CIRCUIT DEVELOPMENT IN THE AUDITORY BRAINSTEM

DEVELOPMENT OF NEUROTRANSMISSION IN THE LATERAL SUPERIOR OLIVE: UNDERSTANDING SYNAPSE MATURATION IN THE DEVELOPING AUDITORY BRAINSTEM

By

DANIEL T. CASE, B.Sc.

A Thesis

Submitted to the School of Graduate Studies

in Partial Fulfillment of the Requirements

for the Degree

Doctorate of Philosophy

McMaster University

DOCTORATE OF PHILOSOPHY (2013) McMaster University

(Neuroscience Graduate Program) Hamilton, ON

TITLE: Development of neurotransmission in the lateral superior olive: understanding synapse maturation in the developing auditory brainstem.

AUTHOR: Daniel T. Case, B.Sc. (University of Alberta)

SUPERVISOR: Dr. Deda Gillespie

NUMBER OF PAGES: xii, 176

ABSTRACT

The lateral superior olive (LSO) is an auditory brainstem nucleus crucial in the determination of sound source. To accomplish sound localization, principal neurons of the LSO compare the intensity of sounds reaching the two ears by integrating an excitatory input from the ipsilateral anteroventral cochlear nucleus (AVCN), which is activated by sound reaching one ear, with an inhibitory input from the ipsilateral medial nucleus of the trapezoid body (MNTB), which is activated by sound reaching the opposite ear. In order for LSO principal neurons to properly integrate these excitatory and inhibitory inputs, the inputs must be matched in a frequency-dependent matter to LSO neurons. The mechanisms that direct the organization, selection, and maturation of both the excitatory and inhibitory pathway during development are not well understood. The experiments presented in this thesis were aimed at understanding the mechanisms that may underlie these processes in the developing LSO.

The excitatory neurotransmitter glutamate is released in both the excitatory AVCN-LSO pathway and the inhibitory MNTB-LSO pathway during their period of functional circuit refinement, and may be important in the development of both of these pathways. Using the patch-clamp technique in acute brainstem slices of rats, we evaluated glutamatergic transmission in both the excitatory AVCN-LSO pathway and the inhibitory MNTB-LSO pathway during their period of functional refinement. Additionally, using the patch-clamp technique in acute brainstem slices of mice, we examined what functions

vesicular glutamate transporter 3 (VGlut3), the protein that supports glutamate release from MNTB terminals, may have in the developing MNTB-LSO pathway. When taken together, the results from the three studies presented support a model in which circuit maturation in the LSO relies on mechanisms driven through a specific glutamate receptor, the N-methyl-D-aspartate (NMDA) receptor.

ACKNOWLEDGEMENTS

First and foremost, I would like to thank my supervisor Dr. Deda Gillespie. Deda is a gifted neuroscientist, excellent teacher, and a talented writer; if I have become a portion of any of these it is due to her guidance. I would also like to thank Dr. Colin Nurse and Dr. Ray Truant for taking the time to serve on my supervisory committee, and for their input and advice on my research projects over the course of my graduate work. Additionally, I would like to thank all the members of the Gillespie lab, particularly Alan Cooper and Dr. Javier Alamilla, whom I have worked closely with over the last several years, and the taxpayer-funded sources that have made my studies possible.

Many people have helped me through my time as a graduate student. Most importantly, my parents have been supportive of all my decisions and have been continually encouraging amid frustrations; I would not have been able to reach this point without their help. Since moving to Hamilton I have spent time with many people that have made coming to a new city and facing a new challenge bearable; these people know who they are, and I value the friendship of all them and their presence in my life has been truly important. Finally, I would especially like to thank Kate Williams: you are my best friend and a constant source of support and encouragement; I am very fortunate and grateful to have met you.

TABLE OF CONTENTS

LIST OF FIGURES AND TABLES

Chapter 1

Chapter 2

Chapter 3

Chapter 4

LIST OF ABBREVIATIONS

AMPA(R) – 2-amino-3-(3-hydroxy-5-methyl-isoxazol-4-yl)propanoic acid receptor

ATP – adenosine triphosphate

AVCN – anteroventral cochlear nucleus

GABA(R) – gamma amino butyric acid receptor

GAD – glutamic acid decarboxylase

Gly(R) – glycine receptor

KCC2 – potassium chloride cotransporter 2

LSO – lateral superior olive

LTD – long term depression

LTP – long term potentiation

mGluR – metabotropic glutamate receptor

MNTB – medial nucleus of the trapezoid body

MSO – medial superior olive

NKCC1 – sodium potassium cotransporter 1

NMDA(R) – N-methyl D-aspartate receptor

SOC – superior olivary complex

STDP – spike timing dependent plasticity

STED – stimulated emission depletion microscopy

TRP – transient receptor potential

VGlut – vesicular glutamate transporter

VIAAT – vesicular inhibitory amino acid transporter

DECLARATION OF CONTRIBUTION TO RESEARCH

For Chapter 2, I designed the experiments with Dr. Deda Gillespie, I performed the experiments with Dr. Xiwu Zhao, I completed the data analysis, and I wrote the paper with Dr. Deda Gillespie.

For Chapter 3, I designed the experiments with Dr. Deda Gillespie, I performed all the experiments and data analyses, and I wrote the paper with Dr. Deda Gillespie.

For Chapter 4, I designed the experiments with Drs. Deda Gillespie and Javier Alamilla, I performed the experiments with Dr. Javier Alamilla, I completed the data analyses, and I wrote the manuscript.

Chapter 2 was published in PLoS One in 2011:

Case DT, Zhao X, Gillespie DC (2011) Functional refinement in the projection from ventral cochlear nucleus to lateral superior olive precedes hearing onset in rat. *PLoS One* 6(6): e20756.

Chapter 3 was published in the Journal of Neurophysiology in 2011:

Case DT and Gillespie DC (2011) Pre- and postsynaptic properties of glutamatergic transmission in the immature inhibitory MNTB-LSO pathway. *J Neurophysiol* 106(5): 2570-2579.

Chapter 1 – General Introduction

1.1 Auditory Brainstem

Organization and Superior Olivary Complex

Hearing is crucial in all aspects of our daily life: it signals us of danger, helps to direct our attention, and, most importantly, connects us with other people. In hearing, our brain deciphers complex patterns in sound waves to allow us to effectively interact with the world around us. The first step in the process of hearing occurs in the cochlea, the sensory organ in the inner ear that transduces auditory information from the external environment in to electrical signals. The cochlea decomposes sound waves in a frequency dependent manner, with high frequency sounds represented on the basal end of the cochlea (nearest to the outer ear) and low frequency sounds represented at the apical end of the cochlea (farthest from the outer ear) (von Bekesy, 1956). This frequency mapping is termed tonotopy, and it persists throughout the auditory system. Electrical signals are sent from the cochlea to the brain by the spiral ganglion neurons, the axons of which make up the auditory portion of the eighth cranial nerve. Spiral ganglion neurons project to the cochlear nucleus, which is recognized to have three divisions: the dorsal cochlear nucleus, the posteroventral cochlear nucleus, and the anteroventral cochlear nucleus. Principal neurons of the cochlear nucleus in turn project to two main areas: the nuclei of the lateral lemniscus, via the dorsal and intermediate acoustic stria, and the superior olivary complex, via the ventral acoustic stria (for review, see Oertel, 1999). Most projection neurons in the lateral lemniscus and in the superior olivary complex project to

the inferior colliculus, which is the principal integration area for information that encodes sound source (Glendenning and Masterton, 1983; Tollin, 2009).

The superior olivary complex (SOC) is a binaural structure consisting of several nuclei crucial for sound localization. The principal nuclei of the SOC are the medial nucleus of the trapezoid body (MNTB), the medial superior olive (MSO), and the lateral superior olive (LSO). All of these nuclei receive major excitatory, glutamatergic input from the anteroventral cochlear nucleus (AVCN): the MNTB receives input from the contralateral AVCN, the MSO receives input from both the ipsilateral and contralateral AVCN, and the LSO receives input from the ipsilateral AVCN. Additionally, the LSO receives major inhibitory, GABA/glycinergic input from the ipsilateral MNTB (Figure 1; Boudreau and Tsuchitani, 1968; Caird and Klinke, 1983; Moore and Caspary, 1983; Cant and Casseday, 1986; Bledsoe et al. 1990; Smith et al, 1991; for review, see Oertel, 1999), and the MSO receives important inhibitory input driven by information from both ears (for review, see Grothe, 2003).

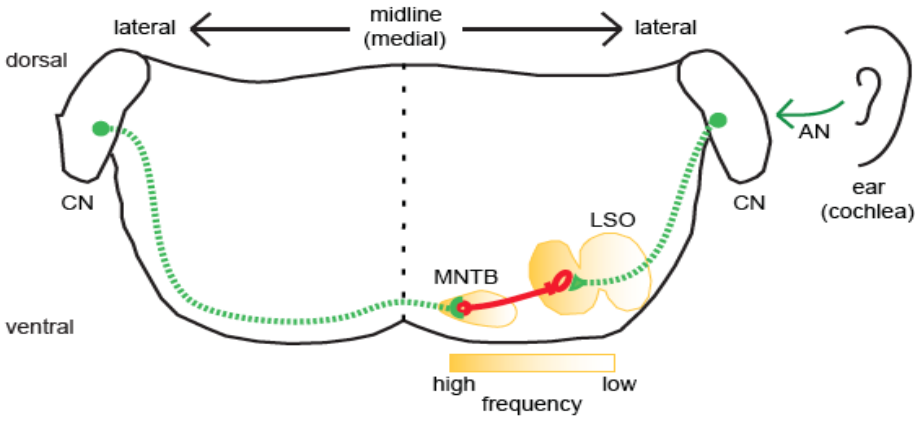

Figure 1. Major input pathways to the LSO (schematic courtesy D. Gillespie)

Principal neurons of the MSO and LSO perform computations necessary for azimuthal (horizontal) sound localization, but use two different cues to do so. Neurons of the MSO integrate the binaural excitatory input they receive from the AVCN to detect the *time* difference of a sound reaching the two ears. MSO neurons are believed to detect the timing difference using a coincidence detection mechanism, or some variation thereof (for review, see Ashida and Carr, 2011). Neurons of the LSO integrate the excitatory input they receive from the ipsilateral AVCN with the inhibitory input they receive from the ipsilateral, contralaterally-driven, MNTB to detect the *intensity* difference of a sound reaching the two ears (Boudreau and Tsuchitani, 1968; Caird and Klinke, 1983). Intensity differences are most useful for localizing the source of high frequency sounds composed of waves the length of the head or smaller, as these waves are effectively reflected and the ear farthest from the sound source falls in a "sound shadow." Intensity differences are signaled by the level of excitation that an LSO neuron generates, with greater excitation being generated in the LSO ipsilateral to the sound source.

For the MSO and LSO to properly perform their respective sound localization computations, the two major inputs reaching principal neurons of these nuclei must be matched in a frequency dependent manner (for review, see Tollin, 2009). A central question in the development of the auditory system is how tonotopic maps originating from the two ears become matched at binaural nuclei in the brainstem (for review, see Sanes and Friauf, 2000, and Kandler et al, 2009). Understanding this process is important not only for the auditory system, but for all systems in which topographic mapping occurs, most notably the visual and somatosensory systems (for example, Triplett et al,

2009). The LSO has proven to be an excellent area in which to study the question of how topographic maps become aligned to their targets during development, in part because its inputs are large projection neurons whose organization and function are well understood (for review, see Kandler and Gillespie, 2005). However, the LSO is very attractive to study for another reason. The development of inhibitory circuits has been very difficult to study because most inhibitory circuits are small local circuits that are made up of many different cell types, they are difficult to access experimentally, and their function is not well understood. The highly organized MNTB-LSO pathway does not present any of these problems, making the LSO an ideal place to study the development of inhibitory circuitry, in addition to sensory mapping (for review, see Kandler, 2004).

Lateral Superior Olive: Neurotransmission

Of the two major inputs to the LSO, relatively little is known about the excitatory AVCN inputs to LSO neurons. The excitatory inputs appear to reach their mature state by approximately the end of the third postnatal week (Sanes and Rubel, 1988). These inputs release glutamate (Wu and Kelly, 1992), and calcium imaging studies in mice have demonstrated that all families of glutamate receptors are activated on LSO neurons by these inputs before hearing onset (Ene et al, 2003). The activation of the different glutamate receptors is dependent on stimulation frequency, and each type of glutamate receptor mediates calcium entry via different sources. Under low frequency stimulation of AVCN fibers, calcium entry into LSO neurons is dependent on 2-amino-3-(5-methyl-3-

oxo-1,2- oxazol-4-yl) propanoic acid (AMPA) receptor activation that leads to membrane depolarization and the activation of voltage-gated calcium channels; at moderate stimulation frequencies N-methyl-D-aspartate (NMDA) receptors also contribute to calcium entry, doing so because they are calcium-permeable; at high stimulation frequencies metabotropic glutamate receptors (mGluRs) are also activated, and elicit an increase in postsynaptic calcium through activation of intracellular calcium stores, and potentially transient receptor potential (TRP) channels (Ene et al, 2003). However, the activation of the different families of glutamate receptors has not been studied electrophysiologically before hearing onset. Consequently, very little is known about the relative contribution of the different families of glutamate receptors during development, and hence about which receptors might principally contribute to refinement of the excitatory inputs.

The inhibitory MNTB inputs to LSO principal neurons undergo several changes over the first three postnatal weeks in rodents. Like the excitatory pathway, the MNTB-LSO pathway appears to reach its mature state by approximately the end of the third postnatal week (Sanes and Rubel, 1988). Once the circuit is mature, a single LSO neuron receives inhibitory input from approximately 3-5 MNTB neurons, and this input is purely glycinergic and strongly hyperpolarizing at the soma (Kim and Kandler, 2003; Moore and Caspary, 1983; Bledsoe et al, 1990). However, at birth, neurotransmission from the MNTB to the LSO is different from the mature state in many ways. First, though the functional reasons remain unclear, gamma-amino-butyric acid (GABA) is released in addition to glycine from MNTB terminals in the LSO (Kotak et al, 1998; Korada and

Schwartz, 1999; Nabekura et al, 2004). This release of GABA lasts in to the second postnatal week, and GABA actually contributes much more than glycine to post-synaptic currents during the first postnatal week. Second, GABA and glycine are depolarizing until late in the first postnatal week, and GABA/glycinergic transmission can elicit action potentials in LSO neurons over the first few postnatal days (Kandler and Friauf, 1995; Ehrlich et al, 1999; Kullmann et al, 2002). This excitatory action of GABA and glycine occurs because activity of the potassium-chloride co-transporter KCC2, which extrudes chloride from neurons, is low in the days following birth, whereas expression of a bicarbonate-chloride exchanger, AE3, which transports chloride into the cell, is highly expressed in the days following birth (Kakazu et al, 1999; Balakrishnan et al, 2003; Becker et al, 2003). Finally, immature MNTB-LSO synapses, although they are ultimately inhibitory, also release the most prevalent excitatory neurotransmitter in the brain, glutamate (Gillespie et al, 2005). Like GABA release, glutamate release from MNTB terminals is transient, and is most prevalent during the first postnatal week.

Lateral Superior Olive: Refinement

The inhibitory inputs from the MNTB are believed to undergo three distinct developmental stages. First, chemical guidance cues, most importantly ephrins and their receptors, the Ephs, are believed to be critical in bringing MNTB axons into the LSO (for review, see Cramer, 2005). This early period occurs mainly before birth in rodents, as functional connections are observed as early as embryonic day 18 (Kandler and Friauf,

1993; Kandler and Friauf, 1995). Second, MNTB inputs on to LSO principal neurons undergo a period of functional refinement that consists of the silencing of many inputs and the strengthening of the remaining inputs (Kim and Kandler, 2003). This middle period occurs before hearing onset in rodents (postnatal day 12; P12), and appears to be dependent on neuronal activity (Kotak and Sanes, 1996). Third, anatomical pruning of silenced MNTB inputs occurs and is believed to support the functional refinement that occurred before hearing onset. This period occurs after hearing onset in rodents, and is also dependent on neuronal activity (Sanes and Siverls, 1991; Sanes and Takacs, 1993). My thesis research has focussed on the second stage of development, because it is an ideal period to study activity-dependent refinement in the auditory system.

Neurotransmission begins at MNTB-LSO synapses as early as embryonic day 18 (3-4 days before birth) in rodents (Kandler and Friauf, 1995). As stated above, neurotransmission from P0 to hearing onset at P12 is a mixed GABA/glycine/glutamate phenotype (Kotak et al, 1998; Korada and Schwartz, 1999; Nabekura et al, 2004; Gillespie et al, 2005). From P0 to P8 GABA and glutamate release is prevalent, and GABA/glycinergic transmission is depolarizing, and even excitatory, in the earliest postnatal days (Kandler and Friauf, 1995; Kotak et al, 1998; Ehrlich et al, 1999; Gillespie et al, 2005). This period, in which GABA/glycinergic signalling is depolarizing and GABAergic and glutamatergic signalling is prevalent, closely correlates with the period of physiological (functional) refinement of the MNTB-LSO synapses (Kim and Kandler, 2003). This period of functional refinement was characterized by Kim and Kandler (2003) in a very nice series of experiments. First, they mapped the input area from the MNTB to

single LSO neurons using photouncaging of glutamate to excite MNTB neurons and whole-cell patch clamp of LSO neurons in acute slices of rat brainstem. Kim and Kandler demonstrated that the proportional area of MNTB that an LSO neuron receives input from is only ¼ the size at P14 as it is at P3. Second, Kim and Kandler stimulated electrically in the MNTB and performed minimal stimulation and input-output curve experiments. Doing this, they were able to estimate the size of the smallest MNTB inputs to LSO neurons, estimate the maximal amplitude of the combined MNTB inputs to an LSO neuron, and determine if there were discrete steps in response amplitude following increases in stimulation strength. All of this information allowed them to estimate the number and strength of MNTB inputs on to LSO neurons over the first two weeks of development. They found that LSO neurons receive approximately ¼ the number of inputs in P9-14 as in P1-5 animals, and that the average input strength is 12-fold greater in P9-14 animals than in P1-5 animals. Overall, results from this study by Kim and Kandler demonstrate that functional refinement of MNTB-LSO inputs, which consists of both a reduction in the number of inputs to a given LSO neuron and an increase in the strength of the remaining inputs, appears to be largely complete by P9.

As stated above, the period of functional refinement in the MNTB-LSO pathway occurs before hearing onset (Kim and Kandler, 2003; Kotak and Sanes, 1996). However, because this period of refinement occurs before hearing onset, neuronal activity must be initiated by something other than environmental sound. In the visual system, spontaneous neural activity generated in the retina is crucial for the proper refinement of retinal ganglion cell projections, and the *pattern* of this activity is likely important for proper

mapping of these connections (for review, see Torborg and Feller, 2005, and Feller, 2009). Like the retina, the cochlea is able to initiate spontaneous neuronal activity (Lippe, 1994; Kros et al, 1998; Beutner and Moser, 2001; Tritsch et al, 2007). A group of supporting epithelial cells in the developing cochlea, known as Kolliker's organ, spontaneously releases adenosine triphosphate (ATP). ATP depolarizes neighboring inner hair cells in the cochlea, initiating calcium spikes in the hair cell and causing them to release glutamate on to spiral ganglion neurons. The calcium spikes pass across hair cells in a theta-burst pattern, and initiate bursting action potential activity in the spiral ganglion (Tritsch et al, 2007; Tritsch and Bergles, 2010; Tritsch et al, 2010). This bursting activity begins in the spiral ganglion at approximately P3, and ends at hearing onset (Tritsch and Bergles, 2010). The bursting activity initiated in the cochlea can propagate through the auditory system (Tritsch et al, 2010), and may be important in establishing nearest-neighbor relationships between cells, and ultimately tonotopic mapping. Once this cochlear driven spontaneous activity ends at hearing onset, sound-evoked activity likely directs the final stages of tonotopic mapping (Sanes and Rubel, 1988; Kandler, 2004).

The results from the studies outlined above have uncovered many events important in the development of the MNTB-LSO pathway. First, MNTB-LSO synapses are functionally refined before hearing onset, mainly between P3 and P8 (Kim and Kandler, 2003). Second, spontaneous activity initiated in the cochlea increases at approximately P3 and is believed to propagate through the lower auditory system (Tritsch et al, 2007; Tritsch and Bergles, 2010). Third, GABA/glycine release at MNTB-LSO synapses is depolarizing in the first postnatal week (Kandler and Friauf, 1995; Kotak et

al, 1998; Ehrlich et al, 1999). Fourth, glutamate release at MNTB-LSO terminals is highly prevalent in the first postnatal week (Gillespie et al, 2005). The correlation of these events leads to a unified model of functional refinement of MNTB-LSO synapses. First, spontaneous activity initiated in the cochlea patterns activity at MNTB-LSO synapses. As has been shown in the retina, the pattern of electrical activity can carry information that is crucial for developmental plasticity and the organization of neural circuits (for review, see Torborg and Feller, 2005, and Feller, 2009). Second, co-release of GABA/glycine and glutamate allows for removal of the magnesium block of NMDARs (by depolarizing GABA/glycine) and opening of NMDARs (by glutamate) postsynaptically. Third, calcium enters through NMDARs, initiating intracellular plasticity mechanisms within the LSO neuron. This is a relatively simple, direct model for plasticity at inhibitory synapses, a topic that is poorly understood.

1.2 Synaptic Plasticity

General Properties of NMDA Receptors

The NMDAR family of glutamate receptors are tetrameric ionotropic receptors (Monyer et al, 1994); of the four subunits comprising the NMDAR, two of the subunits are always of the GluN1 subtype (also known as NR1), and the other two subunits can be a mixture of GluN2 (NR2) or GluN3 (NR3) subunits (Monyer et al, 1992; Ishii et al, 1993; for review, see Cull-Candy et al, 2001). There are four subtypes of GluN2 subunits (GluN2A-D) and two subtypes of GluN3 subunits (GluN3A-B). Generally, the two non-

GluN1 subunits will be of the same type, but mixed receptor types have been observed (for review, see Cull-Candy et al, 2001, and Cull-Candy and Leszkiewicz, 2004). NMDARs are known for having a much longer open time than other ionotropic neurotransmitter receptors: Generally, NMDARs containing GluN2A subunits have shorter open times (100-200ms) than NMDARs containing GluN2B, GluN2C (300-400ms), or GluN2D subunits (>1000ms) (Monyer et al, 1994). Binding affinity of glutamate is higher for GluN2B, GluN2C, and GluN2D containing receptors than for GluN2A containing receptors (for review, see Feldmeyer and Cull-Candy, 1996). Additionally, NMDARs are blocked by the divalent cation magnesium at membrane potentials ~ -20mV, causing them to display voltage-dependent activation (Nowak et al, 1984; Mayer et al, 1984); magnesium blockade of NMDARs is highest for GluN2A and GluN2B containing receptors and lowest for GluN2C and GluN2D containing receptors (Monyer et al, 1994; Kuner and Schoepfer, 1996).

Like the other families of ionotropic glutamate receptors, NMDARs pass mainly sodium and potassium (Mayer and Westbrook, 1985). However, unlike most other ionotropic glutamate receptors, NMDARs also pass calcium (MacDermott et al, 1986). Additionally, unlike most other ionotropic glutamate receptors, more than just glutamate must bind to NMDARs in order for them to be activated: NMDARs require glycine to bind to the receptor in order for the channel to open (Kleckner and Dingledine, 1988), and, as mentioned above, NMDARs are blocked by magnesium at negative membrane potentials and therefore the cell membrane must be depolarized, though not at the NMDAR reversal potential of ~0mV, in order for the NMDAR to pass current (Nowak et

al, 1984; Mayer et al, 1984). Because NMDARs require both neurotransmitter release and membrane depolarization in order to pass current, they detect both presynaptic activity, via neurotransmitter binding, and postsynaptic activity, via membrane depolarization. This characteristic allows NMDARs to act as coincidence detectors, because they detect the coordinated activity of the pre- and postsynaptic terminals. Because NMDARs pass calcium, and because they can detect coordinated cellular activity by acting as coincidence detectors, they are very important for many forms of synaptic plasticity.

Excitatory Synaptic Plasticity

Santiago Ramon y Cajal was the first to suggest that changes in synaptic strength could underlie learning (Cajal, 1911). Donald Hebb later proposed a model for how synaptic strength could be altered. "Hebb's postulate" generally stated that if one cell (cell A) consistently participates in initiating the firing of another cell (cell B), there will be a change in one or both of the cells to increase cell A's ability to cause cell B to fire (Hebb, 1949). This idea has often been summarized as "cells that fire together, wire together," and underlies what has become known as activity-dependent plasticity.

Terje Lomo and Timothy Bliss were the first to demonstrate activity-dependent plasticity of synapses (Lomo, 1966; Bliss and Lomo, 1973). Studying rabbit hippocampus, Bliss and Lomo used extracellular recording to show that excitatory postsynaptic potentials (EPSPs) between perforant pathway fibers and neurons in the dentate gyrus of the hippocampus were increased in amplitude if a high frequency tetanus

was delivered to the perforant pathway (Bliss and Lomo, 1973). This finding was very exciting, because it closely related to Cajal's and Hebb's predictions from decades earlier, and created a model for long-term potentiation (LTP) paradigms that are still used, albeit in several different forms, today.

Though Bliss and Lomo first described LTP in the perforant pathway to the dentate gyrus in the hippocampus, long-term plasticity of excitatory synapses has been studied most extensively in the Schaffer collateral pathway between areas CA3 and CA1 in the hippocampus, and in the mossy fiber pathway between the dentate gyrus and area CA3 in the hippocampus. Differences in results of plasticity experiments performed in these two pathways resulted in the early "pre-post wars" of long-term potentiation. At CA3-CA1 synapses, early studies suggested that LTP is a postsynaptic phenomenon, dependent on NMDARs. Conversely, at mossy fiber-CA3 synapses, early studies suggested that LTP is a presynaptic phenomenon, with no dependence on NMDARs (for review, see Nicoll et al, 1988). The initial disagreements on the locus of plasticity were part of a crucial quest in understanding where plasticity can occur, and work over the past 30 years has established that different synapses can exhibit different forms of plasticity, and that the induction and expression of a single "type" of plasticity can differ (for review, see Malenka and Bear, 2004). In recent years, the importance of long-term depression (LTD; for review, see Collingridge et al, 2010), spike-timing dependent plasticity (STDP; for review, see Caporale and Dan, 2008), homeostatic plasticity (for review, see Turrigiano, 2012), and short-term presynaptic plasticity, such as paired-pulse depression or facilitation, have become obvious (for review, see Castillo, 2012). Despite

this, NMDAR-dependent plasticity (LTP and LTD) has remained a model mechanism for synaptic strengthening and weakening, particularly during neural circuit development.

Excitatory Synaptic Plasticity: Role of NMDARs

In the visual and somatosensory systems, and likely in the other sensory systems, periods of heightened plasticity exist in which the neural circuits serving these senses are refined (Hubel and Wiesel, 1970; Fox, 1992). There are several cellular mechanisms that may limit the timing of these "critical periods" and the heightened plasticity observed during them, but NMDAR-mediated transmission has proven to be a particularly common limiting factor in critical period plasticity (for example, Carmignoto and Vicini, 1992; Crair and Malenka, 1995). Rather than include exhaustive details about the many locations that NMDAR dependent plasticity has been observed, or the many intracellular pathways that are activated in different forms of NMDAR dependent plasticity, I will focus on one example of NDMAR dependent plasticity that beautifully outlines its role in the development of sensory systems.

Rats gain somatosensory information largely through their whiskers, which have a stereotyped arrangement. When rat primary somatosensory cortex (S1) is stained for Nissl substance, it is apparent that groups of neuronal cell bodies are organized in to several cylindrical arrangements that extend radially through the cortex (Woolsey and Van der Loos, 1970). Each of these cylinders, or "barrels," represents a single whisker on the face of the rat. S1 has thus been termed "barrel cortex" in rats, and it is here that NMDARs

were first nicely linked to critical period plasticity. Sensory deprivation perturbs the organization of the axons that convey somatosensory information between thalamus and barrel cortex, though this effect is most evident in the first postnatal week (Fox, 1992). To understand more about what contributes to sensory circuit development, Crair and Malenka (1995) studied LTP in acutely dissected thalamocortical slices from early postnatal rats. To induce LTP, an electrode was inserted into the presynaptic (thalamic) region of the slice and electrical current was injected in a repetitive manner. Postsynaptic responses were recorded in layer IV barrel cortex using whole-cell patch-clamp. Following a repetitive presynaptic stimulus, Crair and Malenka observed LTP that had several important characteristics. First, LTP could only be induced in the first postnatal week and could not be induced thereafter, mirroring the period in which sensory deprivation can disrupt neuronal organization in this area. Second, to induce LTP the postsynaptic cell had to be depolarized *and* coupled with thalamic afferent stimulation, pointing to a role of NMDARs, which must be in depolarized membrane and must bind neurotransmitter to be active. Third, LTP induction was blocked by the calcium chelator BAPTA, again suggesting a role for calcium, and hence calcium-permeable NMDARs. Finally, D-APV, a selective antagonist of NMDARs, completely inhibited LTP induction. Together, this evidence demonstrated that NMDARs are crucial for LTP induction at thalamocortical synapses in layer IV of barrel cortex. Importantly, at these synapses the contribution of NMDARs to synaptic current is large in the first postnatal week and greatly declines thereafter, paralleling the timing of the critical period in this area. This finding gives strong correlative evidence that the factor limiting the critical period for

development of the thalamocortical synapses in layer IV of barrel cortex is the expression of either specific subtypes of NMDARs (for example, Liu et al, 2004, and Barria and Malinow, 2005), or NMDARs in general.

This initial finding in somatosensory cortex is extremely similar to our current understanding of the development of the inhibitory MNTB-LSO synapses in auditory brainstem: MNTB-LSO synapses are functionally refined mainly between P3 and P8, suggestive of a narrow window, or even critical period in development (Kim and Kandler, 2003), and NMDAR-mediated transmission is highest at the same time functional refinement occurs at MNTB-LSO synapses (Gillespie et al, 2005). The parallels apparent in the development of the somatosensory and auditory systems therefore make NMDAR-dependent plasticity a very attractive model for the development of the inhibitory MNTB-LSO pathway.

Inhibitory Synaptic Plasticity

Inhibitory synaptic plasticity has proven very difficult to study. Most inhibitory circuits in the brain are very local, composed of small interneurons of many different types, and the function of these circuits is not well understood (for review, see Kandler, 2004). Despite these problems, several different forms of inhibitory synaptic plasticity have been identified in many areas of the central nervous system, including the cerebellum, auditory brainstem, hippocampus, and cortex (for review, see Gaiarsa et al, 2002). Changes in inhibitory synapses can be induced by a variety of patterns of activity,

and these changes can be mediated by a variety of cellular mechanisms. However, the need for calcium entry is common for almost every form of inhibitory synaptic plasticity (Gaiarsa et al, 2002).

The source of calcium for inhibitory plasticity is usually NMDARs or voltage-gated calcium channels. For reasons that aren't understood, calcium entry through NMDARs often leads to LTD of inhibitory synapses, whereas calcium entry through voltage gated calcium channels often leads to LTP of inhibitory synapses (Gaiarsa et al, 2002). For plasticity mechanisms dependent on voltage-gated calcium channels or NMDARs to be possible, postsynaptic depolarization needs to occur in order to open the voltage-gated calcium channels or to relieve the magnesium block of NMDARs. This poses a problem for inhibitory plasticity, because opening of GABA (or glycine) receptors typically leads to hyperpolarization of the neuronal membrane, as chloride has an equilibrium potential near to or more negative than the resting membrane potential of the neuron. This means that models of activity-dependent synaptic plasticity do not fit well at inhibitory synapses: if an inhibitory synapse is performing its job well, neuronal firing should be decreased, and a coincidence detection model is not possible. However, in developing neurons, the chloride equilibrium potential is much more positive than the neuronal resting membrane potential, and opening of GABARs causes depolarization of the cell membrane (Cherubini et al, 1991). Therefore, activity-dependent plasticity could be possible during development when chloride signalling is depolarizing. The chloride equilibrium potential is higher in developing neurons than in mature neurons because the sodium-potassium-chloride cotransporter NKCC1 (in the LSO, the bicarbonate-chloride

transporter AE3 appears to perform this role (Becker et al, 2003)) is predominant in young neurons, and this transporter does not as effectively extrude chloride as the potassium-chloride cotransporter KCC2, which is predominant in mature neurons (Delpire, 2000; Rivera et al, 1999). However, a gradient in the expression of the NKCC1 and KCC2 transporters can occur in neurons, and this is reflected by differences in GABA equilibrium potential between the dendrites and soma (Woodin et al, 2003; Szabadics et al, 2006; Romo-Parra et al, 2008). Activity-dependent plasticity could then be possible at inhibitory synapses not only during development, but also in mature neurons if chloride signalling is very tightly buffered and is depolarizing at some synapses.

In visual cortex, several examples of inhibitory long-term plasticity have been demonstrated. For example, long-term plasticity of layer 4 to layer 5 inhibitory connections was demonstrated by recording inhibitory postsynaptic potentials in layer 5 cells following stimulation of layer 4. Here, plasticity only occurred if groups of neuronal fibers were stimulated. The stimulation protocol drove plasticity in opposite directions depending on which type of neurotransmitter receptors were blocked. Furthermore, LTP in this circuit involved $GABA_B$ receptors, monoamine receptors and calcium release from intracellular stores (Komatsu and Iwakiri, 1993; Komatsu, 1994; Komatsu, 1996). Another form of LTP that has been identified in visual cortex occurs between inhibitory interneuron-pyramidal cell pairs in layer 4 (Maffei et al, 2006, Maffei et al, 2010). LTP in this circuit is occluded by deprivation that causes ocular dominance shifts, suggesting that this plasticity observed *in vitro* actually contributes to *in vivo* plasticity.

Spike-timing dependent plasticity has been shown at inhibitory synapses in the hippocampus (Woodin et al, 2003). Here, the strength of inhibitory transmission is decreased at mature inhibitory synapses when they are active within 20ms before or after an action potential fires in the postsynaptic cell. This synaptic depression is mediated by a reduction in KCC2 activity, which causes a depolarizing shift in the chloride reversal potential. In contrast, at immature hippocampal inhibitory synapses the same conditioning protocol increases the strength of inhibition. This is mediated by a reduction in NKCC1 activity, which causes a hyperpolarizing shift in the chloride reversal potential (Balena and Woodin, 2008).

Inhibitory Synaptic Plasticity: Role of NMDARs

NMDAR-dependent inhibitory plasticity appears to arise in the same way as NMDAR-dependent excitatory plasticity. For example, it is observed most commonly when GABA and glycine are depolarizing and can remove the magnesium block of NMDARs, as AMPARs do at excitatory synapses (for review, see Gaiarsa et al, 2002). Additionally, the level of calcium entry appears to dictate the direction of synaptic plasticity (LTP versus LTD) at inhibitory synapses, as it does at many excitatory synapses (Gaiarsa et al, 2002).

That NMDARs are important in many forms of inhibitory synaptic plasticity is quite surprising, considering that there is no direct source of glutamate release at inhibitory synapses, nor is there NMDAR expression at inhibitory synapses, generally

speaking. This means that in most forms of inhibitory plasticity observed to date, inhibitory synapses have to use signals from excitatory synapses for plasticity, and the effect observed can be considered a global cellular event. The mechanism proposed in cases of NMDAR-dependent inhibitory plasticity requires that excitatory synapses be activated close to inhibitory synapses, both in space and time. From this, calcium entry through NMDARs at excitatory synapses could essentially "spillover" within the intracellular milieu to inhibitory synapses that are simultaneously activated. A seemingly homeostatic plasticity mechanism such as this may be sufficient to arrange many inhibitory circuits, assuming that the main function of an inhibitory circuit is to limit excitatory activity and pattern electrical signalling in a small area of the cell membrane. However, it is known that inhibitory synapses in most circuits are targeted to the cell body and proximal dendrites of neurons, whereas excitatory synapses are targeted predominantly to the apical dendrites (Kapfer et al, 2002). A non-synapse specific plasticity mechanism such as the one described above is an unsatisfying model for the direction of such segregated excitatory and inhibitory synapse pools during development. Moreover, in the mature state in which synapse segregation is complete, the degree to which calcium spillover between excitatory and inhibitory synapses occurs in the postsynaptic cell is unknown, making the mechanism described more difficult to imagine. Given the importance of inhibitory synapses in shaping cell output, a synapse specific mechanism for inhibitory synaptic plasticity is more attractive, particularly for an inhibitory projection circuit like the MNTB-LSO pathway. The MNTB-LSO pathway almost certainly requires a mechanism for synapse specific refinement, due to the

tonotopy that this pathway must achieve; the fact that this pathway releases glutamate on to NMDARs during development offers a way in which this circuit can accomplish synapse specificity (Kim and Kandler, 2003; Gillespie and Kandler, 2005; Noh et al, 2010). Additionally, bidirectional spillover of glutamate between excitatory and inhibitory terminals in the immature LSO appears extensive, and may play a role in coordinated refinement of the excitatory and inhibitory inputs (Alamilla and Gillespie, 2011). Whether a model like the one at MNTB-LSO synapses is feasible or not for other inhibitory circuits remains to be seen.

Inhibitory Synaptic Plasticity in the Lateral Superior Olive

As described above, neurons of the LSO receive highly organized inhibitory inputs from the MNTB. The inhibitory neurons from the MNTB are large projection neurons of a single phenotype, and the role of these neurons in sound processing is reasonably well understood. This means that the inhibitory MNTB-LSO circuit is an excellent place to study development and plasticity of inhibitory circuits (for review, see Kandler, 2004). Currently, much more is known about the characteristics of developmental refinement of the MNTB-LSO pathway than the mechanisms of plasticity underlying the developmental refinement. However, work from Dan Sanes' laboratory has provided one example of long-term plasticity during the period of functional refinement of the MNTB-LSO pathway. Performing whole-cell patch-clamp on LSO neurons in acute brainstem slices from pre-hearing onset age (P7-P12) and post-hearing onset age

(P17-P19) gerbils, Kotak and Sanes (2000) found that delivering low frequency stimulation (1Hz stimulation for a 15 minute period) to the MNTB decreases inhibitory postsynaptic potentials or currents in LSO neurons by up to 50%. This LTD was much more prominent in the younger age group, and was also decreased by the calcium chelator BAPTA, demonstrating that the LTD is dependent on calcium. In subsequent studies, LTD of MNTB-LSO terminals was found to be blocked by inhibiting $GABA_B$ receptors (Kotak et al, 2001). Additionally, it was found that LTD could be induced by applying neurotrophic factors (BDNF and NT-3) or cyclic AMP analogs to the slice, and also that LTD could be blocked by applying inhibitors of intracellular tyrosine kinases, protein kinase C, protein kinase A, or CaM kinase II (Kotak et al, 2001; Kotak and Sanes, 2002). Finally, using focal application of GABA and glycine coupled with pharmacology, Chang et al. (2003) demonstrated that LTD of MNTB-LSO synapses was dependent on GABAB receptor activation, but not glycine receptor activation. Additionally, analysis of miniature synaptic events and paired-pulse ratios of neurotransmitter release indicate that LTD at MNTB-LSO synapses is a postsynaptic phenomenon.

Though intriguing, this LTD has never been directly linked to synapse elimination in the MNTB-LSO pathway. It also does not offer a mechanism for strengthening of MNTB-LSO synapses, and was not demonstrated during the main period of functional refinement. The finding that glutamate is released on to NMDARs at developing MNTB-LSO synapses gives rise to a more elegant model for bidirectional plasticity and synaptic refinement in the MNTB-LSO pathway.

1.3 Vesicular Glutamate Transporters

Glutamate is packaged in to synaptic vesicles by a group of H+-dependent cotransporters known as the vesicular glutamate transporters, or VGluts (for review, see Fremeau et al, 2004). There are three members of this transporter family, named VGlut1, VGlut2, and VGlut3. The first two members, VGlut1 and VGlut2, were originally identified as Na+-dependent transporters known as BNPI and DNPI, and were believed to be important for neuronal inorganic phosphate homeostasis (Ni et al, 1994; Aihara et al, 2000; Bellochio et al, 2000, Fremeau et al, 2001). The expression pattern of VGlut1 and VGlut2 are essentially complementary in the central nervous system, with VGlut1 being expressed primarily at glutamatergic terminals in cortex and cerebellum, and VGlut2 being expressed primarily at glutamatergic terminals in midbrain and hindbrain regions (Herzog et al, 2001). VGlut3, which was identified later than VGlut1 and VGlut2, has a much more sparse, distributed expression pattern than VGlut1 and VGlut2, and is often expressed in neurons that are not typically glutamatergic (Fremeau et al, 2002; Gras et al, 2002). VGlut3 can also be found in dendrites, not just synaptic terminals (Fremeau et al, 2002). It is VGlut3 that supports glutamate release at MNTB-LSO synapses during their period of functional refinement (Gillespie et al, 2005; Blaesse et al, 2005; Noh et al, 2010).

VGlut3 is usually expressed at “non-glutamatergic” terminals (Herzog et al, 2004), and often shows significant developmental changes in its expression (Gras et al, 2005). In rodents, VGlut3 is expressed immediately following birth, and peaks at P10; after this, VGlut3 expression again peaks in adulthood, but only in rostral brain regions

(Gras et al, 2005). This biphasic expression pattern is highly suggestive of two roles for VGlut3, one transient and developmental, the other maintained through adulthood. Recent findings are beginning to indicate what these, rather surprising, roles may be.

Understanding of the function of VGlut3 was greatly aided by the generation of VGlut3 knockout (KO) mice. VGlut3 KO mice are congenitally deaf, and also experience non-convulsive seizures (Seal et al. 2008). This phenotype arises because VGlut3 is normally expressed in inner hair cells of the cochlea, and also in GABAergic basket cells in the hippocampus (Seal et al, 2008; Somogyi et al, 2004). VGlut3 knockout mice also fail to undergo normal refinement in the MNTB-LSO pathway: without VGlut3, MNTB-LSO connections remain numerous and weak, whereas the excitatory AVCN-LSO connections appear to undergo normal refinement (Noh et al, 2010). This phenotype does not appear to arise simply because the mice are deaf, as mice that do not express otoferlin, a protein necessary for normal vesicular release from inner hair cells (Roux et al, 2006), appear to have normal development of the MNTB-LSO pathway (Noh et al, 2010). Additionally, neither the size of the GABA/glycine response before the functional refinement period nor neuronal membrane properties differ between VGlut3 wild-type and VGlut3 knockout mice. These findings give further support to the hypothesis that glutamate release is what is crucial for functional refinement of the MNTB-LSO pathway (Noh et al, 2010).

Another surprising role of VGlut3 has been described in the striatum. Here, VGlut3 is expressed in cholinergic neurons, and, rather than being necessary for glutamatergic transmission, the primary role of VGlut3 in these neurons appears to be to

increase cholinergic signalling (Gras et al, 2008). This effect, termed "vesicular synergy," has also been observed in serotonergic neurons of the raphe nuclei, where VGlut3 has been shown to increase serotonergic signalling (Amilhon et al, 2010). In line with this, knockout of VGlut3 in mice has been shown to increase anxiety-like behaviours, suggesting a very important role for VGlut3 in serotonergic transmission (Amilhon et al, 2010).

The studies outlined above offer two potential roles for VGlut3 at developing MNTB-LSO synapses: 1) VGlut3 is necessary for glutamate release on to NMDARs which mediate developmental refinement of MNTB-LSO synapses (Gillespie et al, 2005; Noh et al, 2010), 2) VGlut3 acts to increase GABA/glycinergic signalling, which may be required to support patterned activity necessary for proper refinement of the MNTB-LSO pathway (Gras et al, 2008; Amilhon et al, 2010; Figure 2). These two possibilities are likely exclusive, but some interplay between the two cannot be ruled out.

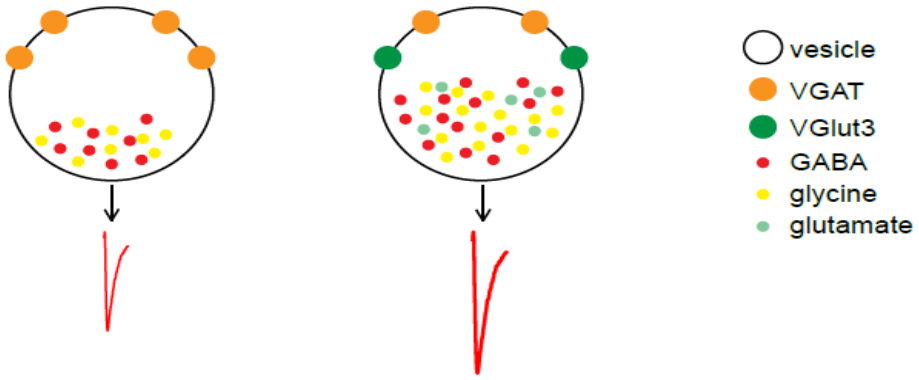

Figure 2. Vesicular synergy model at developing MNTB-LSO synapses.

1.4 Background and Rationale for Studies Performed in Chapters 2-4

The research presented in chapters 2-4 was performed to gain insight into two important open questions in the developing nervous system: 1) How do topographic maps become aligned? 2) How are inhibitory synapses refined? Specifically, we wanted to further understand: 1) how excitatory and inhibitory topographic (tonotopic) maps are aligned in the auditory brainstem; 2) what role glutamate release and VGlut3 serve at developing inhibitory synapses in the auditory brainstem. I examined these questions in three separate projects, which I have described below.

Chapter 2: Functional refinement in the projection from ventral cochlear nucleus to lateral superior olive precedes hearing onset in rat.

Before this project was completed, functional refinement of the inhibitory MNTB-LSO pathway was well described by Kim and Kandler (2003), but nothing was known about the time course of functional refinement of the excitatory AVCN-LSO pathway. Additionally, little was known about the development and prevalence of specific glutamate receptors at AVCN-LSO synapses. We performed whole-cell patch-clamp recordings in acute brainstem slices taken from rats between P1 and P12 and asked: 1) When are the excitatory AVCN-LSO synapses functionally refined? 2) What glutamate receptors are active at AVCN-LSO synapses during this period of refinement? 3) Are there changes in the subunits making up these glutamate receptors? 4) Do properties of glutamate release change at AVCN-LSO synapses between birth and hearing onset? The

results of this study furthered our understanding of the development of the excitatory AVCN-LSO inputs, because we now know what glutamate receptors are active during the period of functional refinement, and the subunits that may be present in these receptors. This gives us insight in to what forms of plasticity are available to drive strengthening and weakening of synapses, and ultimately functional refinement. Additionally, the results furthered our understanding of how the excitatory AVCN-LSO topographic map may be matched with the inhibitory MNTB-LSO topographic map, because by comparing the time periods in which the excitatory and inhibitory maps are refined we can determine whether or not these two maps use a template-matching model; that is, we can determine if one map is refined before the other, so that the other map can be matched to it.

Chapter 3: Pre- and postsynaptic properties of glutamatergic transmission in the immature MNTB-LSO pathway.

Gillespie et al. (2005) demonstrated that glutamate release at MNTB-LSO synapses is present from birth (P0) to hearing onset (P12), that glutamate release is most prevalent from birth to P8, and that glutamate release from MNTB-LSO synapses activates both AMPA and NMDA receptors. However, to fully understand how NMDAR-mediated plasticity may occur at MNTB-LSO synapses, we wanted to characterize further glutamate release at these synapses. To do this we asked: 1) What glutamate receptors are active at MNTB-LSO synapses between birth and hearing onset? 2) Are there changes in the subunits making up these glutamate receptors? 3) Are release properties of GABA/glycine similar or different to release properties of glutamate at MNTB-LSO synapses? Like the results of the first study outlined, the results of this study give us a

better idea of what forms of plasticity are available for functional refinement of MNTB-LSO synapses, because we now know the receptors and receptor subunits that are active during functional refinement. Additionally, by comparing release properties of GABA/glycine and glutamate, we have a better idea of how these neurotransmitters may be packaged into vesicles within a single terminal, and also the patterns of activity that may initiate release of each type of transmitter.

Chapter 4: VGlut3 does not synergize the loading of GABA/glycine into synaptic vesicles at MNTB-LSO synapses.

VGlut3 may play a role more complicated than simply loading glutamate into synaptic vesicles. For example, VGlut3 has been shown to synergize the loading of acetylcholine into synaptic vesicles in neurons in the striatum (Gras et al, 2008), and the loading of serotonin into synaptic vesicles in neurons in the raphe nuclei (Amilhon et al, 2010). This finding has important implications for the development of MNTB-LSO synapses: If VGlut3 synergizes with VIAAT to increase loading of GABA/glycine into synaptic vesicles, GABA/glycine-containing vesicles may be refilled at higher rates than normal, strengthening MNTB-LSO synapses by increasing quantal content. Additionally, increasing the rate of vesicle filling may also allow MNTB-LSO synapses to better follow patterned bursting activity that may guide their refinement. If VGlut3 is present to increase loading of GABA/glycine into vesicles, then glutamate release may simply be a

by-product of this operation and the model of NMDAR-dependent plasticity may have to be re-evaluated. In order to test for the possibility that VGlut3 influences loading of synaptic vesicles at MNTB-LSO synapses, we compared properties of short-term plasticity in VGlut3 knockout mice and littermate control mice using whole-cell patch-clamp in acute brainstem slices. We asked three questions: 1) Does short-term synaptic plasticity (measured as paired-pulse ratios) differ between wild-type and VGlut3 knockout mice? 2) Does the time for recovery of neurotransmitter release following a train of electrical stimuli differ between wild-type and VGlut3 knockout mice? 3) Do amplitudes of miniature inhibitory postsynaptic currents (mIPSCs) differ between wild-type and VGlut3 knockout mice? The results of this study have yielded more information on the function of VGlut3 at developing of MNTB-LSO synapses, and have given us more information on the primary role of VGlut3 during early postnatal development.

References

Aihara Y, Mashima H, Onda H, Hisano S, Kasuya H, Hori T, Yamada S, Tomura H, Yamada Y, Inoue I, Kojima I, Takeda J (2000) Molecular cloning of a novel brain-type Na(+)-dependent inorganic phosphate cotransporter. J Neurochem 74(6):2622-5.

Alamilla J, Gillespie DC (2011) Glutamatergic inputs and glutamate-releasing immature inhibitory inputs activate a shared postsynaptic receptor population in lateral superior olive. Neuroscience 196:285-96.

Amilhon B, Lepicard E, Renoir T, Mongeau R, Popa D, Poirel O, Miot S, Gras C, Gardier AM, Gallego J, Hamon M, Lanfumey L, Gasnier B, Giros B, El Mestikawy S (2010). VGLUT3 (vesicular glutamate transporter type 3) contribution to the regulation of serotonergic transmission and anxiety. J Neurosci 30(6):2198-2210.

Ashida G, Carr CE (2011) Sound localization: Jeffress and beyond. Curr Opin Neurobiol 21(5):745-51.

Balakrishnan V, Becker M, Löhrke S, Nothwang HG, Güresir E, Friauf E (2003) Expression and function of chloride transporters during development of inhibitory neurotransmission in the auditory brainstem. J Neurosci 23(10):4134-45.

Barria A, Malinow R (2005) NMDA receptor subunit composition controls synaptic plasticity by regulating binding to CaMKII. Neuron 48(2):289-301.

Becker M, Nothwang HG, Friauf E (2003) Differential expression pattern of chloride transporters NCC, NKCC2, KCC1, KCC3, KCC4, and AE3 in the developing rat auditory brainstem. Cell Tissue Res 312(2):155-65.

Bellocchio EE, Reimer RJ, Fremeau RT Jr, Edwards RH (2000) Uptake of glutamate into synaptic vesicles by an inorganic phosphate transporter. Science 289(5481):957-60.

Beutner D, Moser T (2001) The presynaptic function of mouse cochlear inner hair cells during development of hearing. J Neurosci 21(13):4593-9.

Blaesse P, Ehrhardt S, Friauf E, Nothwang HG (2005) Developmental pattern of three vesicular glutamate transporters in the rat superior olivary complex. Cell Tissue Res 320(1):33-50.

Bledsoe SC, Jr., Snead CR, Helfert RH, Prasad V, Wenthold RJ, Altshuler RA (1990) Immunocytochemical and lesion studies support the hypothesis that the projection from the medial nucleus of the trapezoid body to the lateral superior olive is glycinergic. Brain Res 517: 189-194.

Bliss TV, Lomo T (1973) Long-lasting potentiation of synaptic transmission in the dentate area of the anaesthetized rabbit following stimulation of the perforant path. J Physiol 232(2):331-56.

Boudreau JC, Tsuchitani C (1968) Binaural interaction in the cat superior olive S segment. J Neurophysiol. 1968 May;31(3):442-54.

Caird D, Klinke R (1983) Processing of binaural stimuli by cat superior olivary complex neurons. Exp Brain Res. 52(3):385-99.

Cajal SR (1911) Histologie du Systeme Nerveux de l'Homme et des Vertebres, Vol. II (Paris: Maloine), pp. 993.

Cant NB, Casseday JH (1986) Projections from the anteroventral cochlear nucleus to the lateral and medial superior olivary nuclei. J Comp Neurol 247:457-476.

Caporale N, Dan Y (2008) Spike timing-dependent plasticity: a Hebbian learning rule. Annu Rev Neurosci 31:25-46.

Castillo PE (2012) Presynaptic LTP and LTD of excitatory and inhibitory synapses. Cold Spring Harb Perspect Biol 4(2). pii: a005728.

Carmignoto G, Vicini S (1992) Activity-dependent decrease in NMDA receptor responses during development of the visual cortex. Science 258(5084):1007-11.

Chang EH, Kotak VC, Sanes DH (2003) Long-term depression of synaptic inhibition is expressed postsynaptically in the developing auditory system. J Neurophysiol 90:1479-1488.

Cherubini E, Gaiarsa JL, Ben-Ari Y (1991) GABA: an excitatory transmitter in early postnatal life. Trends Neurosci 14(12): 515-519.

Collingridge GL, Peineau S, Howland JG, Wang YT (2010) Long-term depression in the CNS. Nat Rev Neurosci 11(7):459-73.

Crair MC, Malenka RC (1995) A critical period for long-term potentiation at thalamocortical synapses. Nature 375:325-328.

Cramer KS (2005) Eph proteins and the assembly of auditory circuits. Hear Res 206(1-2):42-51.

Cull-Candy S, Brickley S, Farrant M (2001) NMDA receptor subunits: diversity, development and disease. Curr Opin Neurobiol 11: 327-335.

Cull-Candy SG, Leszkiewicz DN (2004) Role of distinct NMDA receptor subtypes at central synapses. Sci STKE 2004(255):re16.

Delpire E (2000) Cation-Chloride Cotransporters in Neuronal Communication. News Physiol Sci 15:309-312.

Ehrlich I, Lohrke S, Friauf E (1999) Shift from depolarizing to hyperpolarizing glycine action in rat auditory neurones is due to age-dependent Cl- regulation. J Physiol 520 Pt 1: 121-137.

Ene FA, Kullmann PH, Gillespie DC, Kandler K (2003) Glutamatergic calcium responses in the developing lateral superior olive: receptor types and their specific activation by synaptic activity patterns. J Neurophysiol 90: 2581-2591.

Feldmeyer D, Cull-Candy S (1996) Functional consequences of changes in NMDA receptor subunit expression during development. J Neurocytol 25(12):857-67.

Feller MB (2009) Retinal waves are likely to instruct the formation of eye-specific retinogeniculate projections. Neural Dev. 2009 Jul 6;4:24.

Fox K (1992) A critical period for experience-dependent synaptic plasticity in rat barrel cortex. J Neurosci 12(5):1826-38.

Fremeau RT Jr, Troyer MD, Pahner I, Nygaard GO, Tran CH, Reimer RJ, Bellocchio EE, Fortin D, Storm-Mathisen J, Edwards RH (2001) The expression of vesicular glutamate transporters defines two classes of excitatory synapse. Neuron 31(2):247-60.

Fremeau RT Jr, Burman J, Qureshi T, Tran CH, Proctor J, Johnson J, Zhang H, Sulzer D, Copenhagen DR, Storm-Mathisen J, Reimer RJ, Chaudhry FA, Edwards RH (2002) The identification of vesicular glutamate transporter 3 suggests novel modes of signaling by glutamate. Proc Natl Acad Sci U S A 99(22):14488-93.

Fremeau RT Jr, Voglmaier S, Seal RP, Edwards RH (2004) VGLUTs define subsets of excitatory neurons and suggest novel roles for glutamate. Trends Neurosci 27(2):98-103.

Gaiarsa JL, Caillard O, Ben-Ari Y (2002) Long-term plasticity at GABAergic and glycinergic synapses: mechanisms and functional significance. Trends Neurosci 25:564-570.

Gillespie DC, Kim G, Kandler K (2005). Inhibitory synapses in the developing auditory system are glutamatergic. Nat Neurosci 8:332-338.

Glendenning KK, Masterton RB (1983) Acoustic chiasm: efferent projections of the lateral superior olive. J Neurosci 3(8):1521-37.

Gras C, Herzog E, Bellenchi GC, Bernard V, Ravassard P, Pohl M, Gasnier B, Giros B, El Mestikawy S (2002) A third vesicular glutamate transporter expressed by cholinergic and serotoninergic neurons. J Neurosci 22(13):5442-51.

Gras C, Vinatier J, Amilhon B, Guerci A, Christov C, Ravassard P, Giros B, El Mestikawy S (2005) Developmentally regulated expression of VGLUT3 during early post-natal life. Neuropharmacology 49(6):901-11.

Gras C, Amilhon B, Lepicard EM, Poirel O, Vinatier J, Herbin M, Dumas S, Tzavara ET, Wade MR, Nomikos GG, Hanoun N, Saurini F, Kemel ML, Gasnier B, Giros B, El Mestikawy S (2008) The vesicular glutamate transporter VGLUT3 synergizes striatal acetylcholine tone. Nat Neurosci 11:292-300.

Grothe B (2003) New roles for synaptic inhibition in sound localization. Nat Rev Neurosci 4(7):540-50.

Herzog E, Bellenchi GC, Gras C, Bernard V, Ravassard P, Bedet C, Gasnier B, Giros B, El Mestikawy S (2001) The existence of a second vesicular glutamate transporter specifies subpopulations of glutamatergic neurons. J Neurosci 21(22):RC181.

Herzog E, Gilchrist J, Gras C, Muzerelle A, Ravassard P, Giros B, Gaspar P, El Mestikawy S (2004) Localization of VGLUT3, the vesicular glutamate transporter type 3, in the rat brain. Neuroscience 123(4):983-1002.

Hebb DO (1949) The Organization of Behavior (New York: John Wiley & Sons, Inc.)

Hubel DH, Wiesel TN (1970) The period of susceptibility to the physiological effects of unilateral eye closure in kittens. J Physiol 206(2): 419-436.

Ishii T, Moriyoshi K, Sugihara H, Sakurada K, Kadotani H, Yokoi M, Akazawa C, Shigemoto R, Mizuno N, Masu M, et al. (1993) Molecular characterization of the family of the N-methyl-D-aspartate receptor subunits. J Biol Chem 268(4):2836-43.

Kakazu Y, Akaike N, Komiyama S, Nabekura J (1999) Regulation of intracellular chloride by cotransporters in developing lateral superior olive neurons. J Neurosci 19: 2843-2851.

Kandler K, Friauf E (1993) Pre- and postnatal development of efferent connections of the cochlear nucleus in the rat. J Comp Neurol 328: 161-184.

Kandler K, Friauf E (1995) Development of glycinergic and glutamatergic synaptic transmission in the auditory brainstem of perinatal rats. J Neurosci 15: 6890-6904.

Kandler K (2004) Activity-dependent organization of inhibitory circuits: lessons from the auditory system. Curr Opin Neurobiol 14:96-104.

Kandler K, Gillespie DC (2005) Developmental refinement of inhibitory sound-localization circuits. Trends Neurosci 28(6):290-6.

Kandler K, Clause A, Noh J (2009) Tonotopic reorganization of developing auditory brainstem circuits. Nat Neurosci 12: 711-717.

Kapfer C, Seidl AH, Schweizer H, Grothe B (2002) Experience-dependent refinement of inhibitory inputs to auditory coincidence-detector neurons. Nat Neurosci 5(3):247-53.

Kim G, Kandler K (2003). Elimination and strengthening of glycinergic/GABAergic connections during tonotopic map formation. Nat Neurosci 6:282-290.

Kleckner NW, Dingledine R (1988) Requirement for glycine in activation of NMDA-receptors expressed in Xenopus oocytes. Scienc 241(4867):835-7.

Komatsu Y and Iwakiri M (1993) Long-term modification of inhibitory synaptic transmission in developing visual cortex. Neuroreport 4(7): 907-910.

Komatsu Y (1994) Age-dependent long-term potentiation of inhibitory synaptic transmission in rat visual cortex. J Neurosci 11(1): 6488-6499.

Komatsu Y (1996) GABAB receptors, monoamine receptors, and postsynaptic inositol trisphosphate-induced Ca2+ release are involved in the induction of long-term potentiation at visual cortical inhibitory synapses. J Neurosci 16(20): 6342-6352.

Korada S, Schwartz IR (1999) Development of GABA, glycine, and their receptors in the auditory brainstem of gerbil: a light and electron microscopic study. J Comp Neurol 409:664-681.

Kotak VC, Sanes DH (1996) Developmental influence of glycinergic transmission: regulation of NMDA receptor-mediated EPSPs. J Neurosci 16:1836-1843.

Kotak VC, Korada S, Schwartz IR, Sanes DH (1998) A developmental shift from GABAergic to glycinergic transmission in the central auditory system. J Neurosci 18:4646-4655.

Kotak VC, Sanes DH (2000) Long-lasting inhibitory synaptic depression is age- and calcium-dependent. J Neurosci 20:5820-5826.

Kotak VC, DiMattina C, Sanes DH (2001) GABA(B) and Trk receptor signaling mediates long-lasting inhibitory synaptic depression. J Neurophysiol 86:536-540.

Kotak VC, Sanes DH (2002) Postsynaptic kinase signaling underlies inhibitory synaptic plasticity in the lateral superior olive. J Neurobiol 53:36-43.

Kros CJ, Ruppersberg JP, Rusch A (1998) Expression of a potassium current in inner hair cells during development of hearing in mice. Nature 394:281-284.

Kullmann PH, Ene FA, Kandler K (2002) Glycinergic and GABAergic calcium responses in the developing lateral superior olive. Eur J Neurosci 15(7):1093-104.

Kuner T, Schoepfer R (1996) Multiple structural elements determine subunit specificity of Mg2+ block in NMDA receptor channels. J Neurosci 16(11):3549-58.

Lippe WR (1994) Rhythmic spontaneous activity in the developing avian auditory system. J Neurosci 14: 1486-1495.

Liu L, Wong TP, Pozza MF, Lingenhoehl K, Wang Y, Sheng M, Auberson YP, Wang YT (2004) Role of NMDA receptor subtypes in governing the direction of hippocampal synaptic plasticity. Science 304:1021-1024.

Lomo T (1966) Frequency potentiation of excitatory synaptic activity in the dentate area of the hippocampal formation. Acta Physiol. Scand. 68 (supplement 277), 128.

MacDermott AB, Mayer ML, Westbrook GL, Smith SJ, Barker JL (1986) NMDA-receptor activation increases cytoplasmic calcium concentration in cultured spinal cord neurones. Nature 321(6069):519-22.

Maffei A, Nataraj K, Nelson SB, Turrigiano GG (2006) Potentiation of cortical inhibition by visual deprivation. Nature 443(7107): 81-84.

Maffei A, Lambo ME, Turrigiano GG (2010) Critical period for inhibitory plasticity in rodent binocular V1. J Neurosci 30:3304-3309.

Malenka RC, Bear MF (2004) LTP and LTD: an embarrassment of riches. Neuron 44:5-21.

Mayer ML, Westbrook GL, Guthrie PB (1984) Voltage-dependent block by Mg2+ of NMDA responses in spinal cord neurones. Nature 309(5965):261-3.

Mayer ML, Westbrook GL (1985) The action of N-methyl-D-aspartic acid on mouse spinal neurones in culture. J Physiol 361:65-90.

Monyer H, Sprengel R, Schoepfer R, Herb A, Higuchi M, et al. (1992) Heteromeric NMDA receptors: molecular and functional distinction of subtypes. Science 256: 1217-1221.

Monyer H, Burnashev N, Laurie DJ, Sakmann B, Seeburg PH (1994) Developmental and regional expression in the rat brain and functional properties of four NMDA receptors. Neuron 12: 529-540.

Moore MJ, Caspary DM (1983) Strychnine blocks binaural inhibition in lateral superior olivary neurons. J Neurosci 3: 237-242.

Nabekura J, Katsurabayashi S, Kakazu Y, Shibata S, Matsubara A, Jinno S, Mizoguchi Y, Sasaki A, Ishibashi H (2004) Developmental switch from GABA to glycine release in single central synaptic terminals. Nat Neurosci 7:17-23.

Ni B, Rosteck PR Jr, Nadi NS, Paul SM (1994) Cloning and expression of a cDNA encoding a brain-specific Na(+)-dependent inorganic phosphate cotransporter. Proc Natl Acad Sci USA 91(12):5607-11.

Nicoll RA, Kauer JA, Malenka RC (1988) The current excitement in long-term potentiation. Neuron 1(2):97-103.

Noh J, Seal RP, Garver JA, Edwards RH, Kandler K (2010) Glutamate co-release at GABA/glycinergic synapses is crucial for the refinement of an inhibitory map. Nat Neurosci 13: 232-238.

Nowak L, Bregestovski P, Ascher P, Herbet A, Prochiantz A (1984) Magnesium gates glutamate-activated channels in mouse central neurones. Nature 307(5950):462-5.

Oertel D (1999) The role of timing in the brain stem auditory nuclei of vertebrates. Annu Rev Physiol 61: 497-519.

Rivera C, Voipio J, Payne JA, Ruusuvuori E, Lahtinen H, Lamsa K, Pirvola U, Saarma M, Kaila K (1999) The K+/Cl- co-transporter KCC2 renders GABA hyperpolarizing during neuronal maturation. Nature 397(6716): 251-255.

Romo-Parra H, Treviño M, Heinemann U, Gutiérrez R (2008) GABA actions in hippocampal area CA3 during postnatal development: differential shift from depolarizing to hyperpolarizing in somatic and dendritic compartments. J Neurophysiol 99(3):1523-34.

Roux I, Safieddine S, Nouvian R, Grati M, Simmler MC, Bahloul A, Perfettini I, Le Gall M, Rostaing P, Hamard G, Triller A, Avan P, Moser T, Petit C (2006) Otoferlin, defective in a human deafness form, is essential for exocytosis at the auditory ribbon synapse. Cell 127(2):277-89.

Sanes DH, Rubel EW (1988) The ontogeny of inhibition and excitation in the gerbil lateral superior olive. J Neurosci 8: 682-700.

Sanes DH, Siverls V (1991) Development and specificity of inhibitory terminal arborizations in the central nervous system. J Neurobiol 22(8):837-54.

Sanes DH, Takacs C (1993) Activity-dependent refinement of inhibitory connections. Eur J Neurosci 5: 570-574.

Sanes DH, Friauf E (2000) Development and influence of inhibition in the lateral superior olivary nucleus. Hear Res 147: 46-58.

Seal RP, Akil O, Yi E, Weber CM, Grant L, Yoo J, Clause A, Kandler K, Noebels JL, Glowatzki E, Lustig LR, Edwards RH (2008) Sensorineural deafness and seizures in mice lacking vesicular glutamate transporter 3. Neuron 57(2):263-75.

Somogyi J, Baude A, Omori Y, Shimizu H, El Mestikawy S, Fukaya M, Shigemoto R, Watanabe M, Somogyi P (2004) GABAergic basket cells expressing cholecystokinin

contain vesicular glutamate transporter type 3 (VGLUT3) in their synaptic terminals in hippocampus and isocortex of the rat. Eur J Neurosci 19(3):552-69.

Smith PH, Joris PX, Carney LH, Yin TC (1991) Projections of physiologically characterized globular bushy cell axons from the cochlear nucleus of the cat. J Comp Neurol 304:387-407.

Szabadics J, Varga C, Molnár G, Oláh S, Barzó P, Tamás G (2006) Excitatory effect of GABAergic axo-axonic cells in cortical microcircuits. Science 311(5758):233-5.

Tollin DJ (2009) The lateral superior olive: a functional role in sound source localization. Neuroscientist 9: 127-143.

Torborg CL, Feller MB (2005) Spontaneous patterned retinal activity and the refinement of retinal projections. Prog Neurobiol 76(4):213-35.

Triplett JW, Owens MT, Yamada J, Lemke G, Cang J, et al. (2009) Retinal input instructs alignment of visual topographic maps. Cell 139: 175-185.

Tritsch NX, Yi E, Gale JE, Glowatzki E, Bergles DE (2007) The origin of spontaneous activity in the developing auditory system. Nature 450: 50-55.

Tritsch NX, Bergles DE (2010) Developmental regulation of spontaneous activity in the Mammalian cochlea. J Neurosci 30: 1539-1550.

Tritsch NX, Rodríguez-Contreras A, Crins TT, Wang HC, Borst JG, Bergles DE (2010) Calcium action potentials in hair cells pattern auditory neuron activity before hearing onset. Nat Neurosci 13(9):1050-2.

Turrigiano G (2012) Homeostatic synaptic plasticity: local and global mechanisms for stabilizing neuronal function. Cold Spring Harb Perspect Biol 4(1):a005736.

Von Bekesy G (1956) Current status of theories of hearing. Science 123(3201):779-83.

Woodin MA, Ganguly K, Poo MM (2003) Coincident pre- and postsynaptic activity modifies GABAergic synapses by postsynaptic changes in Cl- transporter activity. Neuron 39(5): 807-820.

Woolsey TA, Van der Loos H (1970) The structural organization of layer IV in the somatosensory region (SI) of mouse cerebral cortex. The description of a cortical field composed of discrete cytoarchitectonic units. Brain Res 17(2):205-42.

Wu SH, Kelly JB (1992) Synaptic pharmacology of the superior olivary complex studied in mouse brain slice. J Neurosci 12: 3084-3097.

Chapter 2

Publication Reference:

Case DT, Zhao X, Gillespie DC (2011) Functional refinement in the projection from ventral cochlear nucleus to lateral superior olive precedes hearing onset in rat. *PLoS One* 6(6): e20756.

Abstract

Principal neurons of the lateral superior olive (LSO) compute the interaural intensity differences necessary for localizing high-frequency sounds. To perform this computation, the LSO requires precisely tuned, converging excitatory and inhibitory inputs that are driven by the two ears and that are matched for stimulus frequency. In rodents, the inhibitory inputs, which arise from the medial nucleus of the trapezoid body (MNTB), undergo extensive functional refinement during the first postnatal week. Similar functional refinement of the ascending excitatory pathway, which arises in the anteroventral cochlear nucleus (AVCN), has been assumed but has not been well studied. Using whole-cell voltage clamp in acute brainstem slices of neonatal rats, we examined developmental changes in input strength and pre- and post-synaptic properties of the VCN-LSO pathway. A key question was whether functional refinement in one of the two major input pathways might precede and then guide refinement in the opposite pathway. We find that elimination and strengthening of VCN inputs to the LSO occurs over a

similar period to that seen for the ascending inhibitory (MNTB-LSO) pathway. During this period, the fractional contribution provided by NMDA receptors (NMDARs) declines while the contribution from AMPA receptors (AMPARs) increases. In the NMDAR-mediated response, GluN2B-containing NMDARs predominate in the first postnatal week and decline sharply thereafter. Finally, the progressive decrease in paired-pulse depression between birth and hearing onset allows these synapses to follow progressively higher frequencies. Our data are consistent with a model in which the excitatory and inhibitory projections to LSO are functionally refined in parallel during the first postnatal week, and they further suggest that GluN2B-containing NMDARs may mediate early refinement in the VCN-LSO pathway.

2.1 Introduction

The superior olivary complex in the auditory brainstem includes the key nuclei responsible for azimuthal sound localization. In particular, the lateral superior olive (LSO) compares converging excitatory and inhibitory inputs to compute sound level differences between the two ears for high frequency sounds (Boudreau and Tsuchitani, 1968; Caird and Klinke, 1983). This computation requires that the LSO be precisely tonotopically organized such that the excitatory and inhibitory inputs converge to the same isofrequency band (for review, see Tollin, 2009). The excitatory, glutamatergic projection arises in the ipsilateral anteroventral cochlear nucleus (AVCN; Cant and Casseday, 1986; Wu and Kelly, 1992), whereas the inhibitory, glycinergic projection

arises in the ipsilateral medial nucleus of the trapezoid body (MNTB), a sign-inverting nucleus driven by the contralateral VCN (Moore and Caspary, 1983; Bledsoe et al, 1990; Smith et al, 1991; Caspary and Finlayson, 1991). A question of fundamental importance is how these primary inputs of opposing sign are coordinately refined during development to provide the finescale tuning necessary for computing interaural level differences in the adult LSO (for reviews, see Sanes and Friauf, 2000, and Kandler et al, 2009).

Axons of both excitatory and inhibitory projections can be detected in the LSO shortly before birth in the rat (Kandler and Friauf, 1993). These early inputs, which are functional but weak (Kandler and Friauf, 1995), undergo developmental refinement that results in frequency-matched excitation and inhibition (Sanes and Rubel, 1988; Oertel, 1999). Of these two pathways, relatively more is known about development of the inhibitory projection. Patterned, spontaneous activity from the cochlea (Lippe, 1994; Kros et al, 1998; Beutner and Moser, 2001; Tritsch et al, 2007), which increases steadily from around postnatal day 3 (P3) to hearing onset at P12 (Tritsch and Bergles, 2010), is thought to direct activity-dependent refinement in the MNTB-LSO pathway (Sanes and Takacs, 1993). Functional refinement of the rat MNTB-LSO pathway is accompanied by changes in quantal size and quantal content and is mediated by largely unknown mechanisms of plasticity that may require glutamate release from MNTB terminals and that occur primarily between P3 and P8 (Kim and Kandler, 2010; Gillespie et al, 2005; Noh et al, 2010; Kim and Kandler, 2003). Although it has often been assumed that during this same period the ipsilateral VCN inputs to the LSO undergo developmental

refinement, in fact much less is known about how the VCN-LSO pathway normally develops.

Ipsilateral VCN afferents invade the LSO at around embryonic day 18 in rat and are excitatory onto LSO neurons within 2 days (Kandler and Friauf, 1993; Kandler and Friauf, 1995). AMPA receptors (AMPARs), NMDA receptors (NMDARs) and metabotropic glutamate receptors (mGluRs) are all expressed in LSO neurons during early postnatal development (Kotak and Sanes, 1996; Caicedo and Eybalin, 1999), and calcium-imaging studies have shown AMPARs, NMDARs and mGluRs to be activated in the VCN-LSO pathway in the first postnatal week in mouse (Ene et al, 2003). Neither functional refinement nor in vitro synaptic plasticity has yet been reported in this pathway, however, and central aspects of pathway development remain to be determined, such as whether, to what degree, and when functional and morphological refinement occur.

Because the LSO's two major input projections must map onto the same space in tonotopic register with one another, an important first question is to understand whether one of the two inputs is initially established and refined—later acting as a template for the opposite projection—or whether both inputs are established and refined relatively independently. In order to better understand the mechanisms that may govern circuit refinement and tonotopic alignment of excitatory and inhibitory inputs, we have examined developmental changes in several synaptic properties in the VCN-LSO pathway, including measures of input strength, receptor types and subunits, and properties

of neurotransmitter release. We find an apparent decrease in input number, and increase in input strength, during a period that parallels that of functional refinement in the MNTB-LSO pathway. We further find that NMDAR-mediated signaling is elevated during the period of functional refinement, and that a GluN2B component is prevalent in the NMDAR-mediated response before P8 and declines thereafter. As the timecourse of refinement and the activation of GluN2B-containing NMDARs in the VCN-LSO pathway closely shadow similar events in the developing MNTB-LSO pathway, our results support a model in which the excitatory and inhibitory inputs to LSO neurons are refined over the same time frame, presumably independently, and likely using some of the same synaptic molecules and mechanisms.

2.2 Materials and Methods

Ethics Statement

All procedures adhered to Canadian Council on Animal Care guidelines and were approved by the Animal Research Ethics Board of McMaster University (Permit #08-08-36).

Slice preparation and physiology

Sprague-Dawley rats (Charles-River Laboratories) aged postnatal days 1 to 12 (P1-12; P0 is day of birth) were anaesthetized with isofluorane and quickly decapitated, and the

brains were removed into ice-cold artificial cerebrospinal fluid (ACSF, pH 7.2) containing (in mM): 125 NaCl, 1 $MgSO_4$, 5 KCl, 1.25 KH_2PO_4, 10 dextrose, 26 $NaHCO_3$, 2 $CaCl_2$•$2H_2O$, 1 kynurenic acid. The brainstem was cut at 300 µm (Vibratome 3000 Series), and slices containing the LSO were transferred to a humidified interface chamber where they were allowed to recover for at least 1 hour at room temperature (~20C). For recording, slices were transferred to a recording chamber at an upright microscope. Slices were kept at room temperature and continuously perfused with ACSF superfused with 95% O_2/5% CO_2. Strychnine (1 µM) and picrotoxin (50 µM) were added to the perfusate to block glycine and $GABA_A$ receptors, respectively; kynurenic acid was not added to ACSF used in recordings. For experiments performed in Mg^{++}-free ACSF (AMPA/NMDA ratios, NMDAR pharmacology), $MgSO_4$ was replaced with K_2SO_4. Stimulating electrodes, 1–2 MΩ glass pipettes filled with ACSF, were placed in the fiber tract at the lateral edge of the LSO and stimuli were delivered via a Master 8 with Iso-Flex SIU. Cells in the higher frequency (medial and middle) limbs of the LSO were targeted using DIC-IR to identify principal cells based on their bipolar morphology and their orientation relative to the mediolateral axis of the nucleus.

Electrodes for whole-cell voltage clamp (8250 borosilicate glass, AM Systems) had resistances of 3–6 MΩ and were filled with a Cs-gluconate solution (pH 7.2) containing (in mM): 64 D-gluconic acid, 64 CsOH, 11 EGTA, 56 CsCl, 1 MgCl2•6H2O, 1 CaCl2, 10 HEPES, 0.3 GTP-Na, 4 ATPMg•3.5H2O, 0.1 mM spermine (Acros Organics). In most cases, the internal solution also contained 0.5% biocytin for subsequent histological verification of cell type. Internal solutions for some recordings of metabotropic glutamate

receptors contained 100 K-gluconate, 20 KCl, 10 Na2-phosphocreatine, 10 HEPES, 0.3 GTP-Na, 4 ATP-Mg•3.5H20 (pH 7.3). Recordings (MultiClamp 700B amplifier with pClamp 10 and Axopatch 200B amplifier with pClamp 9.2; Molecular Devices) were sampled at 5 or 10 kHz, filtered at 5 kHz and saved for offline analysis with custom Matlab software. Recordings were compensated by a minimum of 80% with <10 μs lag, and were discarded if series resistance changed by more than 15% from its initial value. All recordings, except for those addressing AMPAR rectification, were made at a holding potential of −60 mV. For AMPA/NMDA ratios, pharmacology, and probability of release experiments, electrical stimulation intensity was set near a minimum intensity that reliably elicited responses and stimulation intensity remained unchanged throughout the experiment; for older cells this likely resulted in stimulation of a single input fiber. To construct input-output curves (I/O curves), initial stimulation intensities were set near zero and stimulation intensity was gradually increased until maximal response was observed (plateau in response amplitude). For minimal stimulation experiments, >150 responses were collected to stimulation that produced a response ~40% of the time, and stimulus strength was adjusted online to maintain a failure rate of >50%. D-APV (Ascent Scientific, Tocris) and CNQX (Tocris) were added to the ACSF perfusate to block NMDARs and AMPARs. To assess AMPA/NMDA ratios, the NMDAR component (in a few cases the AMPAR component) was pharmacologically isolated using CNQX (D-APV for AMPAR), and the peak NMDAR response was measured. The mean isolated NMDAR trace was subtracted from the mean mixed glutamatergic current to obtain the mean AMPAR response, from which peak AMPAR response was measured. Ifenprodil

(Ascent), a selective antagonist against GluN2B-containing NMDARs, was used to evaluate NMDAR subunit composition pharmacologically. The presence of GluR2-lacking AMPARs was assessed both by degree of rectification, assessed from recordings at −60 mV, −40 mV, 0 mV, +40 mV, and +60 mV, and by pharmacology, assessed by bath application of the selective GluR2-lacking AMPAR antagonist IEM 1460 (Tocris). In paired-pulse experiments cyclothiazide (Ascent) was included in the perfusate to prevent AMPAR desensitization. Drug concentrations used in the perfusate were: DAPV, 50 µM; CNQX, 5 µM; ifenprodil, 10 µM; IEM 1460, 100 µM; cyclothiazide, 100 µM.

To obtain minimal response amplitudes for P1-2 cells, peak current amplitude within the expected temporal window was obtained, and then all "responses" were matched to an average minimal response trace. All "responses" judged not to match the template were discarded as noise, and the remaining responses were averaged to determine minimum response strength. The rectification index RI was defined here as RI = $[(I_{+40mV}/(V_{+40}-V_{rev})]/[(I_{-60mV}/(V_{-60}-V_{rev})]$. Decay time constants were obtained from pharmacologically isolated NMDAR-mediated currents and were calculated as the time for the response amplitude to decay to 37% of peak. Probability of release was examined by delivering 10 pulses of electrical stimulation at 10, 20, 50, and 100 Hz. The peak current amplitudes resulting from the second to tenth pulses were divided by the peak current amplitude resulting from the first pulse (In/Ii) to determine paired-pulse ratios; peak current was measured relative to current immediately before the stimulus for each pulse. Data were analyzed using MiniAnalysis (Synaptosoft) or custom programs in

Matlab (Mathworks). In general, for post-hoc statistical tests, results of significant tests ($p<0.05$) only are provided.

2.3 Results

Using whole-cell voltage-clamp in acute brainstem slices from rats age P1-12, we recorded from 143 principal cells of the LSO to examine developmental changes in input number and strength, functional expression of post-synaptic receptors, and release properties of the presynaptic terminal, for the glutamatergic VCN inputs to LSO principal neurons. All recordings were made in the presence of picrotoxin (50 µM) and strychnine (1 µM) to ensure that only the isolated glutamatergic components were recorded.

Refinement of the VCN-LSO pathway occurs during a temporal window that parallels refinement of the MNTB-LSO pathway

In order to understand whether and how input number and strength change before hearing onset in the VCN-LSO pathway, we recorded responses to stimuli of increasing amplitude in brainstem slices from animals P1-12 and then plotted input-output curves (I/O curves) of response amplitude as a function of stimulus amplitude for each neuron. In theory, at the weakest stimulation strengths no fibers are activated, whereas stimuli of increasing strength successively recruit additional fibers, the activation of which can be

seen as discrete increases in response amplitude. We found that I/O-curves from the youngest slices differed qualitatively from those obtained from slices around hearing onset. As shown in the example figure, most of the I/O curves from slices younger than P3 rose smoothly with increasing stimulus intensity, as expected for neurons that receive many weak inputs (Fig. 1A). In most of the neurons from P4-5 slices, discrete steps were apparent in the I/O relationships (Fig. 1B), and by P9 most of the I/O-curves exhibited only 1–3 steps (Fig. 1C). As shown in these representative examples, some of the steps in response amplitude at P9 were as large as the maximal responses seen before P3 (Compare the P2 example, Fig. 1A, with average maximal amplitude 427.8±9.2 pA to the P9 example, Fig. 1C, with average step sizes 174.1±15.0 pA, 418.1±21.8 pA, 153.2±22.8 pA. Note different y-axis scales.). Thus, single fibers at the older ages were able to drive LSO neurons as strongly as did the entire projection in slices of the youngest ages. Because steps in response amplitude were rare in the I/O curves of the youngest cells, it was generally not possible to directly determine the number of inputs to a single LSO cell from the I/O curves alone. In order to estimate this number for the youngest ages, we divided the average maximal response obtained from the plateau phase of the I/O-curve (Fig. 1D) by the mean observable single-fiber strength obtained from minimal stimulation (Fig. 1E) (for this P1 example cell, average maximal response = 73.8±3.0 pA and average minimal response = 18.3±0.9 pA; therefore, estimated #inputs = 4). For these youngest cells, responses were sparsely sampled at the lower stimulus intensities in order to focus on the plateau phase; thus, the appearance of steps in this example is a sampling artifact.

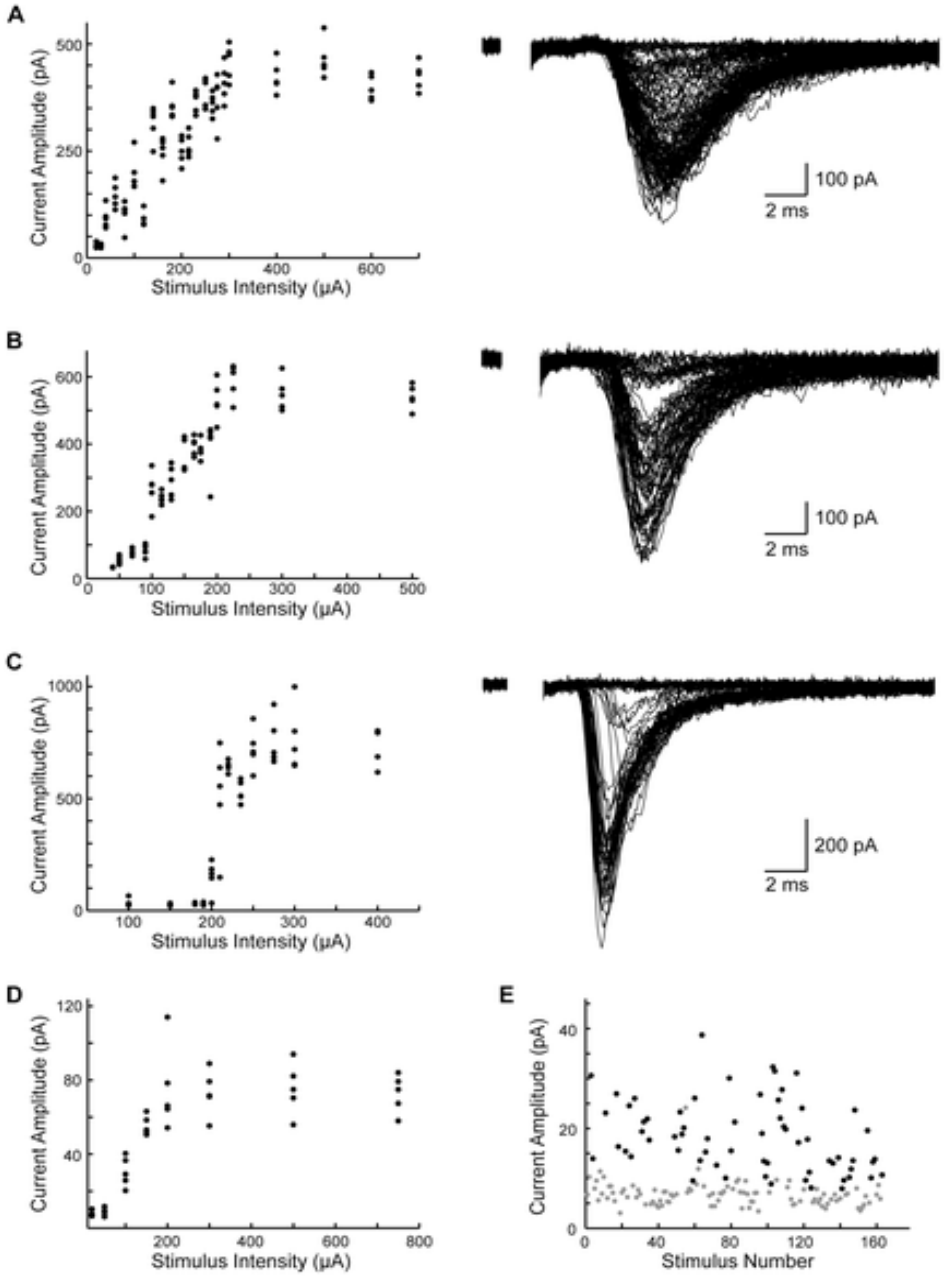
A
Current Amplitude (pA)
Stimulus Intensity (μA)
100 pA
2 ms
B
Current Amplitude (pA)
Stimulus Intensity (μA)
100 pA
2 ms
C
Current Amplitude (pA)
Stimulus Intensity (μA)
200 pA
2 ms
D
Current Amplitude (pA)
Stimulus Intensity (μA)
E
Current Amplitude (pA)
Stimulus Number

Figure 1. Representative input-output curves between P1 and P9. **A**: P2 cell: example individual traces and input-output curve in the VCN-LSO pathway. As shown here, input-output curves obtained for the youngest ages typically lacked clear steps. Higher stimulus amplitudes elicited no increase in response size, and have been removed for clarity. **B**: P5 cell: example individual traces and input-output curve. Stepwise increases in response amplitude could typically be distinguished at this age. Higher stimulus amplitudes elicited no increase in response size, and have been removed for clarity. **C**: P9 cell: example individual traces and input-output curve. Stepwise increases in current amplitude were nearly always distinguishable, with the number of steps rarely exceeding 3. Higher stimulus amplitudes elicited no increase in response size, and have been removed for clarity. **D**: Representative I/O-curve of P1 cell, showing average maximal response in plateau phase of 73.8±3.0 pA. In order to focus on the plateau phase, lower stimulation intensities were sparsely sampled in the youngest cells and thus the appearance of discrete steps in this example is an artifact of sparse sampling. **E**: Response amplitudes to minimal stimulation for the cell shown in D (mean minimal response of 18.3±0.9 pA). Black circles indicate "signal" responses whose shape matched an average minimal-response template; "noise" responses (gray) are shown for comparison.

Estimated number of inputs, mean input strength, and maximal input strength all varied as a function of age in LSO principal cells. Significantly, neurons from the youngest slices were in a distinctly different population from those in the oldest slices: before P3, 67% of all cells (10/15) received more than 3 VCN inputs, whereas from P7 onward less than 10% of all cells (2/24) had more than 3 inputs. Furthermore, before P3 no cells received fewer than 3 inputs, whereas from P7 onward 63% of all cells (15/24) received fewer than 3 inputs (Fig. 2A). For statistical testing, we assigned age groups of P1-3, P4-8 and P9-12, ages corresponding to the periods before, during, and after MNTB-LSO functional refinement, and found statistically significant differences for nearly all comparisons (Kruskal-Wallis for P1-3 vs P4-8 vs P9-12: $p = 1.4*10^{-4}$; posthoc Mann-Whitney tests: P1-3 vs P4-12 $p = 3.2*10^{-5}$; P1-8 vs P9-12 $p = 0.0073$; P1-3 vs P9-12 $p = 2.54*10^{-4}$; P1-3 vs P4-8 $p = 7.0*10^{-4}$; P4-8 vs P9-12 $p = 0.39$). At P1-2, the mean single-fiber strength was 33.9±8.2 pA and the mean maximal response was 150.3±30.3 pA, suggesting that each LSO principal cell received about 5 VCN inputs. Mean single-fiber strength increased significantly before hearing onset ($p = 2.1*10^{-7}$; Kruskal-Wallis). By P9/10, the mean single-fiber strength had increased over five-fold to 231.9±44.2 pA and the mean maximal response to 449.4±77.3 pA, suggesting that each principal cell received only about 2 inputs (Fig. 2B,C). On average, the response to single-fiber stimulation at P9-10 was as big as the largest response that could be obtained in P1-4 slices (maximal response strength for P1-4 172.3±23.9 pA). These data are consistent with the functional elimination of immature synapses in the VCN-LSO pathway between about P3/4 and P8/9 and with an overall strengthening of those synapses that remain (mean input

strength: P1-2, 33.9±8.2 pA, n = 15; P3-4, 57.7±10.7 pA, n = 11; P5-6, 136.1±24.2 pA, n = 8; P7-8, 141.7±33.0 pA, n = 7; P9-10, 231.9±44.2 pA, n = 8; P11-12, 296.8±41.7 pA, n = 9; maximal input strength: P1-2, 150.3±30.3 pA, n = 15; P3-4, 202.3±38.4 pA, n = 11; P5-6, 431.9±120.0 pA, n = 8; P7-8, 267.9±79.2 pA, n = 7; P9-10, 449.4±77.3 pA, n = 8; P11-12, 675.0±129.6 pA, n = 8). Interestingly, although elimination was apparently complete by about P8, further strengthening of VCN-LSO inputs occurred at least until hearing onset at P12 (mean input strength: $p = 2.1*10^{-7}$, Kruskal-Wallis; P3/4 vs P5/6, p = 0.013; P7/8 vs P11/12, p = 0.011, Mann-Whitney; maximal input strength: $p = 5.0*10^{-4}$, Kruskal-Wallis; P1/2 vs P11/12, $p = 4.3*10^{-4}$; P3/4 vs P9/10, p = 0.011, Mann-Whitney).

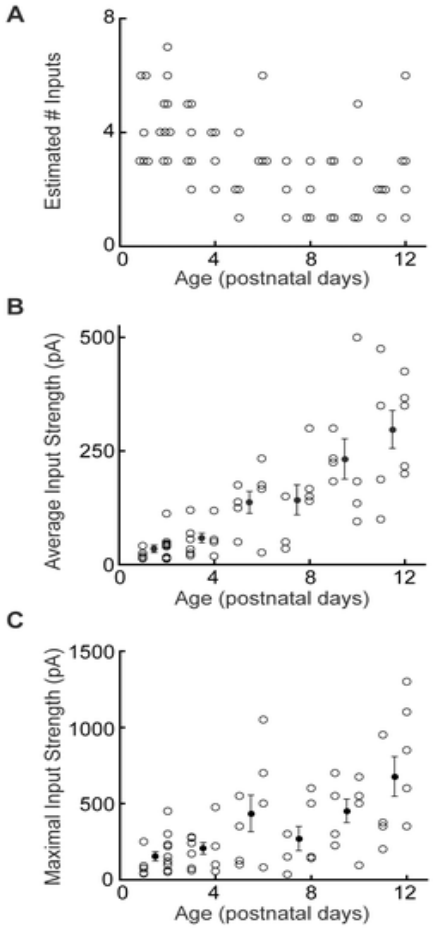

Figure 2. Input number and strength changes with age. **A**: Number of estimated inputs, as a function of age, for 58 LSO principal cells. On average, cells in the youngest slices receive more VCN inputs than do cells from slices around hearing onset. **B**: Mean response to stimulation of the ventral acoustic stria increased by a factor of 9 between P1/2 and P11/12 ($p = 2.1 * 10^{-7}$, Kruskal-Wallis; P3/4 vs P5/6 p = 0.013; P7/8 vs P11/12 p = 0.011, Mann-Whitney). Filled circles represent means ± SEMs at two-day intervals. **C**: Mean maximal response to VCN input increased by a factor of 4.5 between P1/2 and P11/12 (maximal input strength: $p = 5.0 * 10^{-4}$, Kruskal-Wallis; P1/2 vs P11/12 p = $4.3 * 10^{-4}$; P3/4 vs P9/10 p = 0.011, Mann-Whitney).

AMPAR/NMDAR ratio increases between birth and hearing onset

Increases in synaptic strength at many glutamatergic synapses result from the insertion of AMPARs in the postsynaptic membrane, which can be seen as an increase in the ratio of AMPAR/NMDAR peak current (Saal et al, 2003). Thus, we examined the relative contribution of NMDARs and AMPARs to stimulation in the VCN-LSO pathway before hearing onset. To minimize possible confounds from incomplete space clamp in these large cells and potential underestimation of NMDAR currents, these experiments were performed in Mg^{++}-free ACSF. Clearly visible in all recordings before the addition of receptor subtype-specific antagonists (Fig. 3A, top) were an early, fast AMPAR-mediated peak and a later, more slowly decaying NMDAR-mediated peak. Shown in Figure 3B, for the cells in Figure 3A, are the pharmacologically isolated NMDAR components from which fractional contributions to peak current were measured. Because the mixed current at all ages was carried solely by AMPA and NMDA receptors, the AMPAR contribution could be calculated by subtracting the NMDAR-mediated current from the mixed glutamatergic current. These values were used to compute the AMPA/NMDA ratio, which increased as a function of age during the postnatal period before hearing onset (Fig 3C). In the youngest cells, NMDARs contributed a larger share to the EPSC than did AMPARs, whereas by hearing onset AMPARs contributed almost three times as much current as NMDARs. (AMPA/NMDA peak current ratio P1-P2, 0.72±0.11, n = 6; P3-P4, 0.97±0.23, n = 8; P5-P6, 1.24±0.25, n = 7; P7-P8, 1.03±0.15, n = 6; P9-P10, 1.35±0.20, n = 7; P11-12, 2.77±0.43, n = 5). This increase in the AMPA/NMDA ratio could be due to an addition of AMPARs or to a loss of NMDARs or both; linear regression for each

current amplitude as function of age (Fig. 3D) offered weak support for an increase in size of the AMPAR-mediated response (slope 9.9 pA/day, r^2 0.10), accompanied by a decrease in size of the NMDAR-mediated response (slope-7.5 pA/day, r^2 0.072).

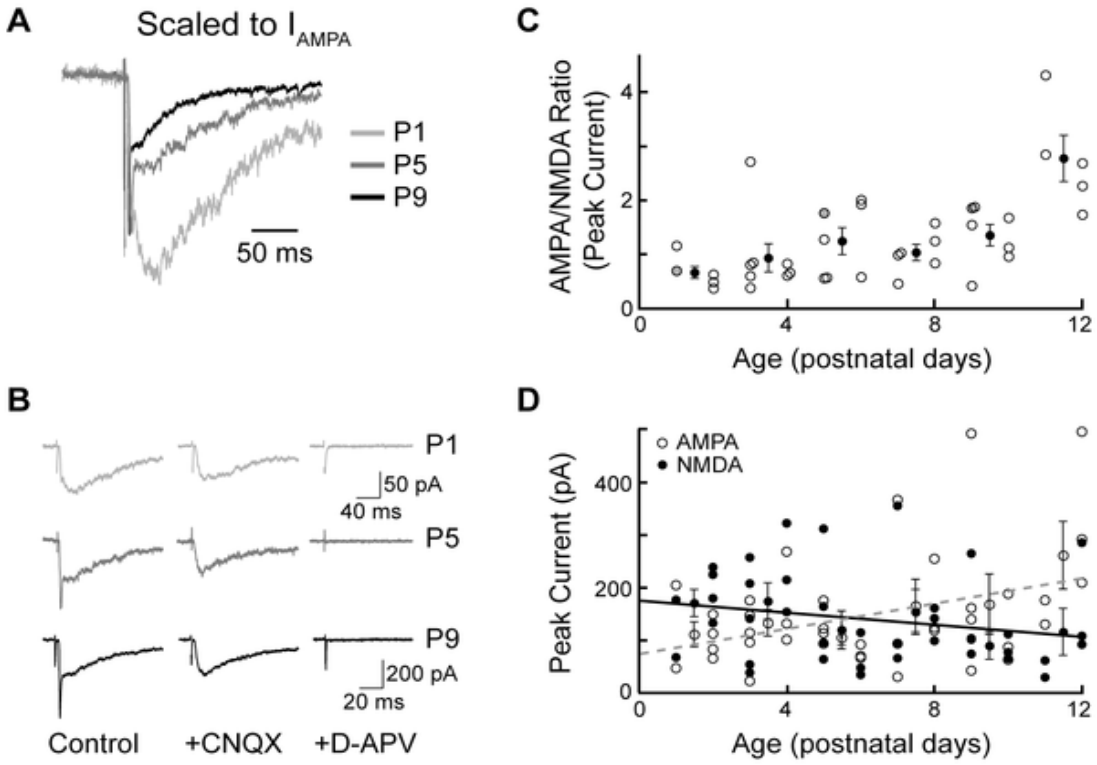

Figure 3. Fractional current mediated by AMPARs increases between birth and hearing onset. **A**: Representative mixed glutamatergic responses from P1, P5 and P9 neurons (average of 10 recordings), scaled to peak AMPA current; distinct AMPA and NMDA components visible in each trace. **B**: Same traces as in A, showing the mixed glutamatergic current, the pharmacologically isolated NMDAR component, and the response after application of AMPAR and NMDAR antagonists, D-APV and CNQX, which abolishes the glutamatergic response. All recordings in Mg^{++}-free ACSF. Note change in scalebars for P9 recordings. **C**: Ratios of peak AMPA/NMDA current in 39 cells from slices P1-P12. During this period, AMPA/NMDA ratio increases as a function of age ($p = 0.012$, Kruskal-Wallis; P1/2 vs P9/10, $p = 0.048$; P7/8 vs P9/10, $p = 0.30$; P9/10 vs P11/12 $p = 0.010$; linear regression slope 0.14/day, $r^2 = 0.32$; exponential fit $r^2 =$

0.36). Filled black circles represent means ± SEMs at two-day intervals. Filled gray circles represent cells shown in A,B. **D**: Increase in AMPA/NMDA ratio with age is accompanied by small increases in average AMPA current (open circles, regressed to gray line) and decreases in average NMDAR current (filled circles, regressed to black line).

A GluN2B subunit component is prevalent before P8

At many glutamatergic synapses, developmental plasticity is mediated by activation of NMDARs (for review, see Malenka and Bear, 2004), and the expression of specific NMDAR subunits may constrain both the magnitude and phenotype of synaptic plasticity available to the synapse (Liu et al, 2004). We asked whether the decrease in NMDAR contribution to peak current with age was due solely to a decrease in NMDAR peak current or whether it was accompanied by a change in receptor kinetics that might point to a developmental change in subunit composition. All experiments on NMDAR composition were performed in Mg^{++}-free ACSF. As seen in the representative traces, the NMDAR component decayed faster at older than at younger ages (Fig. 4A). Additionally, mean charge transfer through NMDARs decreased by a factor of 5 between birth and hearing onset (Fig. 4B; P1-2, 152.2±33.9 pC, n = 6; P3-4, 133.1±26.0 pC, n = 8; P5-6, 94.8±28.6 pC, n = 7; P7-8, 76.8±10.2 pC, n = 6; P9-10, 66.2±25.6 pC, n = 7; P11-12, 26.8±10.3 pC, n = 5).

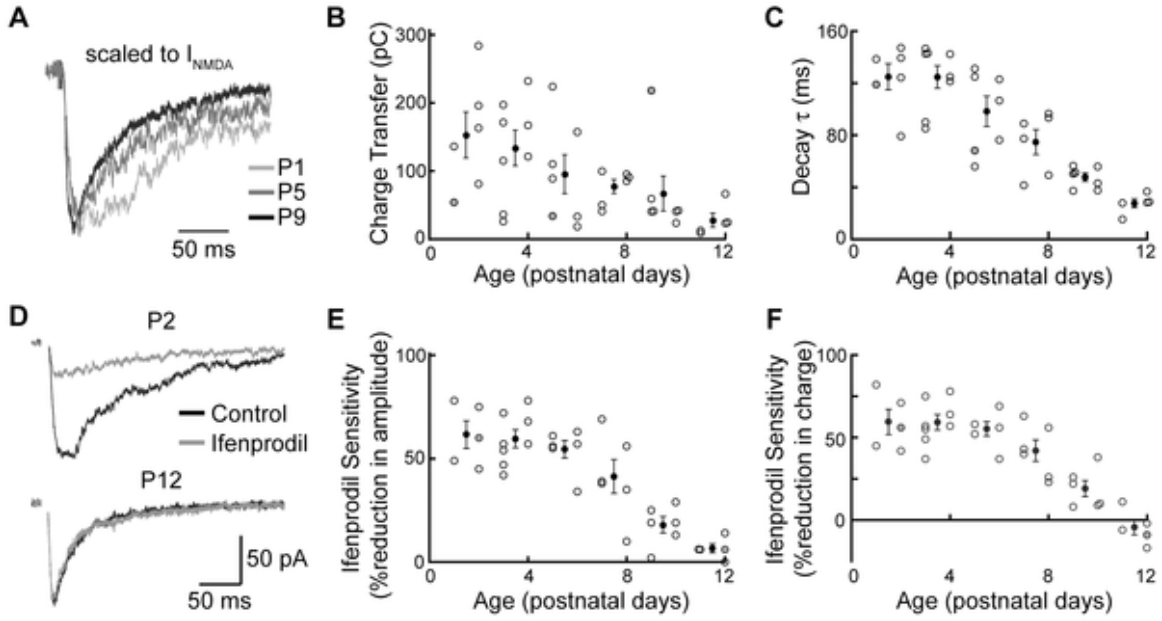

Figure 4. NMDAR kinetics change between P5 and P12 due to loss of GluN2B subunits. **A**: Pharmacologically isolated responses from P1, P5 and P9 neurons (same responses shown in Fig 3), scaled to peak NMDA current, overlay. Note that though these responses are somewhat unrepresentative for charge transfer (gray symbols in B and C), a change in kinetics is nevertheless apparent. **B**: NMDAR-mediated charge transfer decreases between birth and hearing onset (open circles represent individual cells; filled circles represent means ± SEMs at two-day intervals. **C**: NMDAR-mediated current decay times as a function of age. Decay times decrease rapidly after the end of the first postnatal week ($p = 2.9*10^{-5}$, Kruskal-Wallis; P5-6 vs P7-8, p = 0.23 P7-8 vs P9-10, p = 0.10; P9-10 vs P11-12, p = 0.0025, Mann-Whitney). **D**: Median ifenprodil sensitivity from a P2 and P12 neuron; NMDAR-mediated responses in control (black) and in presence of the GluN2B-preferring antagonist ifenprodil (gray). **E**: Sensitivity to ifenprodil (10 μM), measured as % reduction from baseline response amplitude, decreases significantly at the end of the

first postnatal week ($p = 2.5*10^{-4}$, Kruskal-Wallis; P5-6 vs P7-8, p = 0.33; P7-8 vs P9-10, p = 0.037; P9-10 vs P11-12, p = 0.082, Mann-Whitney). Filled black circles indicate means in 2-day groups; filled gray circles correspond to the cells shown in D. **F**: Sensitivity to ifenprodil (10 μM), shown as % reduction from baseline charge transfer, decreases significantly at the end of the first postnatal week (p = 2.7*10−4, Kruskal-Wallis; P5-6 vs P7-8, p = 0.19; P7-8 vs P9-10, p = 0.017, P9-10 vs P11-12, p = 0.030, Mann-Whitney).

To examine more closely the change in charge transfer with age, we plotted decay time constants for the NMDAR-mediated currents as a function of age. Decay time constants, which at P1 were larger than 100 ms, by hearing onset had decreased by a factor of 4.5 (Fig. 4C; P1-2, 125.1±10.1 ms, n = 6; P3-4, 125.0±8.7 ms, n = 8; P5-6, 98.3±11.7 ms, n = 7; P7-8, 74.7±9.7 ms, n = 6; P9-10, 47.5±3.1 ms, n = 7; P11-12, 27.3±3.4 ms, n = 5). Decay time constants of order 100 ms are seen for recombinant diheteromers of both GluN1/GluN2B and GluN1/GluN2C (Vicini et al, 1998). In order to determine which of these GluN2 subunits was likely responsible for the slower decay kinetics seen before P8, we applied the GluN2B-selective antagonist ifenprodil (10 μM) while recording from cells of different ages. As seen in the representative recordings, ifenprodil affected both peak amplitude and kinetics of the NMDAR-mediated response in the first postnatal week, but had little effect thereafter (Fig. 4D). On average, bath application of ifenprodil before P8 reduced both NMDAR-mediated peak current amplitude (Fig. 4E) and charge transfer (Fig. 4F) by over 50%. In P11-12 neurons, however, ifenprodil had almost no effect on either peak current amplitude or charge transfer (% reduction of current amplitude in ifenprodil: P1-2, 61.4±6.6%, n = 5; P3-4, 59.4±4.4%, n = 8; P5-6, 54.3±4.3%, n = 6; P7-8, 41.7±8.2%, n = 6; P9-10, 17.8±3.8%, n = 6; P11-12, 6.4±2.2%, n = 5; % reduction of charge transfer in ifenprodil: P1-2, 59.2±7.6%; P3-4, 59.0±4.7%; P5-6, 55.0±4.3%; P7-8, 41.8±6.5%; P9-10, 18.8±4.9%; P11-12, −4.6±4.6%). These findings indicate that maturation of synaptic currents in the VCN-LSO pathway is due not solely to an increase in the ratio of AMPARs to NMDARs, but also to a subunit switch in the NMDARs at the end of the first postnatal week.

EPSCs are not mediated by GluA2-lacking AMPA receptors or by metabotropic glutamate receptors

We asked whether other glutamate receptors known to mediate synaptic plasticity, such as either the GluA2-lacking, calcium-permeable AMPARs (CP-AMPARs) or the metabotropic glutamate receptors (mGluRs), might contribute to the EPSCs measured after stimulation of VCN-LSO fibers. After applying APV to isolate the AMPAR-mediated response, we obtained current-voltage relationships and used subunit-specific pharmacology to test for the presence of CP-AMPARs at VCN-LSO synapses (Fig. 5A). AMPARs did not exhibit substantial inward rectification at any age examined (Fig. 5B; mean RI = 0.83±0.03, n = 21). Despite an apparent trend toward lower rectification indices (RIs) immediately before hearing onset, no significant age-dependent effects were seen (Kruskal-Wallis for age effects: $p = 0.13$). Additionally, the CP-AMPAR specific antagonist IEM 1460 had no effect on AMPAR-mediated currents at any age (% reduction = 7.0±6.6%, n = 10; data not shown). These data agree with earlier Ca^{++}-imaging results in neonatal mouse VCN-LSO showing that AMPAR-elicited Ca^{++} transients are not due to influx through CP-AMPARs (Ene et al, 2003).

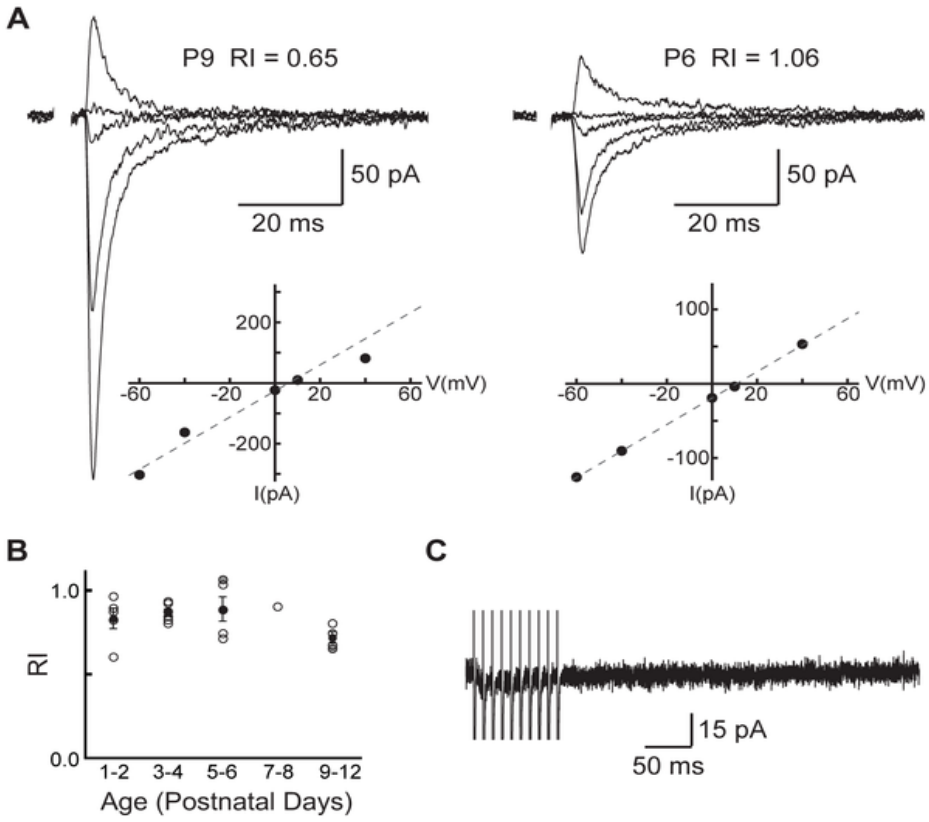

Figure 5. AMPARs contain GluA2 subunits.

A: Example AMPAR responses at various holding potentials for cells with low (left) and high (right) rectification indices. Rectification indices indicate that AMPARs contain GluA2 subunits during the period of VCN-LSO input functional refinement (n = 21). **B**: Rectification indices of pharmacologically isolated AMPAR responses (average RI = 0.83±0.03, n = 21, P1-12). Symbols corresponding to cells shown in A are shaded. **C**: Representative recording from a cell (P1) in response to high-frequency stimulation in an attempt to activate mGluRs. With CNQX and APV in the perfusate, stimulation at 100 Hz failed to elicit mGluR-mediated currents in any cell thus examined (n = 21).

We also did not observe postsynaptic currents resulting from mGluR activation. As shown in Figure 3, the EPSC to single-pulse stimulation in the ventral acoustic stria was abolished by application of CNQX and APV. With CNQX and APV in the perfusate, we further stimulated VCN afferents at 100 and/or 500 Hz, frequencies shown to activate mGluR-mediated Ca^{++}-transients in the mouse VCN-LSO pathway, and we did not observe any mGluR-mediated currents when recording for 1 second or less in response to high frequency stimulation (Fig. 5C; n = 21).

Paired-pulse depression at VCN-LSO synapses decreases between birth and hearing onset

Circuits in the auditory brainstem are capable of supporting among the fastest firing rates in the nervous system. Additionally, varying patterns of activity in the mouse VCN-LSO pathway have been shown to differentially activate different glutamate receptor subtypes and different calcium sources (Ene et al, 2003). To determine the capability of VCN-LSO synapses to support repetitive activity in the developing circuit, we added cyclothiazide to the perfusate to prevent AMPAR desensitization and measured responses to 50 Hz pulse-train stimuli delivered to the ventral acoustic stria. As judged by paired-pulse depression (PPD), neurons in the youngest slices were unable to follow at 50 Hz, a relatively slow frequency for the auditory brainstem (Fig. 6A). In order to ask how frequency-following matures between P1 and P12 we delivered pulse trains of 10 stimuli at 10, 20, 50, and 100 Hz to VCN-LSO fibers. Stimulation at lower frequencies (10 and 20 Hz, or 100 and 50 ms inter-stimulus intervals) yielded similar response profiles at all ages (Fig. 6B),

whereas stimulation at higher frequencies (50 and 100 Hz, or 20 and 10 ms inter-stimulus intervals) revealed distinctly different profiles for the different age groups (50 Hz: $p = 3.3*10^{-5}$; 100 Hz: $p = 0.071$, one-way ANOVA). PPD at 50 Hz (Fig. 6C) was significantly larger in P1-2 than in P3-4 cells ($p = 0.014$) and in P5-8 than in P9-12 cells ($p = 0.041$; [Paired-pulse ratios at 50 Hz: P1-P2, 0.36±0.06; P3-P4, 0.58±0.05; P5-P8, 0.65±0.05; P9-P12, 0.84±0.07]). At 100 Hz, PPD was also significantly larger in P1-2 and in P3-4 cells than in P9-12 cells ($p = 0.0018$; $p = 0.012$; [Paired-pulse ratios at 100 Hz: P1-P2, 0.19±0.03; P3-P4, 0.28±0.07; P5-P8, 0.32±0.12; P9-P12, 0.66±0.10]). These data suggest that changes in probability of neurotransmitter release, rate of vesicle recruitment, number of postsynaptic receptors, or some combination of these, follow a developmental trend that coincides with functional refinement at VCN-LSO synapses.

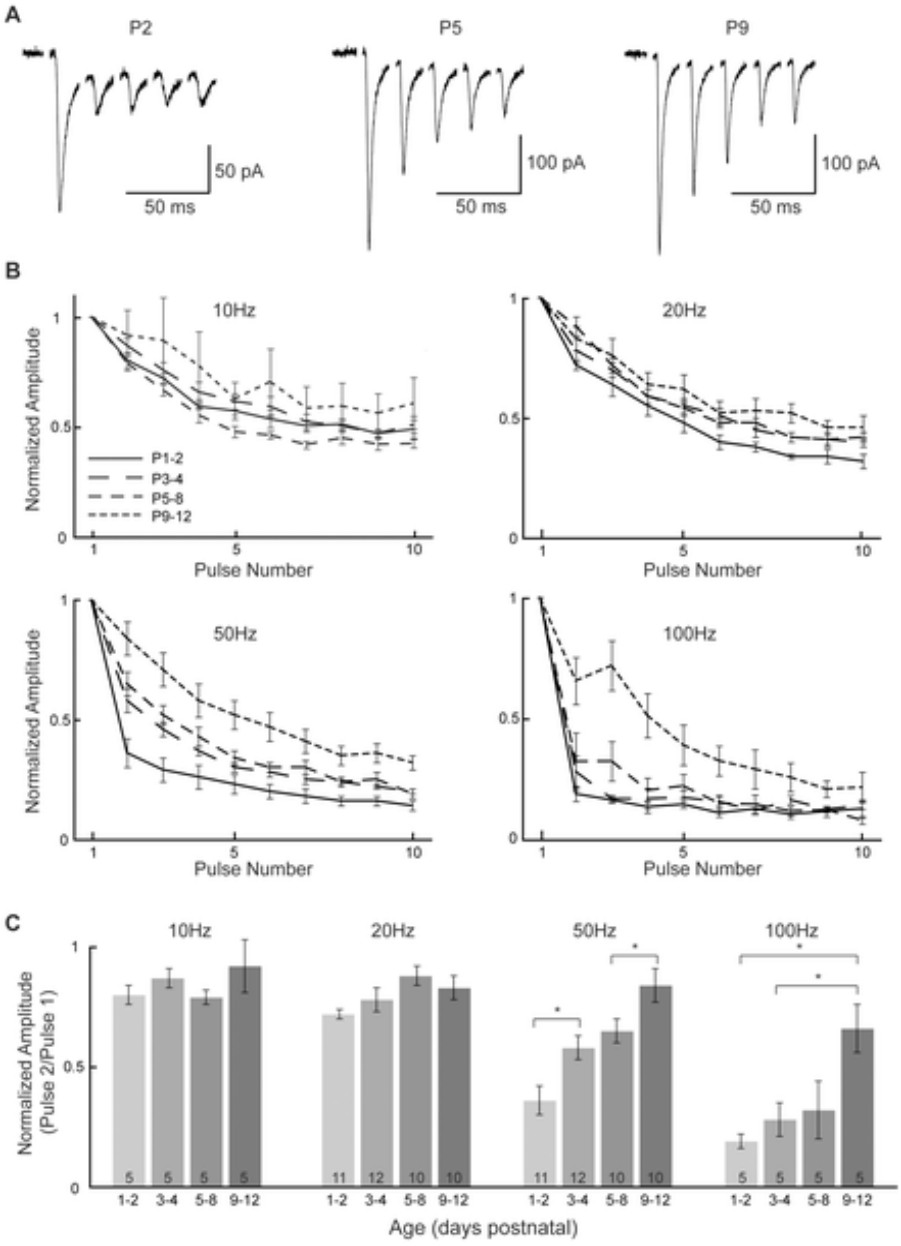

Figure 6. Paired-pulse depression decreases between birth and hearing onset.

A: Representative responses to 50 Hz pulse-trains in P2, P5, and P9 cells; responses to the first five pulses only are shown. Greater paired-pulse depression between pulse 1 and 2 is evident in the youngest cell than in the older cells. **B**: Average responses to 10-pulse

trains at four frequencies. At stimulation frequencies of 20 Hz or less, few differences are seen between ages. At 50 and 100 Hz, clear differences are obvious between age groups, and only the oldest (P9-12) cells are able to follow 100 Hz trains. **C**: Group data from **B**, showing paired-pulse ratios as pulse 2/pulse 1. At 10 and 20 Hz, age differences are not significant at the $p<0.05$ level ($p = 0.48$ and $p = 0.063$, one-way ANOVA). At 50 Hz, significant age differences are seen in paired-pulse depression (one-way ANOVA: = $3.3*10^{-5}$), with greater depression in P1-2 slices than in P3-4 slices (posthoc Mann-Whitney $p = 0.014$) and in P5-8 slices than in P9-12 slices ($p = 0.041$). At 100 Hz, significant age differences are also seen (one-way ANOVA $p = 0.071$), with paired-pulse depression greater in P1-2 ($p = 0.0018$) and P3-4 slices than in P9-12 slices ($p = 0.012$).

2.4 Discussion

Functional refinement in the VCN-LSO pathway parallels refinement in the MNTB-LSO pathway

Using whole-cell patch recordings in the acute slice preparation, we have examined developmental refinement in the excitatory VCN-LSO pathway. We find that the number of functional inputs decreases, and that mean and maximal input strength increase, during the first postnatal week, and thus that refinement in the VCN-LSO pathway occurs during a similar period to that in the opposing, MNTB-LSO pathway. We find that refinement in the VCN-LSO pathway is accompanied by a decrease in the NMDAR fractional contribution and an increase in the AMPAR contribution. Additionally, during the period of functional synapse elimination, much of the NMDAR-mediated current is borne by GluN2B-containing receptors, which disappear rapidly after P8. Finally, frequency-following at VCN-LSO synapses increases progressively between birth and hearing onset.

Our estimates of input number and of percentage decrease are lower than those reported for the MNTB pathway (Kim and Kandler, 2003). These discrepancies may reflect real differences between the two pathways or may be artifacts of slice preparation. Our data should be used cautiously for inferring exact numbers of inputs. Because in any slice preparation an unknown number of fibers is severed, precise input numbers cannot be taken from this study, which provides information about lower bounds and about relative numbers of inputs. Also, because the geometry of rat auditory brainstem precludes a viable slice containing the VCN cell bodies with their fibers that project to the LSO, we

cannot apply the more elegant techniques used to demonstrate major refinement in the MNTB-LSO pathway during the period P3-8 (Kim and Kandler, 2003). Despite our likely underestimation of input number, clear trends are apparent: all P1-3 neurons received ≥3 VCN inputs whereas most P9-12 neurons received <3 inputs, differences supported by non-parametric ANOVA. Our results thus suggest that functional elimination in the VCN-LSO pathway occurs before P8.

Converging neural pathways can be refined either by first establishing and refining one projection and then refining the second projection to match the first, or by refining the two projections simultaneously (Knudsen, 2002; Triplett et al, 2009; Deeg et al, 2009). The refinement observed here is consistent with the second model. We suggest that, like the MNTB-LSO pathway, the VCN-LSO pathway undergoes synaptic silencing during the first postnatal week, possibly using similar mechanisms, and that the excitatory and inhibitory maps are brought into tonotopic registration after hearing onset (Sanes and Rubel, 1988; Sanes and Friauf, 2000, for review). We note a continued strengthening in the VCN-LSO pathway between P8 and hearing onset that has not been reported in the MNTB-LSO pathway. Further strengthening after the period of synaptic silencing could use activity-dependent mechanisms proposed to operate in the first postnatal week, or could involve generalized homeostatic strengthening of the excitatory pathway to compensate for a progressive increase in driving force for hyperpolarizing inhibitory inputs between P8 and hearing onset (Ehrlich et al, 1999). Finally, little is known about glial cells and glutamate re-uptake in the immature LSO, and spillover to peri- or extra-synaptic NMDARs, in which the GluN2B subunit would likely predominate, could be

especially prevalent at young ages (Tovar and Westbrook, 1999). If so, maturation of glutamate uptake and reduction of spillover (Scimemi et al, 2009) might cause an increase in AMPAR/NMDAR ratio. Alternatively, increases in AMPAR/NMDAR ratio are commonly attributed to insertion of AMPARs, which could also contribute to increases in input strength.

Glutamate receptor subtypes in the VCN-LSO pathway change before hearing onset

In addition to similarities of time course, we observed other similarities between the MNTB and VCN inputs to LSO before hearing onset. At MNTB-LSO synapses, NMDAR-mediated signaling is high before P8, coinciding with the period of major synapse elimination in the MNTB-LSO pathway and declines thereafter as glutamate release declines (Gillespie et al, 2005; Kim and Kandler, 2003). Furthermore, NMDAR signaling is lost just as chloride transporter expression matures and these synapses transition from depolarizing to hyperpolarizing GABA/glycinergic transmission (Kandler and Friauf, 1995; Ehrlich et al, 1999; Kakazu et al, 1999; Kullmann and Kandler, 2001). The finding that glutamate is released onto NMDARs at depolarizing GABA/glycinergic synapses during a period of developmental refinement has led to the hypothesis that co-release of glutamate together with depolarizing GABA/glycine activate NMDARs that in turn mediate plasticity in this immature inhibitory pathway, a model corroborated by the report that mice lacking glutamate release from MNTB terminals exhibit perturbed refinement of the MNTB-LSO pathway (Noh et al, 2010). As in the MNTB-LSO

pathway, the developmental changes in NMDAR-mediated signaling in the VCN-LSO pathway occur during a period of functional refinement and are characterized by prominent GluN2B activation that is lost after about P8 (this study; Case and Gillespie, unpublished observations). Regardless of the exact composition of NMDARs in the first postnatal week, we suggest that GluN2B is likely replaced by GluN2A, in a subunit switch similar to that seen in many other areas during development (Sheng et al, 1994; Monyer et al, 1994).

The expression of specific GluN2 subunits determines receptor open probability and conductance, interactions with scaffolding proteins, kinase affinities, and mobility in the plasma membrane, among other factors (Monyer et al, 1992; Strack and Colbran, 1998; Barria and Malinow, 2005; Cull-Candy et al, 2001; Prybylowski et al, 2005; Groc et al, 2006). The GluN2 subunits also show widely different developmental expression profiles in space and time (Sheng et al, 1994; Monyer et al, 1994), and a large body of work has focused on the roles of specific GluN2 subunits, and the ratios of these subunits, in mediating developmental plasticity directly or through control of metaplasticity (reviewed in Malenka and Bear, 2004, and Philpot et al, 2007). Substantial debate has emerged over whether GluN2A or GluN2B may specifically mediate depression versus potentiation (Liu et al, 2004; Morishita et al, 2007); we note that a GluN2B component is prominent during a period that includes both silencing and strengthening, whereas GluN2B is rapidly downregulated during a subsequent period of generalized strengthening. If NMDAR activation is required for developmental plasticity in this pathway, these correlations may suggest that GluN2B mediates synaptic silencing.

In addition to NMDARs, the GluA2-lacking, Ca^{++}-permeable AMPARs (CP-AMPARs) and various mGluRs can also be developmentally expressed and/or can mediate plasticity at central synapses (Liu and Cull-Candy, 2000; Ho et al, 2007; Oliet et al, 1997). Our electrophysiological results agree with an earlier Ca^{++}-imaging study in mouse (Ene et al, 2003), and we conclude that synapses in the early postnatal VCN-LSO pathway do not express CP-AMPARs. In contrast to the imaging study, we found no evidence for mGluR-initiated EPSCs in our recordings, even with high-frequency stimulation. This discrepancy could result from species differences, but a more likely cause may be that as conductances initiated by mGluR activation require release of Ca^{++} from internal stores and downstream activation of TRP channels (Ene et al, 2007), any EPSCs resulting from mGluR activation here would have occurred at latencies too long to appear in whole-cell recordings of ≤500–1000 ms.

Paired-pulse depression declines between birth and hearing onset

We found that at P1 the VCN-LSO pathway could support synaptic transmission at 20 Hz, but not at frequencies ≥50 Hz. The ability of this pathway to support repetitive synaptic transmission increased with age, however, as has also been reported in the MNTB-LSO pathway of mouse (Kim and Kandler, 2010). Although the significant differences seen at 50 and 100 Hz may represent step-increases in the ability of this pathway to support repetitive firing (e.g., at the opening of the P3-8 window for refinement of the MNTB-LSO pathway and again at hearing onset), we suggest that

frequency-following varies smoothly with age and stimulation frequency and that these apparent step-increases represent sampling artifacts. Possibly, the graded differences in frequency-following seen almost until hearing onset result from the staggered maturation of multiple, interacting processes, such as calcium-channel proximity, vesicle population, and vesicle recycling, among others (Cooper and Gillespie, 2011; Wang et al, 2008). Interestingly, PPD observed in the VCN-LSO pathway was similar to that seen for glutamate, but not for GABA/glycine, release in the MNTB-LSO pathway (Case and Gillespie, unpublished observations), despite the fact that the glutamatergic vesicle populations in the two pathways likely use both different vesicular glutamate transporters and different synaptotagmins (Cooper and Gillespie, 2011). Finally, we expect the mature VCN-LSO pathway to exhibit release probabilities and frequency-following similar to that in the MNTB-LSO pathway. Estimating *in vivo* release probabilities from *in vitro* experiments can be problematic (Lorteije et al, 2009), and the different release properties we note may result from slight variability among slices. Nevertheless, understanding how release probability and frequency-following are related in these opposing circuits may contribute to understanding the computation performed by the mature LSO.

References

Barria A, Malinow R (2005) NMDA receptor subunit composition controls synaptic plasticity by regulating binding to CaMKII. Neuron 48: 289-301.

Beutner D, Moser T (2001) The presynaptic function of mouse cochlear inner hair cells during development of hearing. J Neurosci 21: 4593-4599.

Bledsoe SC, Jr., Snead CR, Helfert RH, Prasad V, Wenthold RJ, et al. (1990) Immunocytochemical and lesion studies support the hypothesis that the projection from the medial nucleus of the trapezoid body to the lateral superior olive is glycinergic. Brain Res 517: 189-194.

Boudreau JC, Tsuchitani C (1968) Binaural interaction in the cat superior olive S segment. J Neurophysiol 31: 442-454.

Caicedo A, Eybalin M (1999) Glutamate receptor phenotypes in the auditory brainstem and mid-brain of the developing rat. Eur J Neurosci 11: 51-74.

Caird D, Klinke R (1983) Processing of binaural stimuli by cat superior olivary complex neurons. Exp Brain Res 52: 385-399.

Cant NB, Casseday JH (1986) Projections from the anteroventral cochlear nucleus to the lateral and medial superior olivary nuclei. J Comp Neurol 247: 457-476.

Caspary DM, Finlayson PG (1991) The lateral superior olive: a functional role in sound source localization. In: Altschuler RA, Bobbin RP, Clopton BM, Hoffman DW, editors. Neurobiology of Hearing: The Central Auditory System: Lippincott. pp. 141-161.

Cooper AP, Gillespie DC (2011) Synaptotagmins I and II in the developing rat auditory brainstem: Synaptotagmin I is transiently expressed in glutamate-releasing immature inhibitory terminals. J Comp Neurol.

Cull-Candy S, Brickley S, Farrant M (2001) NMDA receptor subunits: diversity, development and disease. Curr Opin Neurobiol 11: 327-335.

Deeg KE, Sears IB, Aizenman CD (2009) Development of multisensory convergence in the Xenopus optic tectum. J Neurophysiol 102: 3392-3404.

Ehrlich I, Lohrke S, Friauf E (1999) Shift from depolarizing to hyperpolarizing glycine action in rat auditory neurones is due to age-dependent Cl- regulation. J Physiol 520 Pt 1: 121-137.

Ene FA, Kullmann PH, Gillespie DC, Kandler K (2003) Glutamatergic calcium responses in the developing lateral superior olive: receptor types and their specific activation by synaptic activity patterns. J Neurophysiol 90: 2581-2591.

Ene FA, Kalmbach A, Kandler K (2007) Metabotropic glutamate receptors in the lateral superior olive activate TRP-like channels: age- and experience-dependent regulation. J Neurophysiol 97: 3365-3375.

Gillespie DC, Kim G, Kandler K (2005) Inhibitory synapses in the developing auditory system are glutamatergic. Nat Neurosci 8: 332-338.

Groc L, Heine M, Cousins SL, Stephenson FA, Lounis B, et al. (2006) NMDA receptor surface mobility depends on NR2A-2B subunits. Proc Natl Acad Sci U S A 103: 18769-18774.

Ho MT, Pelkey KA, Topolnik L, Petralia RS, Takamiya K, et al. (2007) Developmental expression of Ca2+-permeable AMPA receptors underlies depolarization-

induced long-term depression at mossy fiber CA3 pyramid synapses. J Neurosci 27: 11651-11662.

Kakazu Y, Akaike N, Komiyama S, Nabekura J (1999) Regulation of intracellular chloride by cotransporters in developing lateral superior olive neurons. J Neurosci 19: 2843-2851.

Kandler K, Friauf E (1993) Pre- and postnatal development of efferent connections of the cochlear nucleus in the rat. J Comp Neurol 328: 161-184.

Kandler K, Friauf E (1995) Development of glycinergic and glutamatergic synaptic transmission in the auditory brainstem of perinatal rats. J Neurosci 15: 6890-6904.

Kandler K, Clause A, Noh J (2009) Tonotopic reorganization of developing auditory brainstem circuits. Nat Neurosci 12: 711-717.

Kim G, Kandler K (2003) Elimination and strengthening of glycinergic/GABAergic connections during tonotopic map formation. Nat Neurosci 6: 282-290.

Kim G, Kandler K (2010) Synaptic changes underlying the strengthening of GABA/glycinergic connections in the developing lateral superior olive. Neuroscience 171: 924-933.

Knudsen EI (2002) Instructed learning in the auditory localization pathway of the barn owl. Nature 417: 322-328.

Kotak VC, Sanes DH (1996) Developmental influence of glycinergic transmission: regulation of NMDA receptor-mediated EPSPs. J Neurosci 16: 1836-1843.

Kros CJ, Ruppersberg JP, Rusch A (1998) Expression of a potassium current in inner hair cells during development of hearing in mice. Nature 394: 281-284.

Kullmann PH, Kandler K (2001) Glycinergic/GABAergic synapses in the lateral superior olive are excitatory in neonatal C57Bl/6J mice. Brain Res Dev Brain Res 131: 143-147.

Lippe WR (1994) Rhythmic spontaneous activity in the developing avian auditory system. J Neurosci 14: 1486-1495.

Liu L, Wong TP, Pozza MF, Lingenhoehl K, Wang Y, et al. (2004) Role of NMDA receptor subtypes in governing the direction of hippocampal synaptic plasticity. Science 304: 1021-1024.

Liu SQ, Cull-Candy SG (2000) Synaptic activity at calcium-permeable AMPA receptors induces a switch in receptor subtype. Nature 405: 454-458.

Lorteije JA, Rusu SI, Kushmerick C, Borst JG (2009) Reliability and precision of the mouse calyx of Held synapse. J Neurosci 29: 13770-13784.

Malenka RC, Bear MF (2004) LTP and LTD: an embarrassment of riches. Neuron 44: 5-21.

Monyer H, Sprengel R, Schoepfer R, Herb A, Higuchi M, et al. (1992) Heteromeric NMDA receptors: molecular and functional distinction of subtypes. Science 256: 1217-1221.

Monyer H, Burnashev N, Laurie DJ, Sakmann B, Seeburg PH (1994) Developmental and regional expression in the rat brain and functional properties of four NMDA receptors. Neuron 12: 529-540.

Moore MJ, Caspary DM (1983) Strychnine blocks binaural inhibition in lateral superior olivary neurons. J Neurosci 3: 237-242.

Morishita W, Lu W, Smith GB, Nicoll RA, Bear MF, et al. (2007) Activation of NR2B-containing NMDA receptors is not required for NMDA receptor-dependent long-term depression. Neuropharmacology 52: 71-76.

Noh J, Seal RP, Garver JA, Edwards RH, Kandler K (2010) Glutamate co-release at GABA/glycinergic synapses is crucial for the refinement of an inhibitory map. Nat Neurosci 13: 232-238.

Oertel D (1999) The role of timing in the brain stem auditory nuclei of vertebrates. Annu Rev Physiol 61: 497-519.

Oliet SH, Malenka RC, Nicoll RA (1997) Two distinct forms of long-term depression coexist in CA1 hippocampal pyramidal cells. Neuron 18: 969-982.

Philpot BD, Cho KK, Bear MF (2007) Obligatory role of NR2A for metaplasticity in visual cortex. Neuron 53: 495-502.

Prybylowski K, Chang K, Sans N, Kan L, Vicini S, et al. (2005) The synaptic localization of NR2B-containing NMDA receptors is controlled by interactions with PDZ proteins and AP-2. Neuron 47: 845-857.

Saal D, Dong Y, Bonci A, Malenka RC (2003) Drugs of abuse and stress trigger a common synaptic adaptation in dopamine neurons. Neuron 37: 577-582.

Sanes DH, Rubel EW (1988) The ontogeny of inhibition and excitation in the gerbil lateral superior olive. J Neurosci 8: 682-700.

Sanes DH, Takacs C (1993) Activity-dependent refinement of inhibitory connections. Eur J Neurosci 5: 570-574.

Sanes DH, Friauf E (2000) Development and influence of inhibition in the lateral superior olivary nucleus. Hear Res 147: 46-58.

Scimemi A, Tian H, Diamond JS (2009) Neuronal transporters regulate glutamate clearance, NMDA receptor activation, and synaptic plasticity in the hippocampus. J Neurosci 29: 14581-14595.

Sheng M, Cummings J, Roldan LA, Jan YN, Jan LY (1994) Changing subunit composition of heteromeric NMDA receptors during development of rat cortex. Nature 368: 144-147.

Smith PH, Joris PX, Carney LH, Yin TC (1991) Projections of physiologically characterized globular bushy cell axons from the cochlear nucleus of the cat. J Comp Neurol 304: 387-407.

Strack S, Colbran RJ (1998) Autophosphorylation-dependent targeting of calcium/ calmodulin-dependent protein kinase II by the NR2B subunit of the N-methyl- D-aspartate receptor. J Biol Chem 273: 20689-20692.

Tollin DJ (2009) The lateral superior olive: a functional role in sound source localization. Neuroscientist 9: 127-143.

Tovar KR, Westbrook GL (1999) The incorporation of NMDA receptors with a distinct subunit composition at nascent hippocampal synapses in vitro. J Neurosci 19: 4180-4188.

Triplett JW, Owens MT, Yamada J, Lemke G, Cang J, et al. (2009) Retinal input instructs alignment of visual topographic maps. Cell 139: 175-185.

Tritsch NX, Yi E, Gale JE, Glowatzki E, Bergles DE (2007) The origin of spontaneous activity in the developing auditory system. Nature 450: 50-55.

Tritsch NX, Bergles DE (2010) Developmental regulation of spontaneous activity in the Mammalian cochlea. J Neurosci 30: 1539-1550.

Vicini S, Wang JF, Li JH, Zhu WJ, Wang YH, et al. (1998) Functional and pharmacological differences between recombinant N-methyl-D-aspartate receptors. J Neurophysiol 79: 555–566.

Wang LY, Neher E, Taschenberger H (2008) Synaptic vesicles in mature calyx of Held synapses sense higher nanodomain calcium concentrations during action potential-evoked glutamate release. J Neurosci 28: 14450-14458.

Wu SH, Kelly JB (1992) Synaptic pharmacology of the superior olivary complex studied in mouse brain slice. J Neurosci 12: 3084-3097.

Chapter 3

Publication Reference:

Case DT and Gillespie DC (2011) Pre- and postsynaptic properties of glutamatergic transmission in the immature inhibitory MNTB-LSO pathway. *J Neurophysiol* 106(5): 2570-2579.

Abstract

The lateral superior olive (LSO) integrates excitatory inputs driven by sound arriving at the ipsilateral ear with inhibitory inputs driven by sound arriving at the contralateral ear in order to compute interaural intensity differences needed for localizing high-frequency sound sources. Specific mechanisms necessary for developmental refinement of the inhibitory projection, which arises from the medial nucleus of the trapezoid body (MNTB), have only been partially deciphered. The demonstration that immature MNTB-LSO synapses release glutamate has led to a model in which early glutamate neurotransmission plays a major role in inhibitory plasticity. We used whole cell electrophysiology in acute auditory brain stem slices of neonatal rats to examine glutamatergic transmission in the developing MNTB-LSO pathway. Unexpectedly, AMPA receptor (AMPAR)-mediated responses were prevalent at the earliest ages. We found a salient developmental profile for NMDA receptor (NMDAR) activation, described both by the proportion of total glutamate current and by current durations, and we found

evidence for distinct release probabilities for GABA/glycine and glutamate in the MNTB-LSO pathway. The developmental profile of NMDAR is consistent with the possibility that the inhibitory MNTB-LSO pathway experiences a sensitive period, driven by cochlear activity and mediated by GluN2B-containing NMDARs, between postnatal days 3 and 9. Differing neurotransmitter release probabilities could allow the synapse to switch between GABA/glycinergic transmission and mixed glutamate/GABA/glycinergic transmission in response to changing patterns of spiking activity.

3.1 Introduction

The lateral superior olive (LSO) is a binaural nucleus of the auditory brain stem whose primary output neurons, the "principal cells," compute the interaural intensity differences necessary for azimuthal sound localization (Boudreau and Tsuchitani 1968; Caird and Klinke 1983). Principal cells of the tonotopically organized LSO integrate excitatory and inhibitory inputs that are themselves precisely tonotopically matched (Kandler 2004; Kotak and Sanes 1996; Sanes and Rubel 1988). The ipsilateral anteroventral cochlear nucleus (AVCN) provides the primary excitatory, glutamatergic, input (Cant and Casseday 1986; Wu and Kelly 1992), whereas the contralateral cochlear nucleus excites principal neurons of the sign-inverting medial nucleus of the trapezoid body (MNTB), which provides the primary inhibitory, glycinergic, input to the LSO (Bledsoe et al. 1990; Caspary and Finlayson 1991; Moore and Caspary 1983; Smith et al. 1991). As tonotopic precision of excitatory and inhibitory inputs to the LSO is achieved in the first few

postnatal weeks in rats, the developing LSO offers a model system for understanding both how inhibitory maps are organized during development and how inhibitory and excitatory inputs are brought into register onto a shared postsynaptic target.

The immature MNTB-LSO pathway exhibits activity-dependent synaptic plasticity in vitro (Chang et al. 2003; Kotak et al. 2001; Kotak and Sanes 2002), and major functional refinement that occurs before hearing onset in rats (Kim and Kandler 2003) is likely directed by patterned, spontaneous activity from the cochlea (Beutner and Moser 2001; Kros et al. 1998; Tritsch et al. 2007; Tritsch and Bergles 2010). During this period of refinement, GABA and glycine are coreleased at MNTB-LSO synapses (Korada and Schwartz 1999; Kotak et al. 1998; Nabekura et al. 2004), GABA and glycine exert depolarizing effects at principal neurons in the LSO (Ehrlich et al. 1999; Kakazu et al. 1999; Kandler and Friauf 1995), and immature MNTB terminals release glutamate onto LSO principal cells (Gillespie et al. 2005). The discovery that glutamate is released during a period characterized both by developmental refinement and by depolarizing GABA/glycine led to the hypothesis that the NMDA glutamate receptor subtype (NMDAR) might mediate developmental refinement in the inhibitory MNTB-LSO pathway. Under this hypothesis, release of depolarizing GABA/glycine can relieve Mg^{2+} block of NMDARs, allowing coreleased glutamate to activate NMDARs; influx of Ca^{2+} through open NMDARs would then provide the immature MNTB-LSO synapse access to a wide array of NMDAR-mediated mechanisms of plasticity (for review, see Malenka and Bear 2004). Consistent with this hypothesis, mice lacking glutamate release in the MNTB-LSO pathway exhibit perturbed developmental refinement in the LSO (Noh et al.

2010). Although NMDAR-dependent plasticity has yet to be demonstrated in this pathway, NMDARs have been shown to mediate plasticity at other inhibitory synapses where the glutamate source is still unknown (Gaiarsa et al. 2002; Marsden et al. 2007; McLean et al. 1996; Ouardouz and Sastry 2000; Wang et al. 2003).

In light of the hypothesized role for NMDARs in the developing inhibitory MNTB-LSO pathway, and in order to better understand the range of responses available to synaptic plasticity mechanisms, we examined glutamatergic transmission at immature MNTB-LSO synapses. Our results suggest that MNTB-LSO synapses may be able to switch between primarily GABA/glycinergic and mixed glutamate/GABA/glycinergic transmission, and that postsynaptic expression of GluN2B-containing NMDARs in part defines a discrete temporal window corresponding to the period of major circuit refinement.

3.2 Materials and Methods

All procedures adhered to Canadian Council on Animal Care guidelines and were approved by the Animal Research Ethics Board of McMaster University. Sprague-Dawley rats (Charles River Laboratories) aged postnatal days 0 to 12 (P0–12) were anesthetized with isoflurane and quickly decapitated, and the brains were removed into ice-cold artificial cerebrospinal fluid (ACSF, pH 7.2) containing (in mM) 125 NaCl, 1 K_2SO_4, 5 KCl, 1.25 KH_2PO_4, 10 dextrose, 26 $NaHCO_3$, 2 $CaCl_2 \cdot 2H_2O$, and 1 kynurenic acid. The

brain stem was cut at 300 μm (Vibratome 3000 Series), and slices containing the MNTB and LSO were transferred to a humidified chamber, where they were allowed to recover for at least 45 min.

For recording, slices were transferred to a recording chamber at an upright microscope. Slices were kept at room temperature and were constantly perfused with ACSF superfused with 95% O_2-5% CO_2. Kynurenic acid was not added to ACSF used in recordings. All of the ifenprodil pharmacology experiments, and ~60% of the developmental profiling experiments, were performed in Mg-free ACSF. To reduce noise through NMDARs, ~40% of the developmental recordings were performed in Mg-containing ACSF; no differences were seen between measurements obtained in Mg-free and Mg-containing ACSF. For experiments performed in Mg-containing ACSF, K_2SO_4 was replaced with $MgSO_4$ (1.3 mM). For experiments performed in Mg-containing ACSF, the internal solution contained 5 mM QX-314 (Ascent Scientific) and control (no drug treatment) recordings were taken at −60 mV and +40 mV. After $GABA_A$ ($GABA_A$Rs) and glycine (GlyRs) receptors were blocked pharmacologically, recordings were taken at −60 mV to observe AMPA receptor (AMPAR)-mediated currents and at +40 mV to observe NMDAR-mediated currents. Peak amplitudes have been converted to conductances, and charge transfers have been corrected to allow for differences in driving force [i.e., current normalized $I_{+40mV} \times (df_{-60mV}/df_{+40mV})$ before charge integrated].

Stimulating electrodes, 1- to 2-MΩ glass pipettes filled with ACSF, were placed in the MNTB or in the fiber tract at the lateral edge of the MNTB, and stimuli were delivered

via Grass S88 with SIU or Master 8 with Iso-Flex. For whole cell recording, cells in the higher-frequency (medial and middle) limbs of the LSO were targeted by using DIC-IR to identify principal cells based on their bipolar morphology and their orientation relative to the mediolateral axis of the nucleus. Cells were targeted in the medial and middle limbs where developmental refinement is best understood; the lateral limb contains cells with different response characteristics and protein expression (Friauf 1993). For all cells examined, a GABA/glycinergic response to MNTB stimulation was recorded before application of the $GABA_AR$ and GlyR antagonists picrotoxin and strychnine. Recordings were made at room temperature (20°C), and for any recording in which the onset of the glutamate component lagged the GABA/glycine component by ≥2 ms, the glutamate response was considered to result from a separate input and the glutamate recording was excluded from analysis. Electrodes for whole cell voltage clamp (8250 borosilicate glass, AM Systems) had resistances of 3–6 MΩ and were filled with a Cs-gluconate solution (pH 7.2) containing (in mM) 64 d-gluconic acid, 64 CsOH, 11 EGTA, 56 CsCl, 1 $MgCl_2 \cdot 6H_2O$, 1 $CaCl_2$, 10 HEPES, 0.3 GTP-Na, and 4 ATP-$Mg \cdot 3.5H_2O$. In most cases, the internal solution also contained 0.5% biocytin for subsequent histological verification of cell type. Some neurons were also recorded with K-gluconate internal solution (in mM: 100 K-gluconate, 20 KCl, 10 Na_2-phosphocreatine, 10 HEPES, 0.3 GTP-Na, 4 ATP-$Mg \cdot 3.5H_2O$, pH 7.3) to avoid blocking K^+ channels possibly involved in metabotropic glutamate receptor (mGluR) responses. Recordings (Axopatch 200B amplifier, pCLAMP 9.2; Molecular Devices) were sampled at 10 kHz, filtered at 5 kHz, and saved for off-line analysis with custom Matlab software. Recordings were compensated by a minimum of

80% with <10-μs lag and were discarded if series resistance changed by >15% from its initial value. Electrical stimulation intensity was set near a minimum intensity that reliably yielded responses.

Strychnine (Sigma) and picrotoxin (Tocris) were added to the ACSF perfusate to block GlyRs and $GABA_A$Rs; D-2-amino-5-phosphovaleric acid (D-APV) (Ascent Scientific, Tocris) and CNQX (Tocris) were added to block NMDARs and AMPARs. Charge transfer measurements were taken after any necessary corrections for driving force. The selective GluN2B-containing NMDAR antagonist ifenprodil (Ascent) was used to evaluate NMDAR subunit composition across age. The presence of GluA2-lacking AMPARs was assessed both by rectification and by application of the selective GluA2-lacking AMPAR antagonist IEM 1460 (Tocris). For AMPAR rectification recordings the internal solution contained 0.1 mM spermine (Acros Organics). In release probability experiments cyclothiazide (Ascent) was included in the perfusate to prevent AMPAR desensitization. Drug concentrations used in the perfusate were (in μM) 10 strychnine, 50 picrotoxin, 50 D-APV, 5 CNQX, 3–100 ifenprodil, 100 IEM 1460, and 100 cyclothiazide.

Rectification of AMPARs was assessed by taking recordings at −60 mV, −40 mV, +40 mV. and +60 mV. The rectification index is defined here as RI = $(I_{+40mV}/V_{+40\text{-}Vrev})/(I_{\text{-}60mV}/V_{\text{-}60\text{-}Vrev})$. Average reversal potential for AMPARs was 7 mV. Probability of release was examined by delivering 10 pulses of electrical stimulation at 20 or 50 Hz. Peak current amplitudes resulting from the second to tenth pulses were divided by the peak current amplitude resulting from the first pulse (I_n/I_i) to determine paired-pulse ratios

(PPRs); peak current was measured relative to current immediately before the stimulus for each pulse.

3.3 Results

We used whole cell voltage clamp in acute brain stem slices of neonatal rat pups to characterize the glutamatergic response to MNTB stimulation at immature LSO principal neurons receiving GABA/glycine- and glutamate-releasing inputs. Because strychnine washout is nearly impossible to achieve, we recorded from a single cell per slice (e.g., Fig. 1*A*), to ensure that all cells analyzed for a glutamatergic response received dual inputs. As shown in Fig. 1, *A* and *B*, after block of $GABA_A$Rs, glyRs, and NMDARs many of the residual, unfiltered, AMPAR-mediated currents were small relative to baseline. These residual components were classified as AMPAR components if *1*) the current amplitude was ≥3 standard deviations above background noise, *2*) the current decay time constant was on the order of microseconds (not 10s or 100s of ms), and *3*) the current disappeared after application of the AMPAR antagonist CNQX (Fig. 1*B*). Recording from 113 cells (P0–P12), we found, consistent with previous results (Gillespie et al. 2005), that glutamatergic responses declined after the first postnatal week (Fig. 1*C*) and that the glutamatergic component lagged the GABA/glycinergic component [onset latencies, in ms, for GABA/gly: P0–P4: 2.5 ± 0.1 (n = 50), P5–P8: 2.3 ± 0.1 (n = 46), P9–P12: 2.7 ± 0.1 (n = 15); for glu: P0–P4: 3.4 ± 0.1, P5–P8: 3.2 ± 0.1, P9–P12: 3.6 ± 0.1; mean % difference in onset latency calculated from these means is within 5% of mean of

individual cell % differences, for each age]. To ask whether we might in some of these experiments have stimulated (hypothetical) glutamatergic fibers of passage rather than fibers from GABA/glycinergic MNTB neurons, in an additional six cells (P3–P7) we puffed glutamate directly in the MNTB while recording from an LSO principal cell. In all (5/5) slices aged P3–P5 an NMDAR-mediated component could be clearly observed before the addition of strychnine/picrotoxin (Fig. 1*D*), and in all cases onset latency for the glutamate component lagged that for the GABA/glycine component.

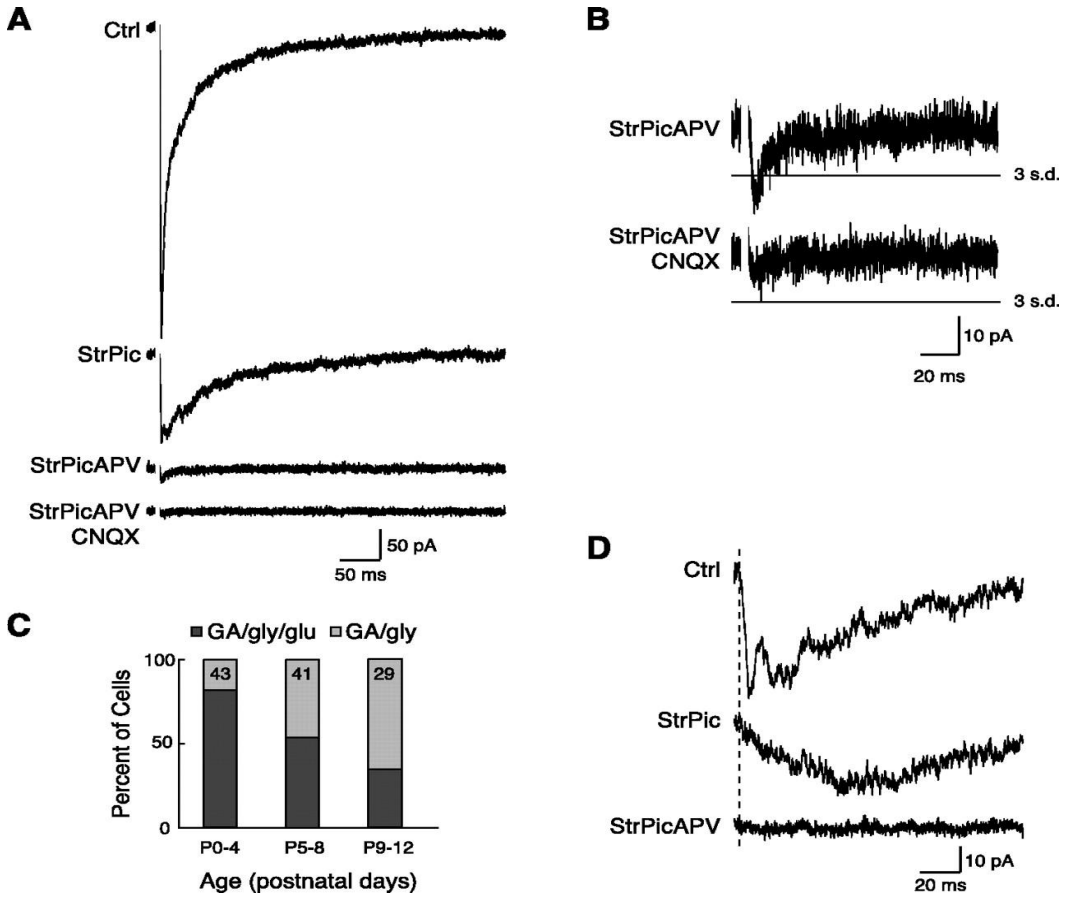

Fig 1. Glutamate responses to medial nucleus of the trapezoid body (MNTB) stimulation recorded in lateral superior olive (LSO) principal neurons. **A**: example traces from an LSO principal neuron exhibiting a mixed GABA/glycine/glutamate response [postnatal day (P)5 slice, Mg^{2+}-free solution, −60 mV]. Traces are averages of 10 responses. Str, strychnine; Pic, picrotoxin; APV, 2-amino-5-phosphonovaleric acid. **B**: AMPA receptor (AMPAR) response from *A*, larger view. Residual responses after addition of strychnine, picrotoxin, and APV were classified as AMPAR responses if the peak amplitude was at least 3 standard deviations (s.d.) greater than mean background noise and the response disappeared when CNQX (5 μM) was added to the perfusate. **C**: distribution of

GABA/glycine (GA/gly) and/or glutamate (glu) responses to MNTB stimulation for cells recorded at different ages between P0 and P12. Note that not all cells analyzed in this study are included in *C*, as in later experiments cell selection was biased toward cells with glutamatergic or NMDAergic components. **D**: example cell (P5) showing response to glutamate puffed directly in MNTB with no drug (Ctrl, *top*), after application of strychnine and picrotoxin (*middle*), and after the additional application of APV (*bottom*). Onset latency for the glutamate component lagged the GABA/glycine component by 0.6 ms.

NMDA receptors are the main contributors to MNTB-elicited glutamatergic responses in LSO neurons.

The proposed role of glutamate release in inhibitory synaptic refinement assumes that postsynaptic NMDARs are present at MNTB-LSO synapses during the period of refinement, and so we first asked what proportion of cells exhibited NMDAR and/or AMPAR components. Figure 2*A* shows receptor subtypes for 67 cells that exhibited glutamatergic responses to MNTB-LSO stimulation, and in which the NMDA and AMPA components could be clearly separated. Surprisingly, in nearly one-third (7 of 22) of cells recorded before P3 the glutamatergic response was mediated solely by AMPARs. By contrast, from P3 onward every glutamatergic response exhibited an NMDAR-mediated component. After P3, not only were the NMDAR-mediated responses more numerous than the AMPAR-mediated responses but they were also larger in magnitude, such that NMDARs contributed on average over half the peak conductance of the glutamatergic responses (Fig. 2*B*). The proportional magnitude of the NMDAR component was noticeably largest between P3 and P9, with the estimated mean contribution larger than 75% at each age tested during this period (see Table 1; Kruskal-Wallis test for NMDA current contribution, $P = 0.0124$; post hoc Mann-Whitney P1 vs. P3, $P = 0.0129$; post hoc Mann-Whitney P9 vs. P10, $P = 0.0047$).

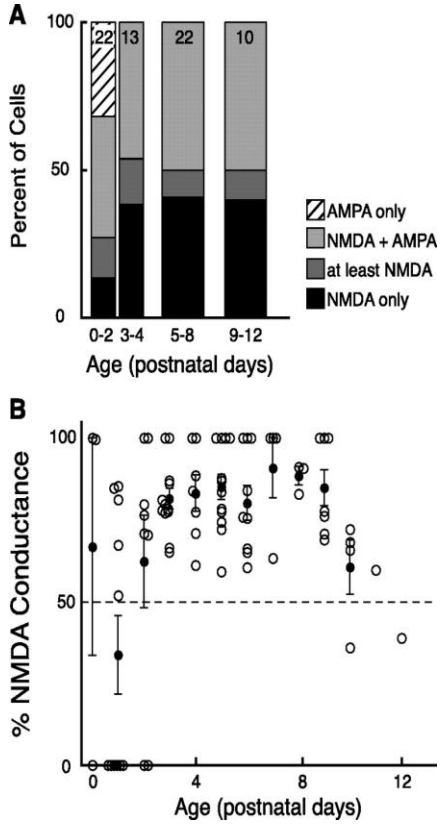

Fig. 2. NMDA receptor (NMDAR)-mediated responses are most prevalent between P3 and P9. **A**: no. of cells showing AMPAR- and/or NMDAR-mediated glutamate responses for ages P0–P12. Before P3, nearly ⅓ of cells exhibited a glutamate response that was mediated solely by AMPARs. From P3 onward, all glutamatergic responses contained an NMDAR-mediated component. "At least NMDA" category includes cells that were found to have an NMDAR-mediated component but for which we could not with confidence assess AMPAR contribution (e.g., because of changes in recording parameters, etc.) **B**: conductance mediated by NMDARs was normalized to the total glutamatergic conductance. Between P3 and P9, >50% of glutamatergic conductance was provided by NMDARs. Open circles represent individual cells; filled circles represent average values for each age. Error bars show SE.

Table 1. Properties of NMDAR-mediated neurotransmission as a function of age

Age	% NMDA Conductance	NMDA Charge Transfer, pC	NMDA CT/Peak, ms
P0	67 ± 33 (3)	28.3 ± 1.0 (2)	1,330.0 ± 215.7 (2)
P1	34 ± 12 (11)	59.2 ± 20.4 (5)	1,355.4 ± 251.0 (5)
P2	62 ± 14 (8)	78.6 ± 14.1 (8)	1,437.4 ± 167.3 (8)
P3	81 ± 3 (12)	193.4 ± 34.9 (13)	1,637.8 ± 112.3 (13)
P4	83 ± 5 (7)	106.9 ± 18.2 (12)	1,603.2 ± 196.0 (12)
P5	85 ± 4 (12)	83.9 ± 16.7 (15)	1,063.2 ± 109.5 (15)
P6	81 ± 5 (9)	150.5 ± 38.4 (12)	1,512.9 ± 139.2 (12)
P7	91 ± 9 (4)	132.5 ± 72.7 (5)	960.7 ± 227.5 (5)
P8	88 ± 3 (3)	244.3 ± 107.1 (5)	1,382.6 ± 133.5 (5)
P9	85 ± 5 (7)	16.6 ± 8.2 (6)	529.0 ± 120.8 (6)
P10–P12	57 ± 6 (6)	18.1 ± 7.4 (4)	464.9 ± 76.1 (4)

Values are means ± SE for % NMDA receptor (NMDAR) conductance [calculated as $g_{NMDA}/(g_{AMPA} + g_{NMDA})$], NMDAR charge transfer (CT), and NMDAR charge transfer normalized to peak (NMDA CT/Peak) as a function of age before hearing onset. Number of values for each measurement are in parentheses. P, postnatal day.

Postsynaptic glutamate receptors activated by glutamate release at MNTB-LSO synapses are ionotropic; AMPARs contain GluA2.

The substantial subset of glutamatergic responses mediated solely by AMPARs appears to run counter to the hypothesis that NMDARs mediate plasticity at MNTB-LSO synapses before hearing onset. However, Ca^{2+}-permeable GluA2-lacking AMPARs (CP-AMPARs) have also been implicated in synaptic plasticity (for review, see Cull-Candy et al. 2006), and so we asked whether CP-AMPARs could have mediated the AMPAR responses observed at MNTB-LSO synapses. For 17 slices, we added spermine to the intracellular solution, isolated the AMPAR-mediated response pharmacologically, and examined the AMPAR responses for the inward rectification characteristic of CP-AMPARs (Fig. 3*A*; Burnashev et al. 1992; Muller et al. 1992). We found neither evidence for significant rectification nor a change in rectification indices between early and later ages (Fig. 3*B*; mean RI = 1.02 ± 0.09, n = 18). To further test for the presence of CP-AMPARs, we isolated AMPAR-mediated responses pharmacologically and applied IEM 1460, an antagonist of GluA2-lacking (and hence calcium permeable) AMPARs. No effect of IEM 1460 was observed (Fig. 3*C*; mean residual current = 101.9 ± 6.7%, n = 14). These findings are consistent with the absence of CP-AMPARs at MNTB-LSO synapses in the first postnatal week.

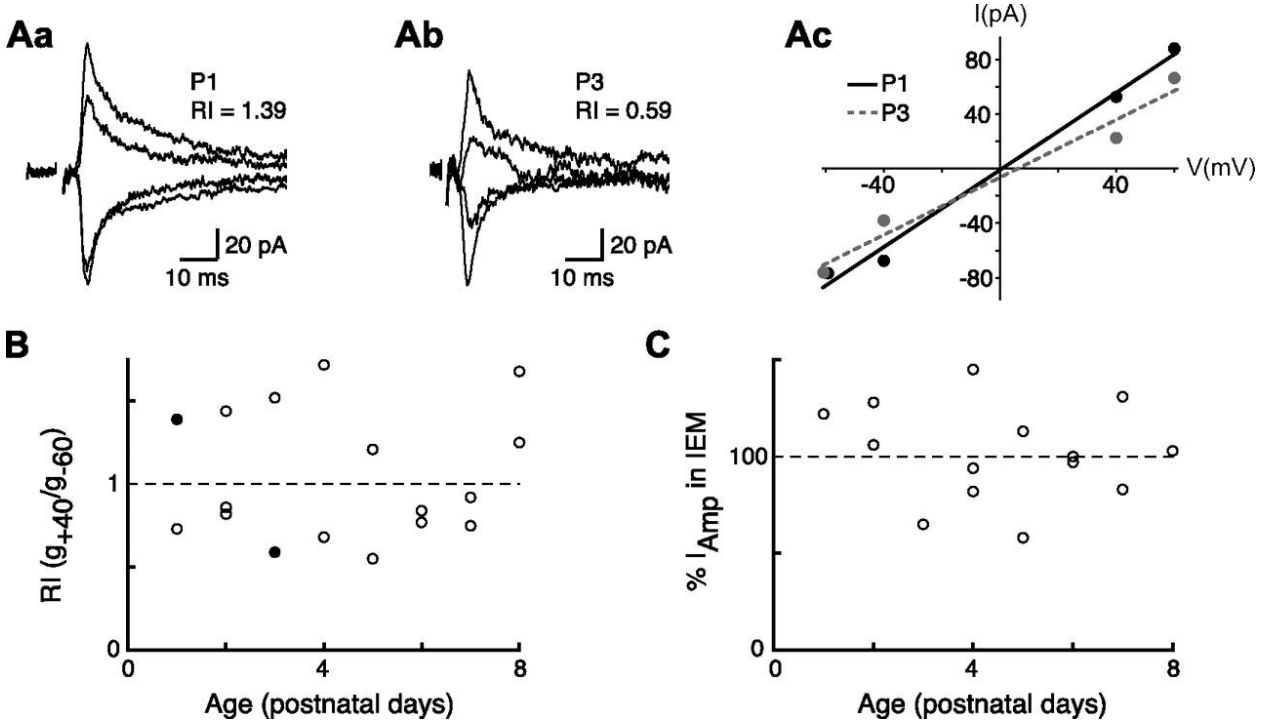

Fig. 3. Glutamate released at MNTB-LSO synapses does not activate Ca^{2+}-permeable AMPARs. **A**: example rectification measurements for 2 cells with relatively extreme rectification index (RI) measurements, showing raw traces for high (*Aa*, P1 cell) and low (*Ab*, P3 cell) RIs and summary measurements with linear fits (*Ac*). Note that although the P3 cell had an RI value below 1.0, significant current was passed at positive membrane potentials. **B**: RIs are distributed around 1 between P1 and P8; $n = 17$. Filled circles correspond to the traces shown in *Aa* and *Ab*. g_{+40}, g_{-60}, conductance at +40 mV and −60 mV. **C**: no consistent change was seen in peak AMPAR current (I_{Amp}) after application of IEM 1460 ($n = 13$).

mGluRs can also mediate synaptic plasticity (Laezza et al. 1999), and high-frequency (100 Hz) stimulation of the glutamatergic AVCN-LSO synapses has been shown to activate mGluRs in immature LSO principal neurons in mouse (Ene et al. 2003). At no point in this study, using single pulses to stimulate in the MNTB, did we see evidence for mGluR-mediated currents (e.g., Fig. 1*A*). To further test for activation of mGluRs at or near MNTB-LSO synapses, we delivered high-frequency stimulation to the MNTB in the presence of antagonists for $GABA_A$Rs, glyRs, AMPARs, and NMDARs. In all LSO cells examined (ages P0–P12, $n = 15$), high-frequency pulse trains to the MNTB (10 pulses at 100 Hz) failed to elicit current responses, and in three slices subjected to higher-frequency (500 Hz) stimulation, LSO principal cells also failed to exhibit mGluR-mediated responses (data not shown). Recording from three additional cells using K-gluconate internal solution, we also failed to observe mGluR-mediated postsynaptic currents (PSCs). We conclude that mGluRs in immature LSO principal neurons of rat do not occupy the membrane postsynaptic to MNTB inputs.

To further investigate the non-NMDAR-mediated glutamatergic response we asked whether there was any relationship between amplitude of the AMPAR response and maturation of the inhibitory pathway. AMPAR currents were larger, relative to GABA/glycine currents, at earlier ages than at later ages (Fig. 4*A*). Peak GABA/glycine current increased between P0 and P8 (Fig. 4*B*), as has been previously reported (Kim and Kandler 2003). The decline in AMPAR amplitude relative to GABA/glycine receptor amplitude during the first postnatal week resulted largely from this maturational

strengthening of the GABA/glycine inputs, while AMPAR responses remained small (Fig. 4*C*).

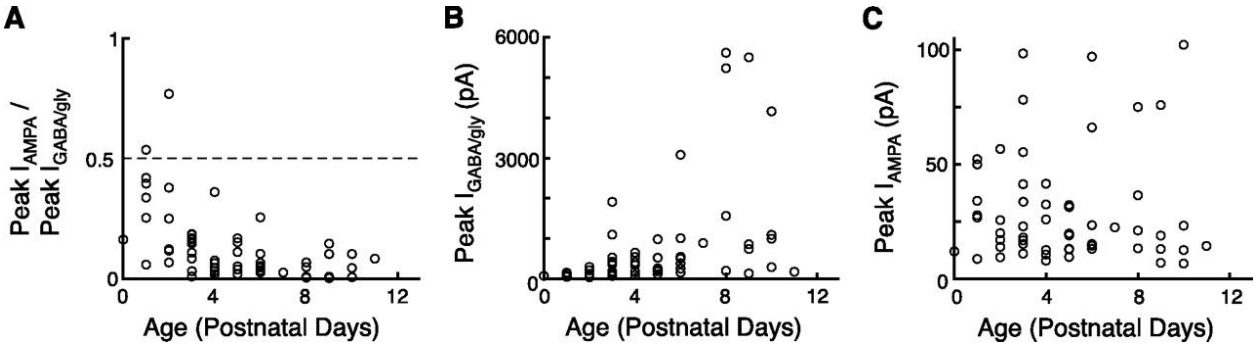

Fig. 4. AMPAR-mediated responses to MNTB stimulation P0–P12. For cells in which an AMPAR component was measured AMPAR-mediated peak current (I_{AMP}) is larger, relative to GABA/glycine peak current ($I_{GABA/gly}$), at the earliest ages than at later ages (**A**); GABA/glycine receptor-mediated currents increase between P0 and P8 (**B**); and AMPAR-mediated currents change little in peak amplitude over the first 2 postnatal weeks (**C**). For clarity, 2 outlying points at P8 (5,615 and 5,235 pA) are not included in *B*.

Changes in NMDAR current duration define a window between P2/3 and P8/9.

The specific subunit composition of NMDARs may influence the plasticity available to a synapse (Liu et al. 2004), and in many areas NMDAR subtype composition changes across development (Monyer et al. 1994; Sheng et al. 1994). We therefore attempted to ascertain whether NMDAR subunit composition at MNTB-LSO synapses changes before hearing onset. In 87 cells, we isolated NMDAR-mediated responses pharmacologically and then assessed charge transfer and used subunit-specific pharmacology to look for evidence of a change in subunit composition. As seen in representative traces (Fig. 5*A*), average charge transfer for the NMDAR current increased over the first few days and dropped sharply at P9 (Fig. 5*B*), recalling the pattern observed for the relative proportion of total glutamatergic current carried by NMDAR (Fig. 2*B*) (see Table 1; Kruskal-Wallis, $P = 2.2 \times 10^{-4}$; post hoc Mann-Whitney P2 vs. P3, $P = 0.0125$; post hoc Mann-Whitney P8 vs. P9, $P = 0.0043$). Additionally, when charge transfer was normalized to peak response to estimate relative NMDAR excitatory PSC (EPSC) duration, a sharp drop was observed between P8 and P9 (Fig. 5*C*) (see Table 1; Kruskal-Wallis, $P = 1.9 \times 10^{-4}$, post hoc Mann-Whitney P8 vs. P9, $P = 0.0087$). These findings are consistent with a change in NMDAR subunit composition, in addition to the decline in NMDAR activation, around P8/9.

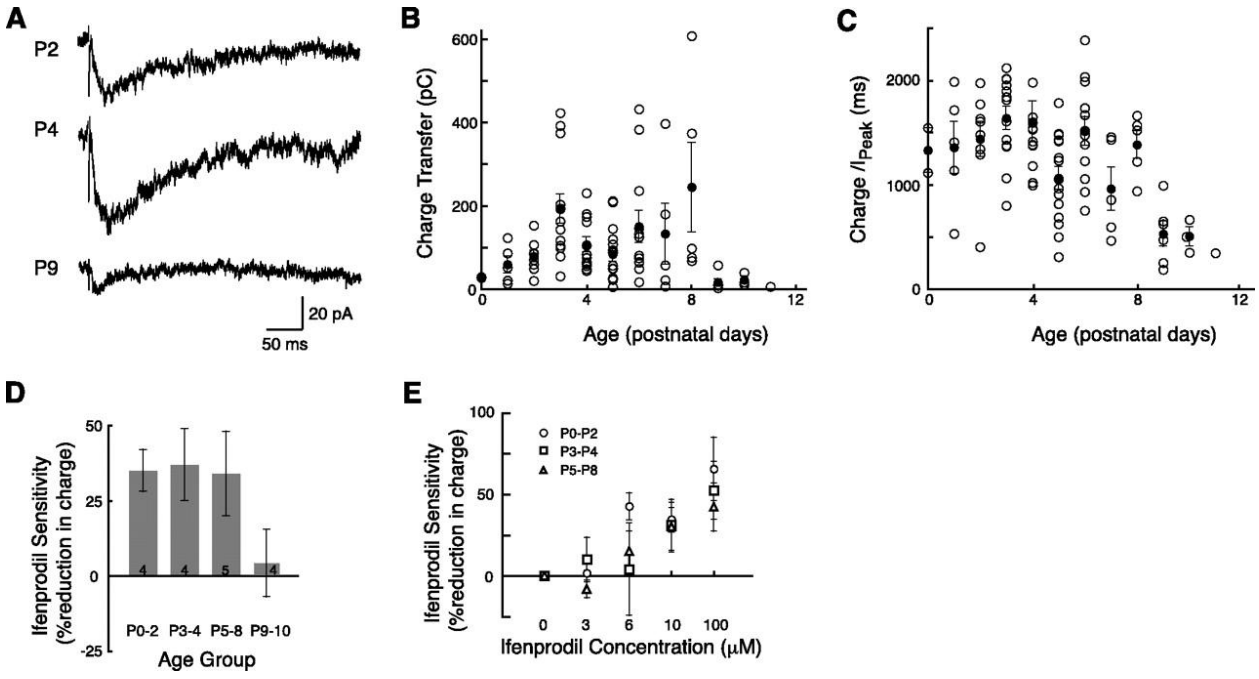

Fig. 5. Elevated NMDAR signaling between P3 and P9 is mediated by GluN2B-containing NMDARs. **A**: example NMDAR-mediated currents at P2, P4, and P9. By P9, peak current amplitude is smaller and decay kinetics are faster than at P2 or P4. **B**: NMDAR-mediated charge transfer before hearing onset. Each open circle represents a single cell; filled circles are means ± SE. Charge transfer for pharmacologically isolated NMDAR-mediated current increases by P3 and drops at P9. **C**: NMDAR-mediated charge transfer normalized to peak current amplitude (I_{Peak}) is relatively high and stable between P0 and P8 and then decreases from P9 onward. **D**: ifenprodil (10 μM) significantly reduces NMDAR-mediated charge transfer in cells from P0–P8 slices but has little effect on cells from older slices (P9/10). **E**: ifenprodil dose-response curves for NMDAR-mediated currents are similar in cells from all ages between P0 and P8. P0–P2, n = 4; P3–P4, n = 3; P5–P8, n = 4.

In many systems, a decrease in NMDAR EPSC duration is caused by a developmental switch from expression of GluN2B- to GluN2A-containing NMDARs. To ascertain whether GluN2B-enriched postsynaptic membranes might account for the longer NMDAR EPSCs seen in the first postnatal week, in slices aged P0–P10 we tested an additional 17 cells for sensitivity to ifenprodil (10 μM), an antagonist that preferentially blocks NMDARs containing the GluN2B subunit. In all cells tested from P0 to P8, addition of ifenprodil to the perfusate caused a reduction in charge transfer (Fig. 5*D*) and in peak current amplitude (data not shown), whereas at P9–P10 ifenprodil had little effect [% reduction: P0–P2, 35 ± 7 (n = 4); P3–P4, 37 ± 12 (n = 4); P5–P8, 34 ± 14 (n = 5); P9–P10, 4 ± 11 (n = 4); 1-way ANOVA, P = 0.1952]. Dose-response curves for ifenprodil were also similar for all ages between P0 and P8 (Fig. 5*E*). In four additional slices from animals <8 days old, the selective GluN2B antagonist Ro25-6981 (3 μM) was added; Ro25-6981 reduced peak current and charge transfer by 34% and 38% (data not shown). These results are consistent with the expression of GluN2B-containing NMDARs at MNTB-LSO synapses in the first postnatal week, and they suggest that the large charge transfer seen in the first postnatal week results from the relatively long decay kinetics conferred by the GluN2B subunit. Finally, we asked whether the size of the NMDAR-mediated response was related to the size of the GABA/glycine response. For these experiments, as in all others, the minimum stimulus intensity that reliably elicited a response was first determined, and this stimulus intensity was then used throughout the experiment in order to ensure that the same single fiber (or small subset of fibers) was stimulated when evaluating both GABA/glycine receptor and the NMDAR-mediated

responses. Neither peak NMDAR current (to reflect total NMDAR contribution; Fig. 6*A*) nor charge transfer (to reflect GluN2B subunit contribution; Fig. 6*B*) was significantly correlated with the size of the initial GABA/glycine response (NMDA I_{peak} vs. GABA/gly I_{peak}: Pearson's $R = 0.30$; NMDA charge transfer vs. GABA/gly I_{peak}: Pearson's $R = 0.26$). Thus, although NMDARs passed substantial charge during the first postnatal week, degree of NMDAR activation was correlated not with strength of GABA/glycine synapses but with postnatal age (Fig. 6*C*).

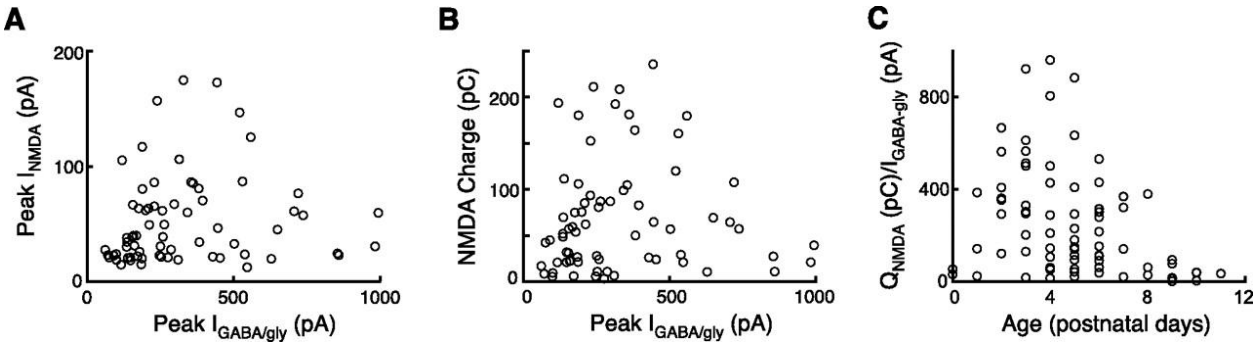

Fig. 6. Peak NMDAR-mediated current and charge transfer as a function of peak GABA/glycine current. **A** and **B**: neither NMDAR-mediated peak current (I_{NMDA}, *A*) nor charge transfer (*B*) correlates strongly with the size of GABA/glycinergic inputs. **C**: NMDAR-mediated charge transfer (Q_{NMDA}) is high relative to GABA/glycine receptor-mediated peak current between P2 and P6. For clarity, extreme outliers have been omitted from *A* (NMDA pA vs. GABA/gly pA: 287 × 424, 122 × 1,584, 32 × 1,910, 363 × 2,802, 52 × 3,280, 96 × 5,615), *B* (NMDA pC vs. GABA/gly pA: 392 × 424, 98 × 1,584, 34 × 1,911, 432 × 2,802, 48 × 3,280, 160 × 5,615), and *C* (1,635 at P3).

Release probabilities differ for GABA/glycine and for glutamate.

An open question surrounding cotransmission of GABA/glycine and glutamate has been whether the two neurotransmitters are released together or whether they could be released independently of one another. To examine this question, we measured release probabilities for GABA/glycine and for glutamate in the same cell by recording responses to 20- and 50-Hz stimulus trains delivered to the MNTB (Fig. 7*A*). To avoid artifact due to possible incomplete washoff of AMPAR antagonists, GABA/glycinergic responses were measured first without any pharmacological antagonists in the perfusate. Strychnine, picrotoxin, and APV were then applied to isolate AMPAR-mediated currents, and pulse trains were delivered again to determine the release probability for glutamate. Release probabilities for both GABA/glycine and glutamate remained fairly stable during the first postnatal week (Fig. 7, *B*–*E*), but at all ages paired-pulse depression was greater for GABA/glycinergic transmission than for glutamatergic transmission (Fig. 7, *B*–*E*), consistent with the release of glutamate and GABA/glycine from distinct vesicle populations. As activation of presynaptic receptors can modulate release, and to control for the possibility that Ca^{2+} entry into the postsynaptic cell might have affected GABA/glycine currents, we recorded from an additional three cells in the presence of the $GABA_B$ receptor antagonist CGP 52432 (10 μM) and the NMDAR antagonist D-APV (50 μM) throughout. Although the PPRs increased slightly (GABA/gly: ~10% at 20 Hz, <1% at 50 Hz; glu: ~5% at 20 and 50 Hz), GABA/glycine and glutamate still exhibited distinctly different release probabilities (data not shown).

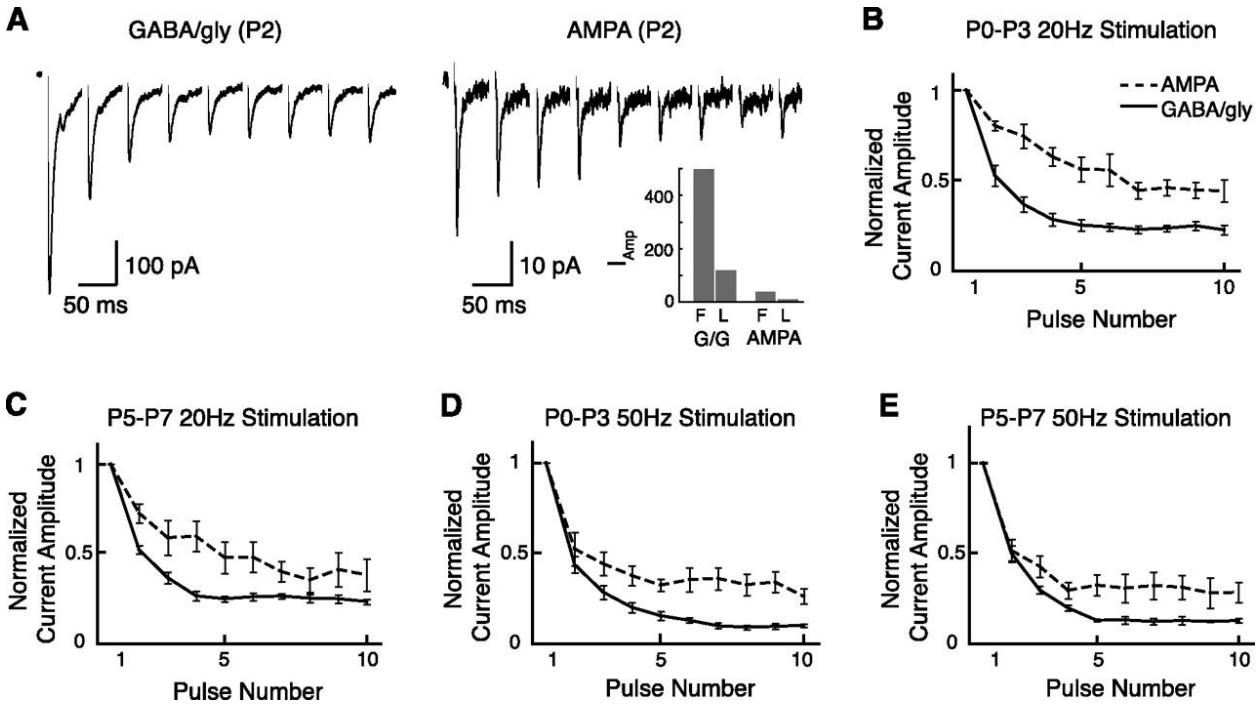

Fig. 7. Glutamate release probability differs from GABA/glycine release probability at MNTB-LSO synapses. **A**: representative LSO response to 10-pulse trains delivered to the MNTB at 20 Hz (P2 slice). $GABA_AR$/glyR-mediated responses are shown on *left* and strychnine/picrotoxin/APV-isolated AMPAR-mediated responses for the same cell on *right. Inset*: absolute current amplitude of the first (F) and last (L) pulses for the GABA/glycine receptor-mediated (G/G) and AMPAR-mediated (AMPA) responses. **B–E**: average pulse train responses for P0–P3 (*B* and *D*) and P5–P7 (*C* and *E*) cells stimulated at 20 Hz (*B* and *C*) or 50 Hz (*D* and *E*); 6 cells/age group. Current amplitudes are normalized to average first peak amplitude. At all ages and at both 20 and 50 Hz, release probability for GABA/glycine is higher than that for glutamate.

3.4 Discussion

Here we have examined glutamatergic neurotransmission at a glutamate-releasing immature inhibitory synapse. We find that NMDARs are the major contributors to glutamatergic responses at immature MNTB-LSO synapses and that activation of GluN2B-containing NMDARs defines a temporal period whose closure correlates with the known decline in major functional refinement in this pathway. Functional refinement of the MNTB-LSO pathway, characterized by a decrease in input area and an increase in strength of individual inputs, is thought to be driven by spontaneous activity generated in the cochlea and is complete in rats by about P9 (Kandler 2004; Kim and Kandler 2003; Tritsch et al. 2007; Tritsch and Bergles 2010). Although recent evidence suggests that glutamate release is necessary for normal functional refinement in this pathway (Noh et al. 2010), glutamate receptors can play many roles in synaptic plasticity at inhibitory and excitatory synapses; these results identify specific receptors and timepoints that may be especially revealing for further studies of refinement in the MNTB-LSO circuit.

AMPA receptors in the MNTB-LSO pathway.

In contrast to the trend from NMDAR-containing "silent synapses" to AMPAR-containing synapses elsewhere (Isaac et al. 1997; Liao et al. 1995), about one-third of MNTB-LSO synapses before P2–P3 lacked NMDARs and were enriched for AMPARs. If Ca^{2+} influx is important for MNTB-LSO refinement, why would much of the early

glutamatergic current be carried by AMPARs? The Ca^{2+}-permeable GluA2-lacking AMPARs that have been implicated in synaptic plasticity elsewhere (Lei and McBain 2002; Mahanty and Sah 1998) appear to be absent from this synapse. In fact, Ca^{2+} influx may not be needed until about P3, after which the mean MNTB input area declines steeply (Kim and Kandler 2003) and NMDARs reliably mediate most of the glutamatergic response.

Do AMPARs play a role in the MNTB-LSO pathway? Possibly, the small AMPAR currents we observed reflect an immature system in which AMPARs destined for AVCN-LSO synapses are inappropriately inserted near MNTB terminals. A scenario in which AMPAR activation unblocks NMDARs very locally as the chloride reversal potential becomes more negative with age is unlikely both because of the typically small size of the AMPAR responses and because these responses were most numerous at ages when GABA and glycine are frankly excitatory (Ehrlich et al. 1999; Kandler and Friauf 1995; Kullmann and Kandler 2001). We suggest that AMPAR-mediated responses reflect glutamate spillover to receptors under AVCN synapses and that this spillover declines with the maturation of functional diffusion barriers. Such spillover would also likely activate extrasynaptic NMDARs, a possibility corroborated by the longer glutamate latencies and by the prominent early GluN2B component in the NMDAR-mediated response (Rumbaugh and Vicini 1999).

NMDA receptors in the MNTB-LSO pathway.

Fractional contribution of NMDARs to peak glutamatergic current defined a temporal window in the MNTB-LSO pathway: NMDAR-mediated currents were seen in most of the glutamatergic responses recorded here and, notably, were present in 100% of glutamatergic responses recorded after P2. The absence of NMDAR-mediated currents in some of the responses before P3 and the increased contribution of NMDARs to peak current suggest a developmental change in NMDAR expression or insertion in the MNTB-LSO pathway. In fact, the increased fractional contribution through NMDARs at P2/3 defined the onset of a temporal window from about P3 to about P9. Although the onset of this window at P3 was not previously predicted, the closure of the window at P9 matched the end of the period of functional refinement in the MNTB-LSO pathway, as would be expected if specific NMDARs mediate developmental plasticity at MNTB-LSO synapses and if these NMDARs are expressed at MNTB-LSO synapses during a period of heightened plasticity.

The P3–P9 window was delineated also in the isolated NMDAR response by larger amounts of charge transferred. This change in current duration strongly suggests a change in subunit composition for the NMDAR population. As the GluN2A and GluN2B subunits interact with distinct synaptic proteins and confer different Mg^{2+} sensitivity and decay kinetics on the NMDAR channels, the relative proportions of these subunits can set several parameters of plasticity (Crair and Malenka 1995; Hrabetova et al. 2000; Liu et al. 2004; Monyer et al. 1992; Philpot et al. 2007). We did not attempt to obtain many

recordings after P10, because of the steadily decreasing probability of glutamate release after the first postnatal week, but note the sharp reduction in ifenprodil sensitivity between P7/8 and P9/10 and suggest that functional GluN2B expression likely remains low after P10. In the glutamatergic VCN-LSO pathway, NMDAR responses also lose sensitivity to ifenprodil and exhibit shorter decay kinetics after P8 (Case et al. 2011). This developmental shortening of NMDAR EPSCs could result from a subunit substitution of GluN2A for GluN2B (Flint et al. 1997; Quinlan et al. 1999).

The developmental profile of glutamatergic transmission—in which NMDAR-mediated charge transfer rises between P3 and P9—could be suggestive of an NMDAR-mediated sensitive period, in light of several correlated events: *1*) the close of major functional refinement occurs around P9 (Kim and Kandler 2003); *2*) GABA/glycine are depolarizing before about P9 (Ehrlich et al. 1999; Kandler and Friauf 1995); *3*) normalized MNTB input area to a given LSO cell changes maximally between P3 and P8 (Kim and Kandler 2003); and *4*) spontaneous activity begins to increase in the cochlea around P3 (Tritsch and Bergles 2010). In light of these events, we speculate that the MNTB-LSO pathway may be another example of an inhibitory circuit that experiences a sensitive period (Maffei et al. 2010), perhaps a window that opens around P3 to permit plasticity driven by spontaneous cochlear activity and then closes around P9.

If NMDARs are necessary for synaptic strengthening, one could ask whether the size of NMDAR EPSCs is inversely correlated with size of developing GABA/glycine synapses. We saw no correlation between size of the two response types, although NMDARs

containing different subunit types could be differentially distributed on subpopulations undergoing strengthening or weakening. Studies in the gerbil slice preparation have linked long-term depression at the MNTB-LSO synapse to several mechanisms that do not specifically involve NMDARs (Kotak and Sanes 2000, 2002; Kotak et al. 2001). Long-term potentiation has not yet been reported in the MNTB-LSO pathway, and, in fact, we still do not know whether NMDAR activation mediates Hebbian developmental refinement in the MNTB-LSO pathway. To our knowledge, no one has yet attempted to induce synaptic plasticity in this pathway in the absence of NMDAR antagonists, and it will be important to determine whether NMDAR-mediated plasticity occurs in the MNTB-LSO pathway.

Release probability at GABA/glycine/glutamatergic MNTB-LSO synapses.

Are GABA, glycine, and glutamate released together at MNTB terminals? If so, they might be expected to occupy the same set of presynaptic vesicles, characterized by coexpression of vesicular transporters for glutamate and GABA/glycine. Such copackaging is possible, as other pairs of distinct transporters can be expressed in the same vesicles (Gras et al. 2008; Herzog et al. 2006). Our results show different PPRs for GABA/glycine and for glutamate-mediated neurotransmission. A minor caveat is that GABA/glycine PPRs were obtained without block of glutamate receptors, whereas glutamate PPRs were obtained in the presence of GABA/glycine antagonists. The different treatments arose from our requirement of obtaining PPRs for both

neurotransmitter types from the same slices, the near impossibility of washing off strychnine within a typical recording period, the small size of most of the AMPAR-mediated currents (Fig. 7*A, inset*), and our consequent concern that incomplete washoff of AMPAR antagonists might compromise the AMPAR recordings. However, given the relative amplitudes for AMPAR-mediated currents and GABA/glycine receptor-mediated currents, AMPARs are unlikely to contribute significantly to differences in apparent GABA/glycine current. Furthermore, if the AMPAR-mediated component with its smaller PPR affected the GABA/glycine PPR, it would make GABA/glycine paired-pulse depression appear smaller than reality; this would have caused us to underestimate the differences in PPRs between the two neurotransmitter systems.

One interpretation for the differences in PPR for GABA/glycine and for glutamate is that GABA/glycine and glutamate are released from different vesicles at MNTB terminals. GABA/glycine and glutamate may occupy distinct vesicle populations, possibly distinguished by their proximity to the synaptic cleft or by their association with different forms of the calcium sensor synaptotagmin (Cooper and Gillespie 2011; Fox and Sanes 2007; Xu et al. 2007), which could confer distinct release probabilities on the two vesicle populations. Alternatively, differences in vesicle filling properties could give rise to the differing paired-pulse depression (Aubrey et al. 2007). Regardless of the cause, these distinct release probabilities might allow the presynaptic terminal—depending on patterns of neural activity—to switch between single (GABA/glycine) and dual (GABA/glycine + glutamate) release. A key implication of such a switch is that if dual release indeed mediates synaptic plasticity, the temporal statistics of the incoming spike train would

determine whether the synapse operated in a normal transmission mode or in a plasticity-inducing mode.

References

Aubrey KR, Rossi FM, Ruivo R, Alboni S, Bellenchi GC, Le Goff A, Gasnier B, Supplisson S (2007) The transporters GlyT2 and VIAAT cooperate to determine the vesicular glycinergic phenotype. J Neurosci 27:6273-6281.

Beutner D, Moser T (2001) The presynaptic function of mouse cochlear inner hair cells during development of hearing. J Neurosci 21:4593-4599.

Bledsoe SC, Jr., Snead CR, Helfert RH, Prasad V, Wenthold RJ, Altschuler RA (1990) Immunocytochemical and lesion studies support the hypothesis that the projection from the medial nucleus of the trapezoid body to the lateral superior olive is glycinergic. Brain Res 517:189-194.

Boudreau JC, Tsuchitani C (1968) Binaural interaction in the cat superior olive S segment. J Neurophysiol 31:442-454.

Burnashev N, Khodorova A, Jonas P, Helm PJ, Wisden W, Monyer H, Seeburg PH, Sakmann B (1992) Calcium-permeable AMPA-kainate receptors in fusiform cerebellar glial cells. Science 256:1566-1570.

Caird D, Klinke R (1983) Processing of binaural stimuli by cat superior olivary complex neurons. Exp Brain Res 52:385-399.

Cant NB, Casseday JH (1986) Projections from the anteroventral cochlear nucleus to the lateral and medial superior olivary nuclei. J Comp Neurol 247:457-476.

Case DT, Zhao X, Gillespie DC (2011) Functional refinement in the projection from ventral cochlear nucleus to lateral superior olive precedes hearing onset in rat. PLoS One 6:e20756.

Caspary DM, Finlayson PG (1991) The lateral superior olive: a functional role in sound source localization. In: Neurobiology of Hearing: The Central Auditory System (Altschuler RA, Bobbin RP, Clopton BM, Hoffman DW, eds), pp 141-161: Lippincott.

Chang EH, Kotak VC, Sanes DH (2003) Long-term depression of synaptic inhibition is expressed postsynaptically in the developing auditory system. J Neurophysiol 90:1479-1488.

Cooper AP, Gillespie DC (2011) Synaptotagmins I and II in the developing rat auditory brainstem: Synaptotagmin I is transiently expressed in glutamate-releasing immature inhibitory terminals. J Comp Neurol 519:2417-2433.

Crair MC, Malenka RC (1995) A critical period for long-term potentiation at thalamocortical synapses. Nature 375:325-328.

Cull-Candy S, Kelly L, Farrant M (2006) Regulation of Ca2+-permeable AMPA receptors: synaptic plasticity and beyond. Curr Opin Neurobiol 16:288-297.

Ehrlich I, Lohrke S, Friauf E (1999) Shift from depolarizing to hyperpolarizing glycine action in rat auditory neurones is due to age-dependent Cl- regulation. J Physiol 520 Pt 1:121-137.

Ene FA, Kullmann PH, Gillespie DC, Kandler K (2003) Glutamatergic calcium responses in the developing lateral superior olive: receptor types and their specific activation by synaptic activity patterns. J Neurophysiol 90:2581-2591.

Flint AC, Maisch US, Weishaupt JH, Kriegstein AR, Monyer H (1997) NR2A subunit expression shortens NMDA receptor synaptic currents in developing neocortex. J Neurosci 17:2469-2476.

Fox MA, Sanes JR (2007) Synaptotagmin I and II are present in distinct subsets of central synapses. J Comp Neurol 503:280-296.

Friauf E (1993) Transient appearance of calbindin-D28k-positive neurons in the superior olivary complex of developing rats. J Comp Neurol 334:59-74.

Gaiarsa JL, Caillard O, Ben-Ari Y (2002) Long-term plasticity at GABAergic and glycinergic synapses: mechanisms and functional significance. Trends Neurosci 25:564-570.

Gillespie DC, Kim G, Kandler K (2005) Inhibitory synapses in the developing auditory system are glutamatergic. Nat Neurosci 8:332-338.

Gras C, Amilhon B, Lepicard EM, Poirel O, Vinatier J, Herbin M, Dumas S, Tzavara ET, Wade MR, Nomikos GG, Hanoun N, Saurini F, Kemel ML, Gasnier B,

Giros B, El Mestikawy S (2008) The vesicular glutamate transporter VGLUT3 synergizes striatal acetylcholine tone. Nat Neurosci 11:292-300.

Herzog E, Takamori S, Jahn R, Brose N, Wojcik SM (2006) Synaptic and vesicular co-localization of the glutamate transporters VGLUT1 and VGLUT2 in the mouse hippocampus. J Neurochem 99:1011-1018.

Hrabetova S, Serrano P, Blace N, Tse HW, Skifter DA, Jane DE, Monaghan DT, Sacktor TC (2000) Distinct NMDA receptor subpopulations contribute to long-term potentiation and long-term depression induction. J Neurosci 20:RC81.

Isaac JT, Crair MC, Nicoll RA, Malenka RC (1997) Silent synapses during development of thalamocortical inputs. Neuron 18:269-280.

Kakazu Y, Akaike N, Komiyama S, Nabekura J (1999) Regulation of intracellular chloride by cotransporters in developing lateral superior olive neurons. J Neurosci 19:2843-2851.

Kandler K (2004) Activity-dependent organization of inhibitory circuits: lessons from the auditory system. Curr Opin Neurobiol 14:96-104.

Kandler K, Friauf E (1995) Development of glycinergic and glutamatergic synaptic transmission in the auditory brainstem of perinatal rats. J Neurosci 15:6890-6904.

Kim G, Kandler K (2003) Elimination and strengthening of glycinergic/GABAergic connections during tonotopic map formation. Nat Neurosci 6:282-290.

Korada S, Schwartz IR (1999) Development of GABA, glycine, and their receptors in the auditory brainstem of gerbil: a light and electron microscopic study. J Comp Neurol 409:664-681.

Kotak VC, Sanes DH (1996) Developmental influence of glycinergic transmission: regulation of NMDA receptor-mediated EPSPs. J Neurosci 16:1836-1843.

Kotak VC, Sanes DH (2000) Long-lasting inhibitory synaptic depression is age- and calcium-dependent. J Neurosci 20:5820-5826.

Kotak VC, Sanes DH (2002) Postsynaptic kinase signaling underlies inhibitory synaptic plasticity in the lateral superior olive. J Neurobiol 53:36-43.

Kotak VC, DiMattina C, Sanes DH (2001) GABA(B) and Trk receptor signaling mediates long-lasting inhibitory synaptic depression. J Neurophysiol 86:536-540.

Kotak VC, Korada S, Schwartz IR, Sanes DH (1998) A developmental shift from GABAergic to glycinergic transmission in the central auditory system. J Neurosci 18:4646-4655.

Kros CJ, Ruppersberg JP, Rusch A (1998) Expression of a potassium current in inner hair cells during development of hearing in mice. Nature 394:281-284.

Kullmann PH, Kandler K (2001) Glycinergic/GABAergic synapses in the lateral superior olive are excitatory in neonatal C57Bl/6J mice. Brain Res Dev Brain Res 131:143-147.

Laezza F, Doherty JJ, Dingledine R (1999) Long-term depression in hippocampal interneurons: joint requirement for pre- and postsynaptic events. Science 285:1411-1414.

Lei S, McBain CJ (2002) Distinct NMDA receptors provide differential modes of transmission at mossy fiber-interneuron synapses. Neuron 33:921-933.

Liao D, Hessler NA, Malinow R (1995) Activation of postsynaptically silent synapses during pairing-induced LTP in CA1 region of hippocampal slice. Nature 375:400-404.

Liu L, Wong TP, Pozza MF, Lingenhoehl K, Wang Y, Sheng M, Auberson YP, Wang YT (2004) Role of NMDA receptor subtypes in governing the direction of hippocampal synaptic plasticity. Science 304:1021-1024.

Maffei A, Lambo ME, Turrigiano GG (2010) Critical period for inhibitory plasticity in rodent binocular V1. J Neurosci 30:3304-3309.

Mahanty NK, Sah P (1998) Calcium-permeable AMPA receptors mediate long-term potentiation in interneurons in the amygdala. Nature 394:683-687.

Malenka RC, Bear MF (2004) LTP and LTD: an embarrassment of riches. Neuron 44:5-21.

Marsden KC, Beattie JB, Friedenthal J, Carroll RC (2007) NMDA receptor activation potentiates inhibitory transmission through GABA receptor-associated protein-dependent exocytosis of GABA(A) receptors. J Neurosci 27:14326-14337.

McLean HA, Caillard O, Ben-Ari Y, Gaiarsa JL (1996) Bidirectional plasticity expressed by GABAergic synapses in the neonatal rat hippocampus. J Physiol 496 (Pt 2):471-477.

Monyer H, Burnashev N, Laurie DJ, Sakmann B, Seeburg PH (1994) Developmental and regional expression in the rat brain and functional properties of four NMDA receptors. Neuron 12:529-540.

Monyer H, Sprengel R, Schoepfer R, Herb A, Higuchi M, Lomeli H, Burnashev N, Sakmann B, Seeburg PH (1992) Heteromeric NMDA receptors: molecular and functional distinction of subtypes. Science 256:1217-1221.

Moore MJ, Caspary DM (1983) Strychnine blocks binaural inhibition in lateral superior olivary neurons. J Neurosci 3:237-242.

Muller T, Moller T, Berger T, Schnitzer J, Kettenmann H (1992) Calcium entry through kainate receptors and resulting potassium-channel blockade in Bergmann glial cells. Science 256:1563-1566.

Nabekura J, Katsurabayashi S, Kakazu Y, Shibata S, Matsubara A, Jinno S, Mizoguchi Y, Sasaki A, Ishibashi H (2004) Developmental switch from GABA to glycine release in single central synaptic terminals. Nat Neurosci 7:17-23.

Noh J, Seal RP, Garver JA, Edwards RH, Kandler K (2010) Glutamate co-release at GABA/glycinergic synapses is crucial for the refinement of an inhibitory map. Nat Neurosci 13:232-238.

Ouardouz M, Sastry BR (2000) Mechanisms underlying LTP of inhibitory synaptic transmission in the deep cerebellar nuclei. J Neurophysiol 84:1414-1421.

Philpot BD, Cho KK, Bear MF (2007) Obligatory role of NR2A for metaplasticity in visual cortex. Neuron 53:495-502.

Quinlan EM, Philpot BD, Huganir RL, Bear MF (1999) Rapid, experience-dependent expression of synaptic NMDA receptors in visual cortex in vivo. Nat Neurosci 2:352-357.

Rumbaugh G, Vicini S (1999) Distinct synaptic and extrasynaptic NMDA receptors in developing cerebellar granule neurons. J Neurosci 19:10603-10610.

Sanes DH, Rubel EW (1988) The ontogeny of inhibition and excitation in the gerbil lateral superior olive. J Neurosci 8:682-700.

Sheng M, Cummings J, Roldan LA, Jan YN, Jan LY (1994) Changing subunit composition of heteromeric NMDA receptors during development of rat cortex. Nature 368:144-147.

Smith PH, Joris PX, Carney LH, Yin TC (1991) Projections of physiologically characterized globular bushy cell axons from the cochlear nucleus of the cat. J Comp Neurol 304:387-407.

Tritsch NX, Bergles DE (2010) Developmental regulation of spontaneous activity in the Mammalian cochlea. J Neurosci 30:1539-1550.

Tritsch NX, Yi E, Gale JE, Glowatzki E, Bergles DE (2007) The origin of spontaneous activity in the developing auditory system. Nature 450:50-55.

Wang J, Liu S, Haditsch U, Tu W, Cochrane K, Ahmadian G, Tran L, Paw J, Wang Y, Mansuy I, Salter MM, Lu YM (2003) Interaction of calcineurin and type-A GABA receptor gamma 2 subunits produces long-term depression at CA1 inhibitory synapses. J Neurosci 23:826-836.

Wu SH, Kelly JB (1992) Synaptic pharmacology of the superior olivary complex studied in mouse brain slice. J Neurosci 12:3084-3097.

Xu J, Mashimo T, Sudhof TC (2007) Synaptotagmin-1, -2, and -9: Ca^{2+} sensors for fast release that specify distinct presynaptic properties in subsets of neurons. Neuron 54:567-581.

Chapter 4

Chapter Statement: Javier Alamilla, a postdoctoral fellow in the lab, was also a contributor to this data chapter.

Abstract

Principal neurons of the lateral superior olive (LSO) integrate tonotopically matched excitatory and inhibitory inputs in order to determine the difference in sound intensity reaching the two ears, a signal crucial for proper sound localization. The inhibitory inputs to LSO neurons, which originate in the medial nucleus of the trapezoid body (MNTB), undergo a period of functional refinement that consists of synaptic strengthening and silencing during a narrow age window before hearing onset. Interestingly, during this refinement window MNTB terminals release glutamate which activates GluN2B-containing NMDARs on LSO neurons, and elimination of VGlut3, the protein that supports glutamate release from developing MNTB terminals, disrupts proper refinement of MNTB-LSO terminals. This finding has led to the hypothesis that NMDAR-dependent plasticity driven by patterned spontaneous activity may underlie developmental refinement of the inhibitory MNTB-LSO inputs. However, at other synapses VGlut3, the transporter that loads glutamate into synaptic vesicles at MNTB terminals, has been shown to increase the level and rate of filling of other neurotransmitters into synaptic vesicles. Therefore, it is possible that VGlut3 is more important for vesicular synergy than for glutamate release, and that synergy of VGlut3

with VIAAT is important for the functional refinement of MNTB-LSO terminals. To determine if VGlut3 synergizes loading of GABA/glycine into vesicles at MNTB-LSO synapses, we used *in vitro* whole-cell patch-clamp to compare properties of GABA/glycinergic transmission at MNTB-LSO synapses in mice expressing and mice lacking VGlut3. We found that paired-pulse ratios, probability of release, recovery from paired-pulse depression, and amplitude of miniature GABA/glycinergic events at MNTB-LSO synapses do not differ between mice expressing and mice lacking VGlut3. These results suggest that VGlut3 does not synergize vesicular loading at MNTB-LSO synapses, and lend further support to the hypothesis that glutamate release from developing MNTB-LSO terminals is most important for initiating NMDAR-dependent refinement.

4.1 Introduction

Interaural intensity differences (IID) used to determine azimuthal sound source are detected by principal neurons of the lateral superior olive (LSO), a binaural brainstem nucleus (Boudreau and Tsuchitani, 1968; Caird and Klinke, 1983). LSO principal neurons compute IID by integrating excitatory, glutamatergic input from the ipsilateral anteroventral cochlear nucleus (AVCN; Cant and Casseday, 1986; Wu and Kelly, 1992) with inhibitory, glycinergic input from the ipsilateral, but contralaterally driven, medial nucleus of the trapezoid body (MNTB; Moore and Caspary, 1983; Bledsoe et al, 1990; Caspary and Finlayson 1991; Smith et al, 1991). In order to accurately determine sound source, these excitatory and inhibitory inputs must be matched tonotopically to LSO

principal neurons (Sanes and Rubel, 1988; Kandler, 2004). How these excitatory and inhibitory inputs become refined and matched are two important questions in the development of the auditory system.

The inhibitory MNTB-LSO pathway undergoes functional refinement consisting of synaptic strengthening and elimination before hearing onset in rodents (Kim and Kandler, 2003). During this refinement, which appears to occur most rapidly between postnatal day 3 and postnatal day 8 (P3-P8), MNTB terminals release GABA and glycine (Kotak et al, 1998; Korada and Schwartz, 1999; Kim and Kandler, 2003; Nabekura et al, 2004), which depolarize the postsynaptic membrane (Kandler and Friauf, 1995; Ehrlich et al, 1999; Kakazu et al, 1999). Interestingly, during functional refinement MNTB terminals also release glutamate (Gillespie et al, 2005), which activates postsynaptic GluN2B-containing NMDARs (Case and Gillespie, 2011). This glutamate release is supported by the vesicular glutamate transporter VGlut3, and expression of this protein at MNTB terminals is crucial for the refinement of the MNTB-LSO pathway (Gillespie et al, 2005; Noh et al, 2010). These findings have led to the model that spontaneous patterned activity generated in the cochlea (Tritsch et al, 2007) propagates throughout the auditory system, driving specific patterns of glutamate release from MNTB terminals that initiate NMDAR-dependent refinement of MNTB-LSO synapses (Noh et al, 2010; Case and Gillespie, 2011).

VGlut3 is expressed in select populations of typically non-glutamatergic neurons (Fremeau et al, 2002; Gras et al, 2002; Herzog et al, 2004), and recent work has demonstrated that VGlut3 can synergize the loading of other neurotransmitters into

synaptic vesicles at “non-glutamatergic synapses” (Gras et al, 2008; Amilhon et al, 2010). This synergistic role of VGlut3 has not been examined extensively at inhibitory terminals, but it is potentially important for increasing loading of GABA and/or glycine into synaptic vesicles (Zander et al, 2010). The synergistic role of VGlut3 could support functional refinement of MNTB-LSO synapses by increasing the loading of GABA/glycine into synaptic vesicles at MNTB terminals, allowing MNTB terminals to better follow the patterned activity that is hypothesized to drive functional refinement.

Is the role of VGlut3 at developing MNTB-LSO synapses to support glutamate release on to postsynaptic NMDARs, or to increase loading of GABA/glycine into synaptic vesicles? To address this question we compared properties of neurotransmission in mice expressing and mice lacking VGlut3. Using whole-cell patch-clamp in acute brainstem slices, we found that the amount of paired-pulse depression, the time for MNTB terminals to recover from paired-pulse depression, and the amplitude of miniature GABA/glycinergic events did not differ across genotypes. These data suggest that VGlut3 does not synergize GABA/glycine release at MNTB-LSO synapses, and support the hypothesis that VGlut3 expression at MNTB-LSO terminals mainly serves to support glutamate release on to postsynaptic NMDA receptors.

4.2 Materials and Methods

All procedures adhered to Canadian Council on Animal Care guidelines and were approved by the Animal Research Ethics Board of McMaster University (Animal Use Protocol #12-05-16).

Slice preparation and physiology

Mice heterozygous (+/-) for the VGLUT3 gene (gift from S. El Mestikawy) were bred to yield litters containing +/+ (wild-type, WT), +/- (het), and -/- (knockout, KO) mice. Pups aged P4-P5 (P0 is day of birth) were anaesthetized with isofluorane and quickly decapitated, and the brains were removed into ice-cold artificial cerebrospinal fluid (ACSF, pH 7.2) containing (in mM): 125 NaCl, 1 MgSO4, 5 KCl, 1.25 KH2PO4, 10 dextrose, 26 NaHCO3, 2 CaCl2•2H2O, 1 ascorbic acid, 1 kynurenic acid. Small segments of tail were also removed at this time for post-hoc genotype identification. The brainstem was cut at 300 µm (Vibratome 3000 Series), and slices containing the MNTB and LSO were transferred to a humidified interface chamber where they were allowed to recover for at least 1 hour at room temperature (~21C). For recording, slices were transferred to a recording chamber at an upright microscope where they were continuously perfused with ACSF heated to near physiological temperature (32-35C) and superfused with 95% O_2/5% CO_2. Perfusion ACSF was the same as cutting ACSF, except that 0.3mM ascorbic acid was used and 0.5mM D-glutamine was also added. GABA/glycine-mediated

responses were isolated by including 1mM kynurenic acid in the perfusion ACSF. To exclude the possibility that metabotropic glutamate receptors (mGluRs) modulate GABA/glycine probability of release, we performed recordings in a number of cells in ACSF lacking kynurenic acid (to confirm the presence of a glutamate response), and compared pulse train values before and after the application of the mGluR antagonist LY 341 495 (Tocris; example shown in Supplemental Figure 1). No differences in paired pulse ratios were observed following blockade of mGluRs.

Electrodes for whole-cell voltage clamp (8250 borosilicate glass, AM Systems) had resistances of 1–4 MΩ and were filled with a high chloride (E_{Cl} = ~ -20mV) Cs-gluconate solution (pH 7.2) containing (in mM): 64 D-gluconic acid, 64 CsOH, 11 EGTA, 56 CsCl, 1 MgCl2•6H2O, 1 CaCl2, 10 HEPES, 0.3 GTP-Na, 4 ATPMg•3.5H2O, 0.1 mM spermine (Acros Organics). In several cases, the internal solution also contained 0.5% biocytin for subsequent histological verification of cell type; in some instances CNQX (5μM; Tocris) was added to the internal solution to increase patch stability. Cells in the higher frequency (medial and middle) limbs of the LSO were targeted using DIC-IR, and principal cells were identified based on their bipolar morphology and their orientation relative to the tonotopic axis of the nucleus. Recordings (MultiClamp 700B amplifier with pClamp 10, and Axopatch 200B amplifier with pClamp 9.2; Molecular Devices) were sampled at 10 kHz, filtered at 5 kHz and saved for offline analysis with custom Matlab software. Series resistance was compensated by a minimum of 80% with <10 μs lag, and were discarded if series resistance changed by more than 15% from its initial value. All recordings were made at a holding potential of −60 mV.

Stimulating electrodes, 1–2 MΩ glass pipettes filled with ACSF, were placed in the MNTB or in the fiber tract leaving the lateral edge of the MNTB and stimuli were delivered via a Master 8 with Iso-Flex SIU. Electrical stimulation intensity was set near a minimum intensity that reliably elicited responses and stimulation intensity remained unchanged throughout the experiment. Probability of release was examined by delivering 10 pulses of electrical stimulation at 50 Hz, or 20 pulses at 100Hz. The peak current amplitudes resulting from the second to tenth (or 20^{th}; I_n) pulses were divided by the peak current amplitude resulting from the first pulse (I_i) to determine paired-pulse ratios (I_n/I_i); peak current was measured relative to current immediately before the stimulus for each pulse. To test recovery from paired-pulse depression, we delivered 10 pulses of electrical stimuli at 50 Hz, waited for a variable delay period, and then delivered another 10 pulses of electrical stimuli at 50 Hz. Many delay times were tested per cell in an attempt to obtain a full recovery time curve for the cell.

To estimate quantal size and probability of release, we delivered 20 pulses of electrical stimuli at 100Hz. The resulting responses were normalized to the amplitude of the first response, and the normalized amplitudes of all 20 responses were added successively to create a cumulative response amplitude curve. The last 6 points in the cumulative response amplitude curve were fit linearly and this fit was extrapolated to determine the sum value at time = 0 (response 1), which can be used to estimate the size of the readily releasable pool of vesicles multiplied by quantal amplitude (N_q) (Inchauspe et al, 2007); from this value, probability of release can be estimated.

Recording of miniature GABA/glycinergic events

Spontaneous GABA/glycinergic events appear to be uncommon in the developing LSO. Therefore, to evaluate the size of miniature GABA/glycinergic events, we delivered high-frequency stimulation (20 pulses at 100Hz) to MNTB fibers, which we found often increases spontaneous activity, or used a perfusion ACSF in which $CaCl_2$ was replaced with $SrCl_2$ (2mM), which results in asynchronous vesicular release, making it possible to evaluate response amplitude following neurotransmitter release from a single vesicle. Miniature events were identified using threshold detection templates in Clampfit (Molecular Devices), and were checked by eye to ensure that they were indeed miniature events.

Genotyping

DNA was isolated from tail clips that were taken from mice during acute slice preparation, and PCR reactions using VGlut3 wild-type (278bp) and VGlut3 knockout cassette (604bp) primers (Gras et al, 2008; Mobix Lab, McMaster University) were completed in separate tubes in a Peltier Thermal Cycler (Dyad DNA Engine). Following the PCR reaction, primer bands were identified using gel electrophoresis.

Data Analysis

Pulse train data were analyzed using custom programs in Matlab (Mathworks); miniature events were analyzed using Clampfit (Molecular Devices). Post-hoc Kruskal-Wallis tests were deemed significant if a p-value less than 0.05 resulted.

4.3 Results

Following functional refinement of the MNTB-LSO pathway, there are changes in quantal size, quantal content, and the probability of GABA/glycine release (Kim and Kandler, 2010). It is unknown whether these changes occur in mice lacking VGlut3 (Kim and Kandler, 2010), but it is possible that they may not given that refinement does not occur properly in these mice (Noh et al, 2010). Therefore, we focussed our study only on P4/P5 mice, because these mice are near the beginning of the refinement period, when glutamate release supported by VGlut3 is normally prevalent but synaptic changes underlying refinement have not occurred, or are just beginning to occur. By doing this, we can more confidently conclude that any differences in GABA/glycine release between normal and VGlut3 knockout mice are due to vesicular synergy, rather than due to differences in the extent of pathway refinement.

Comparison of vesicle release following 50Hz stimulation

We first wanted to determine if there are differences in paired-pulse ratios between VGlut3 wild-type (WT), heterozygote (het), and knockout (KO) mice. To do this, we

delivered 10 electrical stimuli at 50Hz to MNTB fibers and performed whole-cell recordings in the LSO. For all genotypes, almost all pulse trains exhibited depression, not always following the second or even third pulse, but always for the final portion of the pulse train. In a small number of instances (n = 1 WT, 4 het, 2 KO) we observed facilitation through the entire pulse train. Because these responses were extremely different from the majority of the data set, they were excluded from analysis.

Representative recordings from WT, het, and KO mice following 50Hz stimulation are shown in figure 1A, and these traces are shown overlaid in figure 1B (normalized to the highest amplitude recording, the het cell, in figure 1A). By simply normalizing these example recordings, it appears that the paired-pulse ratio (PPR) in the WT cell is different from the PPR in the het and KO cells. However, this apparent difference arises due to the responses in the WT cell exhibiting longer decay times than the responses in the het and KO cells. This difference may occur due to the relative amount of GABA and glycine being released presynaptically, or to the relative number of $GABA_A$ and glycine receptors expressed postsynaptically in these particular cells (Nabekura et al, 2004). By resetting the baseline of each response to the same point, it is evident that the amplitudes of the responses do not differ between these three representative pulse trains (figure 1C).

PPRs did not significantly differ across genotypes, though KO mice did appear to experience less depression on average (figure 1D; PPRs (response2/response1): WT = 0.79+/-0.05, n = 21; het = 0.75+/-0.02, n=49; KO = 0.83+/-0.08, n = 9; Kruskal-Wallis test: p = 0.32). The cumulative normalized amplitude of the pulse train, calculated by

adding the normalized amplitude of all 10 responses in a train together (see Methods), also did not significantly differ across genotypes, though KO mice did appear to experience more summation on average (figure 1E; cumulative amplitudes of 10 responses: KO = 5.97+/-0.36, n = 21; het = 5.69+/-0.20, n = 49; KO = 6.15+/-0.58, n = 9; Kruskal-Wallis: p = 0.60) This is representative of the responses in KO depressing less through the entire pulse train than WT or het mice. Because VGlut3 has been shown to increase the rate of filling of synaptic vesicles (Gras et al, 2008; Amilhon et al, 2010), we would expect KO mice to be less able to follow high frequency stimulation than WT or het mice are; these results are in direct contradiction to what we would expect to see if vesicular synergy was occurring between VGlut3 and VIAAT.

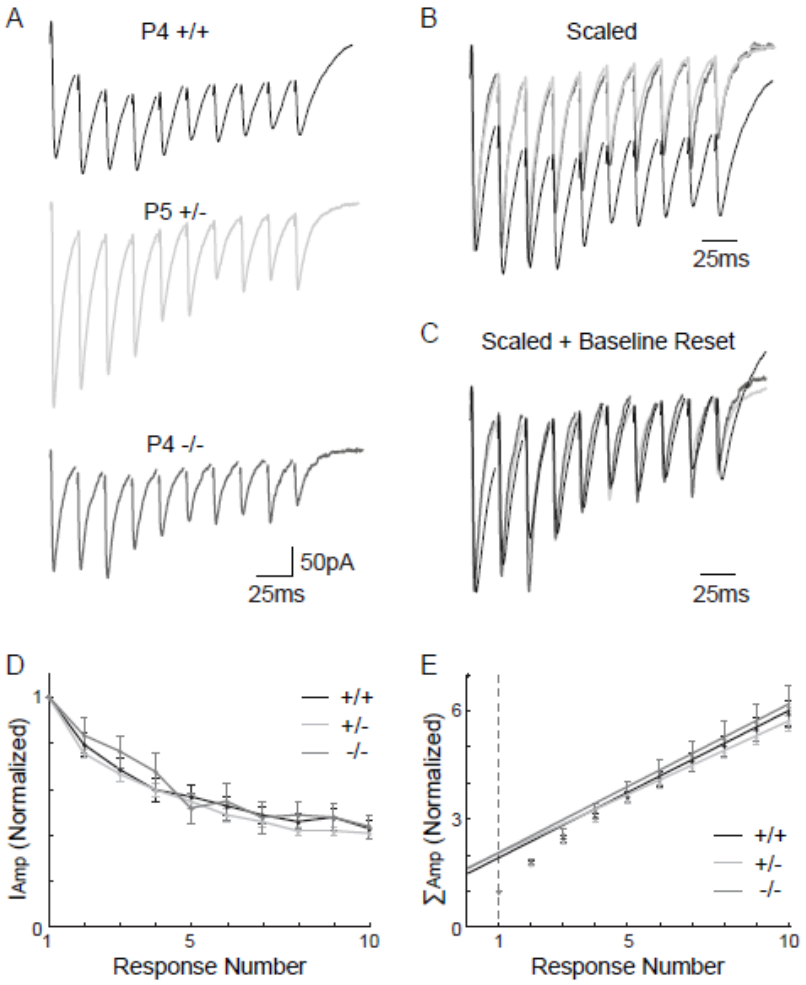

Figure 1. Paired-pulse ratios (PPR) resulting from 50Hz pulse trains do not differ between VGlut3 WT, het, and KO mice. **A**. Example pulse train recordings from WT (P4), het (P5), and KO (P4) mice. **B**. Recordings from A scaled to the het recording and overlaid. **C**. Scaled recordings in B overlaid with current baselines matched between each response. It is apparent in this figure that there is little difference in PPR between VGlut3 WT, het, and KO mice. **D**. Mean PPRs for VGlut3 WT, het, and KO mice are not significantly different. **E**. Cumulative normalized amplitudes for VGlut3 WT, het, and KO mice are not significantly different.

Comparison of vesicle release following 100Hz stimulation

It is possible that any genotypic differences in paired-pulse ratio between VGlut3 WT, het, and KO mice may only be borne out with stimulation at frequencies higher than 50Hz. Therefore, to further evaluate paired-pulse depression we delivered 20 electrical stimuli at 100Hz to MNTB fibers and performed whole-cell recordings in the LSO. Representative recordings from WT, het, and KO mice following 100Hz stimulation are shown in figure 2A, and these traces are shown overlaid in figures 2B and 2C (normalized to the highest amplitude recording, the WT cell, in figure 2A). Similar to the results obtained using 50 Hz stimulation, no difference in paired-pulse depression was observed between WT, het, and KO mice (figure 2D; PPRs (response2/response1): WT = 0.68+/-0.09, n = 8; het = 0.68+/-0.08, n = 9; KO = 0.64+/-0.09, n = 8; Kruskal-Wallis: p = 0.75). Additionally, the cumulative normalized amplitude of the pulse train did not significantly differ across genotypes (figure 2E; cumulative amplitudes of 20 responses: WT = 8.06+/-0.86, n = 8; het = 7.43+/-0.74, n = 9; KO = 6.68+/-0.81, n = 8; Kruskal-Wallis: p = 0.28).

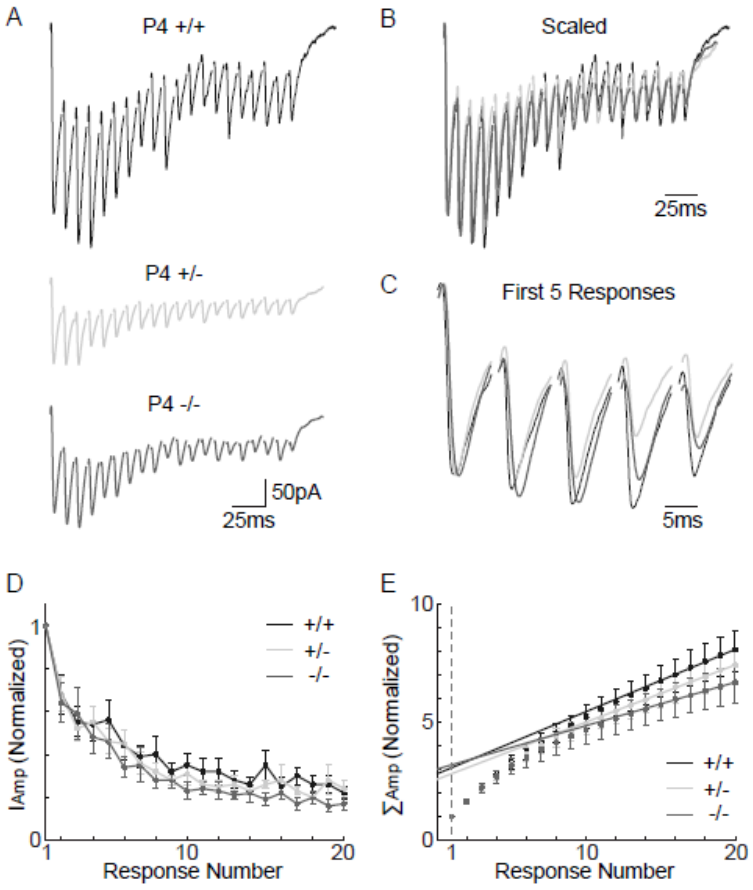

Figure 2. PPRs resulting from 100Hz pulse trains and probability of release do not differ between VGlut3 WT, het, and KO mice. **A**. Example pulse train recordings from WT (P4), het (P4), and KO (P4) mice. **B**. Recordings from A scaled to the WT recording and overlaid. **C**. First 5 responses from the scaled recordings in B are shown on an expanded time base for clarity. **D**. Mean PPRs for VGlut3 WT, het, and KO mice are not significantly different. **E**. Cumulative normalized amplitudes for VGlut3 WT, het, and KO mice are not significantly different. Additionally, probability of release values calculated by using linear regression from the last 6 points in the cumulative amplitude curves for VGlut3 WT, het, and KO mice are not significantly different.

The cumulative amplitude plot can also be used to estimate the probability of release of neurotransmitter for each genotype (see Methods; Inchauspe et al, 2007). The estimated N_q values obtained from the linear regression of the final 6 points in each curve are very similar (figure 2E; WT = 3.1+/-0.3; het = 2.8+/-0.3; KO = 3.2+/-0.4; Kruskal-Wallis test, p=0.74), as are the probability of release values (WT = 0.35+/-0.04; het = 0.39+/-0.05; KO = 0.35+/-0.05; Kruskal-Wallis test, p=0.71). Together, these data demonstrate that MNTB-LSO synapses in VGlut3 WT, het, and KO mice have similar probabilities of release.

Comparison of release recovery following 50Hz stimulation

Though our pulse train experiments indicate that there are no differences in probability of release between genotypes, it is possible that any differences in neurotransmission between VGlut3 WT, het, and KO mice may occur on a timescale longer than a 180ms pulse train. To test this, we determined the length of time it takes for neurotransmission to recover to its original level (see Dittman and Regehr, 1998) following high frequency stimulation, by delivering two 50Hz pulse trains of 10 stimuli each, separated by varying intervals (figure 3A).

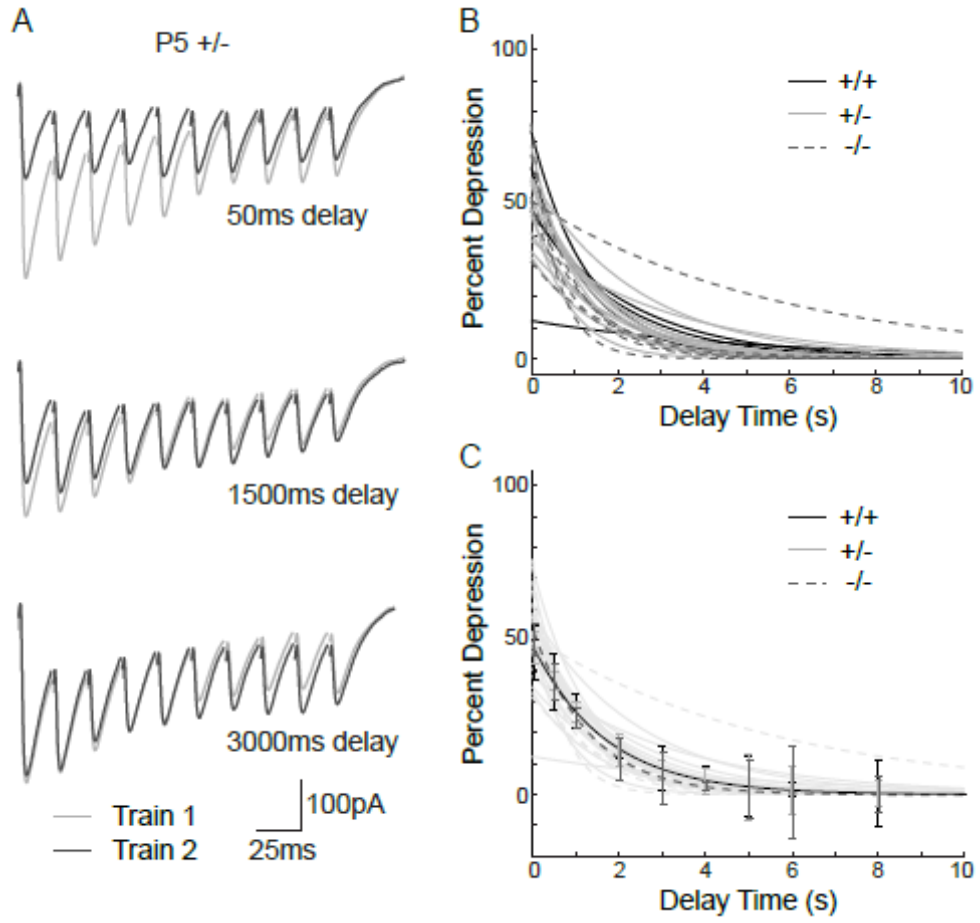

Figure 3. Rate of recovery from paired pulse depression does not differ between VGlut3 WT, het, and KO mice. **A**. Example recordings from a P5 VGlut3 het neuron demonstrating recording protocol and recovery from depression. **B**. Single exponential curves were fit to recovery data for each neuron analyzed. No differences between VGlut3 WT, het, and KO mice are apparent. **C**. Averaged single exponential recovery curves for VGlut3 WT, het, and KO mice are not significantly different.

Cells in which we were able to test at least 8 different recovery intervals, test a recovery interval of at least 4 seconds, and that displayed at least 90% recovery (amplitude of first pulse of second train/amplitude of first pulse of first train) were included in the analysis. Percent depression was plotted against recovery interval, and the resulting data points were fitted with a single exponential curve (individual cells, figure 3B; averages, figure 3C). We found that the exponential fits for recovery from paired-pulse depression did not differ between VGlut3 WT, het, and KO mice (Kruskal-Wallis tests on exponential coefficients: $p = 0.77$; $p = 0.32$), nor did the average time to 90% recovery (WT = 3.2+/-0.7s, het = 2.9+/-0.2s, KO = 3.0+/-1.0s; Kruskal-Wallis test, $p=0.76$).

Comparison of miniature GABA/glycinergic events

VGlut3 has been shown not only to increase the rate of vesicle filling, but also to elevate the amount of transmitter that can be loaded into synaptic vesicles (Gras et al, 2008). Therefore, if VGlut3 synergizes with VIAAT, responses to the release of neurotransmitter from a single vesicle may be higher at MNTB-LSO synapses of WT mice than of KO mice. To test this, we compared the amplitude of miniature GABA/glycinergic events across genotypes. Spontaneous vesicle release is uncommon in the developing LSO, so to estimate response sizes arising from single vesicle release we artificially increased spontaneous release by delivering high frequency stimulation to the

MNTB-LSO pathway, or we desynchronized vesicular release using ACSF containing strontium (see Methods).

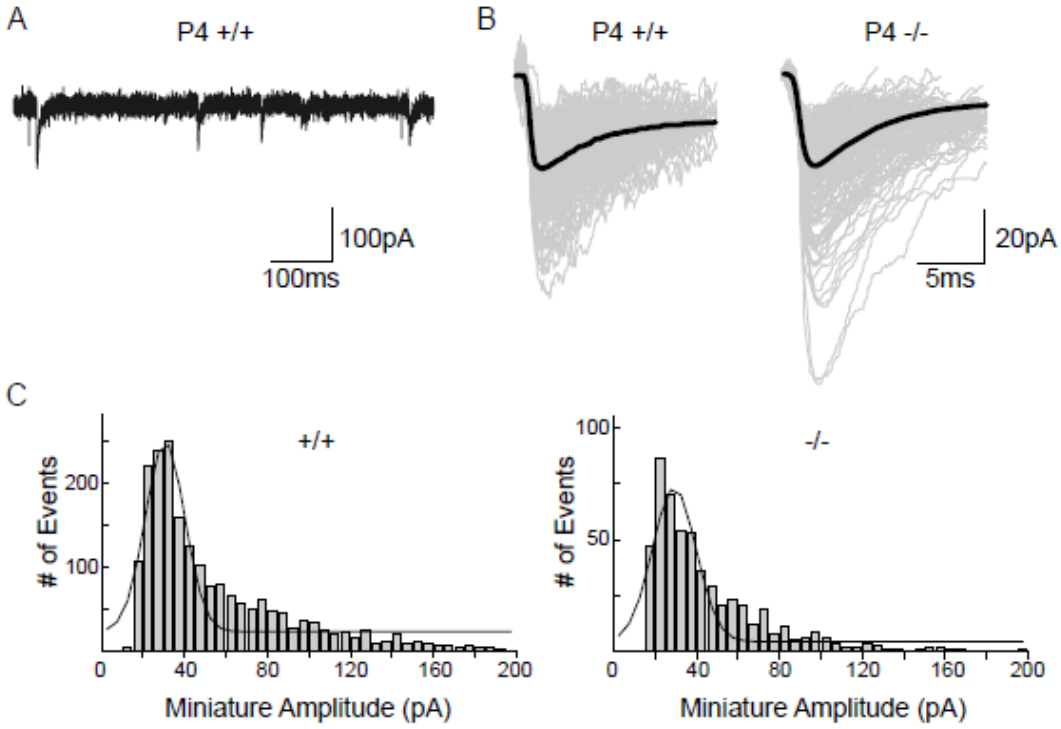

Figure 4. The amplitude of miniature GABA/glycinergic events does not differ between VGlut3 WT and KO mice. **A**. Example recording from a P4 VGlut3 WT neuron that displayed miniature events following 100Hz stimulation. **B**. Example miniature events from a P4 WT (left) and a P4 KO (right) neuron. All events from each neuron are overlaid (grey) and the average event is shown in black. **C**. Mean amplitude of miniature GABA/glycinergic events from VGlut3 WT and KO mice are not significantly different.

An example of miniature events from a P4 WT neuron is shown in figure 4A, and all the miniature events from an example WT neuron and an example KO neuron are shown in figure 4B. Miniature events from all cells of the same genotype were pooled to make event amplitude histograms, and to determine the average miniature GABA/glycinergic amplitude (Figure 4C). Event amplitude histograms for each cell are shown in appendix 2. We found that VGlut3 WT and KO mice display a small difference in mean miniature GABA/glycinergic event amplitude at MNTB-LSO synapses (mean event amplitude WT = 54.8 +/- 0.8 pA, n = 1981 events from 9 neurons; KO = 50.7 +/- 1.9 pA, n = 554 events from 4 neurons; unpaired t-test: $p = 0.03$). However, fitting a Gaussian peak to the event amplitude histograms suggests that there is very little difference in miniature event size between VGlut3 WT and KO mice (Gaussian Peaks: WT = 30.6 +/- 0.8 pA; KO = 29.2 +/- 1.0 pA). These Gaussian peak values are more representative of the smallest miniature event amplitudes for VGlut3 WT and KO mice. Additionally, the difference in miniature event amplitude means between VGlut3 WT and KO mice is much smaller proportionally than differences observed in transmitter release due to vesicular synergy in the striatum (Gras et al, 2008). These results are further evidence that VGlut3 does not synergize vesicular loading at developing MNTB-LSO synapses.

4.4 Discussion

VGlut3 is expressed in select populations of typically non-glutamatergic neurons, and has been shown to increase the *rate* of filling of cholinergic vesicles in the striatum and serotonergic vesicles in the raphe nuclei (Gras et al, 2008; Amilhon et al, 2010). Additionally, VGlut3 increases the *level* of vesicle filling in the striatum and raphe nuclei (Gras et al, 2008; Amilhon et al, 2010).We used whole-cell patch-clamp recordings in VGlut3 WT, het, and KO mice to examine the role that VGlut3 plays in release of GABA/glycine at developing MNTB-LSO synapses. Paired-pulse ratios and time to recovery from paired-pulse depression did not differ between VGlut3 WT, het, and KO mice, arguing against a difference in the rate of vesicle filling between the two genotypes (figures 1-3). The amplitude of miniature GABA/glycinergic events also did not differ between VGlut3 WT and KO mice, arguing against a difference in the level of vesicle filling between the two genotypes (figure 4). These results suggest that VGlut3 does not synergize with VIAAT at developing MNTB-LSO terminals.

The primary function of VGlut3 may depend on the time and location of expression

Though our results are different from what have been observed in the striatum (Gras et al, 2008) and the raphe nuclei (Amilhon et al, 2010), they should not be taken as a contradiction of those findings; rather, they should be taken as complementary. VGlut3 displays a unique expression profile: it is expressed for a brief period during early postnatal life, peaking at approximately P10, then experiences a decline in expression,

and finally is expressed again in adulthood, though only in rostral areas of the brain (Gras et al, 2005). It is possible that our results differ from those of Gras et al (2008) and Amilhon et al (2010) because our study was performed during a discrete developmental stage, as opposed to in adulthood. Together, these studies may suggest that the role of VGlut3 may vary between developing and adult circuits. For example, during development VGlut3 expression may primarily support different forms of refinement of typically non-glutamatergic terminals (Noh et al, 2010), whereas in adulthood VGlut3 expression may primarily support synergistic release of other neurotransmitters, such as acetylcholine and serotonin (Gras et al, 2008; Amilhon et al, 2010), or may serve to suppress excitability (Zander et al, 2010). Additionally, if VGlut3 is expressed biphasically at a single synapse type, it would further suggest that VGlut3 plays distinct roles over the lifespan. Our results also should not be taken to suggest that vesicular synergy does not occur at any type of inhibitory terminal; VGlut3 is also expressed at inhibitory terminals in the hippocampus and in other brain regions (Herzog et al, 2004). It is possible that the role of VGlut3 at inhibitory synapses is dependent on its location of expression, and to fully understand the role of VGlut3 it must be studied at a variety of synapse types, and at temporally and functionally distinct stages.

Lack of vesicular synergy is consistent with a model of NMDAR-dependent plasticity at developing MNTB-LSO terminals

The MNTB-LSO pathway appears to undergo two different periods of refinement. The first, which we focussed on in this study, occurs before hearing onset and consists of functional refinement (Kim and Kandler, 2003); the second occurs after hearing onset and consists of anatomical refinement (Sanes and Siverls, 1991; Sanes and Takacs, 1993). Though neither of these refinement processes is completely understood, the mechanisms underlying the pre-hearing functional refinement are becoming much better known. There appears to be a short window, defined by the correlation of several events, in which this refinement occurs. First, the synaptic strengthening and elimination that characterize MNTB-LSO pathway refinement occurs most rapidly between P3 and P8 (Kim and Kandler, 2003). Second, glutamate is released from MNTB terminals from P0 to P8, and NMDAR activation is most prevalent between P3 and P8 (Gillespie et al, 2005; Case and Gillespie, 2011). Additionally, NMDARs contain the GluN2B subunit, and it appears that the receptor subunit population is of a mixed phenotype at this time (Case and Gillespie, 2011), which may be important for bidirectional NMDAR-mediated plasticity (Liu et al, 2004; Barria and Malinow, 2005). Third, GABA and glycine are depolarizing at MNTB-LSO synapses until up to P8 (Kandler and Friauf, 1995; Ehrlich et al, 1999; Kakazu et al, 1999). This means that GABA and glycine can remove the magnesium blockade from NMDARs at these synapses. Finally, spontaneous activity is generated in the cochlea beginning around P3 due to the release of ATP from Kolliker's Organ, which initiates calcium transients in hair cells that lead to patterned spiking in the spiral ganglion (Tritsch et al, 2007; Tritsch and Bergles, 2010; Tritsch et al, 2010). The correlation of all these events has led to the model that patterned cochlear-driven spontaneous activity

propagates through the auditory system, creating patterned glutamate release from MNTB terminals that initiates NMDAR-dependent plasticity that directs physiological refinement of MNTB-LSO synapses. Because our results indicate that vesicular synergy does not occur at MNTB-LSO synapses during this period, they lend further support to this hypothesis. Our results are also consistent with experiments showing that GABA/glycine and glutamate exhibit different probabilities of release at developing MNTB-LSO synapses, which suggests that GABA/glycine and glutamate are released from separate synaptic vesicles (Case and Gillespie, 2011).

Additional Considerations

What dictates which neurotransmitter transporter proteins are directed to a particular vesicle? Because our results indicate that VGlut3 and VIAAT are not expressed in the same vesicles in MNTB terminals, it suggests that vesicles must be directed to specific recycling pathways to create distinct vesicle pools, as has been suggested for vesicular monoamine transporter 2 and VGlut1 in midbrain dopaminergic neurons (Onoa et al, 2010). At developing MNTB-LSO synapses, the calcium sensors synaptotagmin 1 and 2 (SYT1 and SYT2) are both expressed, and the time course of SYT1 expression closely follows the time course of VGlut3 expression (Cooper and Gillespie, 2011). This suggests that SYT1 and VGlut3 may be expressed on vesicles together, whereas SYT2 and VIAAT may be expressed on vesicles together. This could potentially be manifested as two separate vesicle pools with different phenotypes, and could arise through directed

recycling of synaptic vesicle proteins. This model is also supported by the experiments demonstrating differential release probability of GABA/glycine and glutamate from MNTB terminals (Case and Gillespie, 2011). Determining both how vesicular proteins are directed to vesicles and how the vesicles themselves are organized in MNTB terminals are important problems to answer in order to understand the development of the MNTB-LSO pathway, and to understand protein sorting and trafficking generally.

References

Amilhon B, Lepicard E, Renoir T, Mongeau R, Popa D, Poirel O, Miot S, Gras C, Gardier AM, Gallego J, Hamon M, Lanfumey L, Gasnier B, Giros B, El Mestikawy S (2010) VGLUT3 (vesicular glutamate transporter type 3) contribution to the regulation of serotonergic transmission and anxiety. J Neurosci 30(6):2198-2210.

Barria A, Malinow R (2005) NMDA receptor subunit composition controls synaptic plasticity by regulating binding to CaMKII. Neuron 48(2):289-301.

Bledsoe SC, Jr., Snead CR, Helfert RH, Prasad V, Wenthold RJ, Altshuler RA (1990) Immunocytochemical and lesion studies support the hypothesis that the projection from the medial nucleus of the trapezoid body to the lateral superior olive is glycinergic. Brain Res 517:189-194.

Boudreau JC, Tsuchitani C (1968) Binaural interaction in the cat superior olive S segment. J Neurophysiol. 1968 May;31(3):442-454.

Caird D, Klinke R (1983) Processing of binaural stimuli by cat superior olivary complex neurons. Exp Brain Res. 52(3):385-399.

Cant NB, Casseday JH (1986) Projections from the anteroventral cochlear nucleus to the lateral and medial superior olivary nuclei. J Comp Neurol 247:457-476.

Case DT, Gillespie DC (2011) Pre- and postsynaptic properties of glutamatergic transmission in the immature inhibitory MNTB-LSO pathway. J Neurophysiol 106(5):2570-2579.

Caspary DM, Finlayson PG (1991) The lateral superior olive: a functional role in sound source localization. In: Neurobiology of Hearing: The Central Auditory System (Altschuler RA, Bobbin RP, Clopton BM, Hoffman DW, ed), pp141–161. New York: Lippincott.

Cooper AP, Gillespie DC (2011) Synaptotagmins I and II in the developing rat auditory brainstem: Synaptotagmin I is transiently expressed in glutamate-releasing immature inhibitory terminals. J Comp Neurol 519(12):2417-2433.

Dittman JS, Regehr WG (1998) Calcium dependence and recovery kinetics of presynaptic depression at the climbing fiber to Purkinje cell synapse. J Neurosci 18(16):6147-6162.

Ehrlich I, Lohrke S, Friauf E (1999) Shift from depolarizing to hyperpolarizing glycine action in rat auditory neurones is due to age-dependent Cl- regulation. J Physiol 520(1):121-137.

Fremeau RT Jr, Burman J, Qureshi T, Tran CH, Proctor J, Johnson J, Zhang H, Sulzer D, Copenhagen DR, Storm-Mathisen J, Reimer RJ, Chaudhry FA, Edwards RH. (2002) The identification of vesicular glutamate transporter 3 suggests novel modes of signaling by glutamate. Proc Natl Acad Sci U S A 99(22):14488-14493.

Gillespie DC, Kim G, Kandler K (2005). Inhibitory synapses in the developing auditory system are glutamatergic. Nat Neurosci 8:332-338.

Gras C, Vinatier J, Amilhon B, Guerci A, Christov C, Ravassard P, Giros B, El Mestikawy S (2005) Developmentally regulated expression of VGLUT3 during early post-natal life. Neuropharmacology 49(6):901-911.

Gras C, Amilhon B, Lepicard EM, Poirel O, Vinatier J, Herbin M, Dumas S, Tzavara ET, Wade MR, Nomikos GG, Hanoun N, Saurini F, Kemel ML, Gasnier B, Giros B, El Mestikawy S (2008). The vesicular glutamate transporter VGLUT3 synergizes striatal acetylcholine tone. Nat Neurosci 11:292-300.

Herzog E, Gilchrist J, Gras C, Muzerelle A, Ravassard P, Giros B, Gaspar P, El Mestikawy S (2004) Localization of VGLUT3, the vesicular glutamate transporter type 3, in the rat brain. Neuroscience 123(4):983-1002.

Inchauspe CG, Forsythe ID, Uchitel OD (2007) Changes in synaptic transmission properties due to the expression of N-type calcium channels at the calyx of Held synapse of mice lacking P/Q-type calcium channels. J Physiol 584(3):835-851.

Kakazu Y, Akaike N, Komiyama S, Nabekura J (1999) Regulation of intracellular chloride by cotransporters in developing lateral superior olive neurons. J Neurosci 19:2843-2851.

Kandler K (2004) Activity-dependent organization of inhibitory circuits: lessons from the auditory system. Curr Opin Neurobiol 14:96-104.

Kandler K, Friauf E (1995) Development of glycinergic and glutamatergic synaptic transmission in the auditory brainstem of perinatal rats. J Neurosci 15:6890-6904.

Kim G, Kandler K (2003). Elimination and strengthening of glycinergic/GABAergic connections during tonotopic map formation. Nat Neurosci 6:282-290.

Kim G, Kandler K (2010) Synaptic changes underlying the strengthening of GABA/glycinergic connections in the developing lateral superior olive. Neuroscience 171(3):924-933.

Korada S, Schwartz IR (1999) Development of GABA, glycine, and their receptors in the auditory brainstem of gerbil: a light and electron microscopic study. J Comp Neurol 409:664-681.

Kotak VC, Korada S, Schwartz IR, Sanes DH (1998) A developmental shift from GABAergic to glycinergic transmission in the central auditory system. J Neurosci 18:4646-4655.

Liu L, Wong TP, Pozza MF, Lingenhoehl K, Wang Y, Sheng M, Auberson YP, Wang YT (2004) Role of NMDA receptor subtypes in governing the direction of hippocampal synaptic plasticity. Science 304:1021-1024.

Moore MJ, Caspary DM (1983) Strychnine blocks binaural inhibition in lateral superior olivary neurons. J Neurosci 3:237-242.

Nabekura J, Katsurabayashi S, Kakazu Y, Shibata S, Matsubara A, Jinno S, Mizoguchi Y, Sasaki A, Ishibashi H (2004) Developmental switch from GABA to glycine release in single central synaptic terminals. Nat Neurosci 7:17-23.

Noh J, Seal RP, Garver JA, Edwards RH, Kandler K (2010) Glutamate co-release at GABA/glycinergic synapses is crucial for the refinement of an inhibitory map. Nat Neurosci 13:232-238.

Onoa B, Li H, Gagnon-Bartsch JA, Elias LA, Edwards RH (2010) Vesicular monoamine and glutamate transporters select distinct synaptic vesicle recycling pathways. J Neurosci 30(23):7917-7927.

Sanes DH, Rubel EW (1988) The ontogeny of inhibition and excitation in the gerbil lateral superior olive. J Neurosci 8:682-700.

Sanes DH, Siverls V (1991) Development and specificity of inhibitory terminal arborizations in the central nervous system. J Neurobiol 22(8):837-54.

Sanes DH, Takacs C (1993) Activity-dependent refinement of inhibitory connections. Eur J Neurosci 5(6):570-574.

Smith PH, Joris PX, Carney LH, Yin TC (1991) Projections of physiologically characterized globular bushy cell axons from the cochlear nucleus of the cat. J Comp Neurol 304:387-407.

Tritsch NX, Yi E, Gale JE, Glowatzki E, Bergles DE (2007) The origin of spontaneous activity in the developing auditory system. Nature 450:50-55.

Tritsch NX, Bergles DE (2010) Developmental regulation of spontaneous activity in the Mammalian cochlea. J Neurosci 30: 1539-1550.

Tritsch NX, Rodríguez-Contreras A, Crins TT, Wang HC, Borst JG, Bergles DE (2010) Calcium action potentials in hair cells pattern auditory neuron activity before hearing onset. Nat Neurosci 13(9):1050-2.

Wu SH, Kelly JB (1992) Synaptic pharmacology of the superior olivary complex studied in mouse brain slice. J Neurosci 12:3084-3097.

Zander JF, Münster-Wandowski A, Brunk I, Pahner I, Gómez-Lira G, Heinemann U, Gutiérrez R, Laube G, Ahnert-Hilger G (2010) Synaptic and vesicular coexistence of VGLUT and VGAT in selected excitatory and inhibitory synapses. J Neurosci 30(22):7634-7645.

Supplemental Figure 1: Blockade of mGluRs does not change GABA/glycine paired-pulse ratios

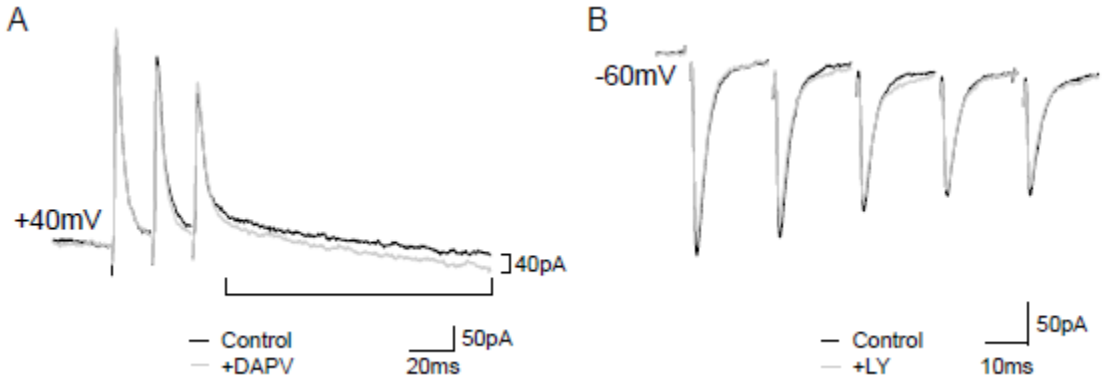

A. A P5 WT cell releases glutamate, as demonstrated by blockade of tail current by the NMDAR antagonist DAPV. **B.** Following application of an mGluR antagonist in the same P5 neuron, GABA/glycine paired-pulse ratios do not differ. A total of 3 cells were tested in this way.

Supplemental Figure 2: Miniature event amplitude histograms fr all neurons tested

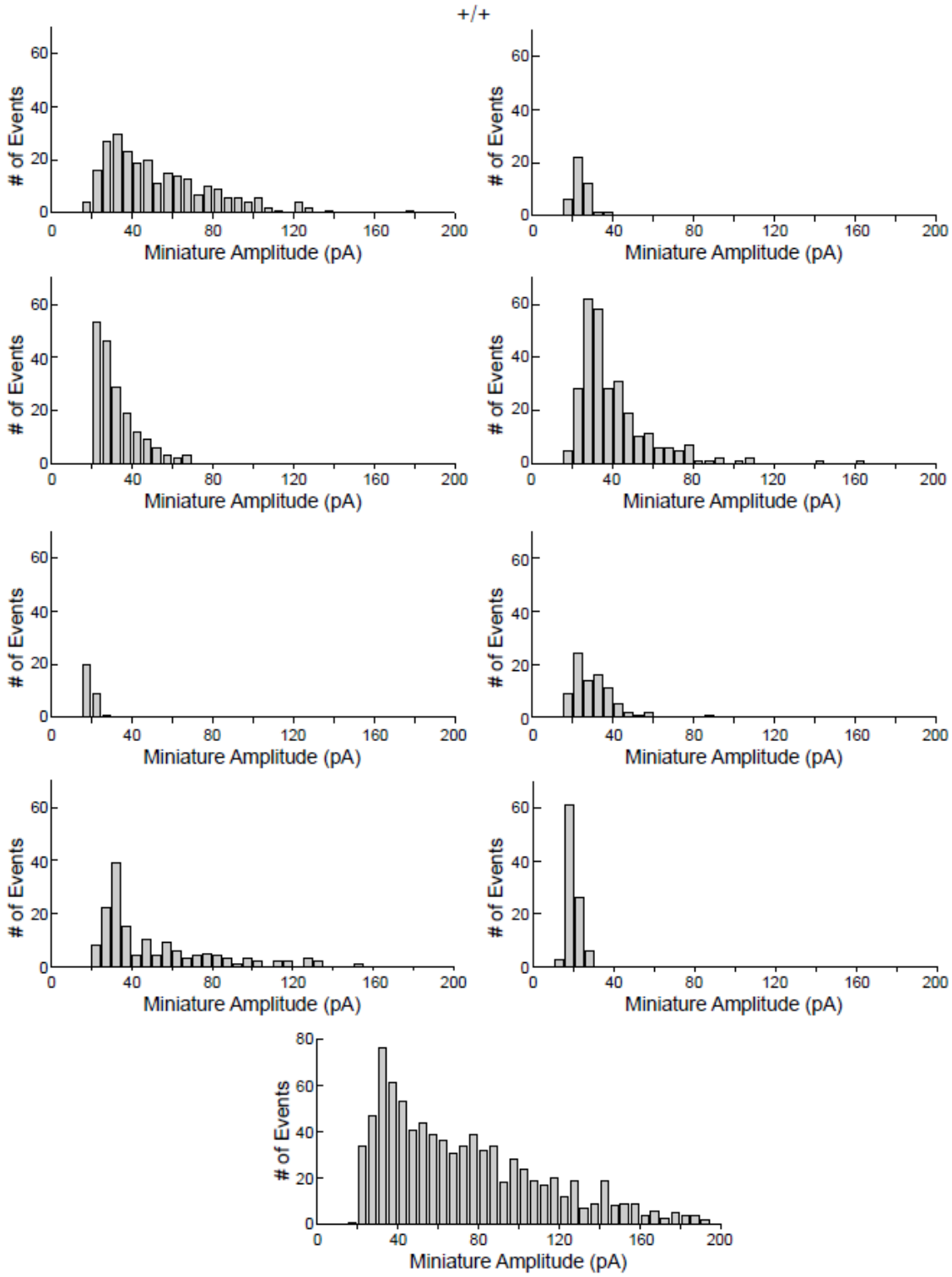

-/-

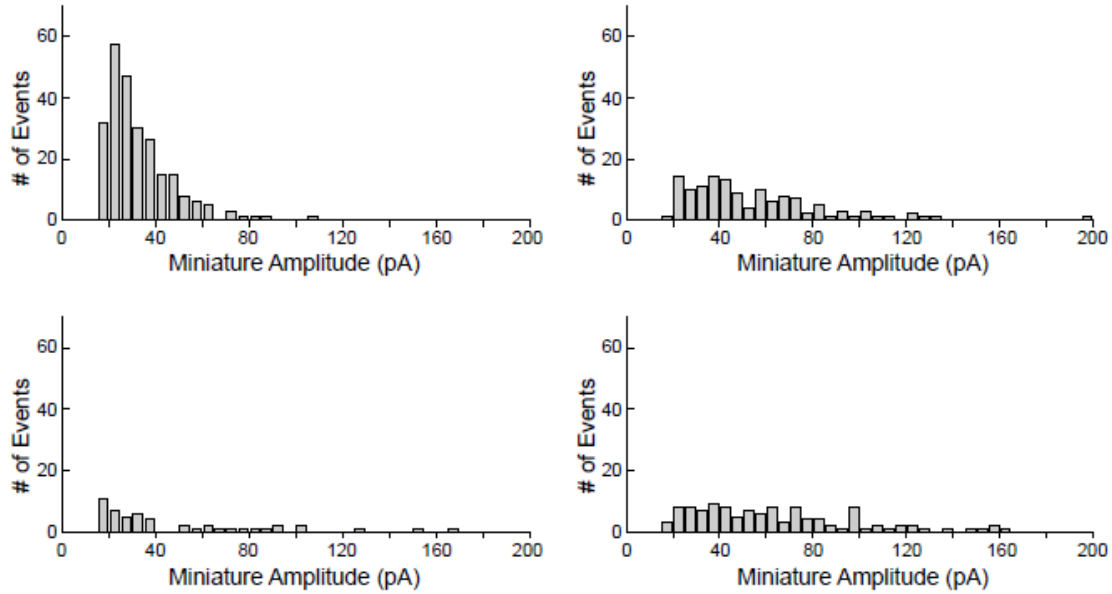
# of Events
Miniature Amplitude (pA)
0
20
40
60
0
40
80
120
160
200

Chapter 5 - Discussion

The research presented in chapters 2 through 4 was directed at understanding what mechanisms underlie the functional refinement of circuits in the lateral superior olive (LSO). More broadly, the research aimed to gain understanding of two basic nervous system questions: 1) How do topographic maps become aligned during development? 2) What are the mechanisms underlying development and plasticity of inhibitory synapses? To understand the development of the excitatory AVCN-LSO pathway and the inhibitory MNTB-LSO pathway, we performed a series of studies to determine how various aspects of neurotransmission develop in the LSO. Interestingly, the development of the excitatory and inhibitory pathways is similar in many ways.

5.1 Results from Chapters 2 to 4

Development of the excitatory AVCN-LSO pathway

Previously, very little was known about the development of the AVCN-LSO pathway. To understand more about the development of this pathway, we sought to characterize its period of functional refinement and the phenotype of neurotransmission during that period. Using whole-cell patch-clamp to record minimal stimulation responses and input-output curves in acute brainstem slices from rats aged P1-P12, we found that principal neurons of the LSO lose inputs from the AVCN mainly between P3 and P7, and

that the remaining inputs are strengthened over this period. This indicates that the AVCN-LSO pathway is refined in the same manner and over the same period as the MNTB-LSO pathway (Kim and Kandler, 2003). Additionally, we found that glutamatergic transmission at AVCN-LSO synapses activates both NMDA and AMPA receptors during this period. NMDAR-mediated transmission, assessed using pharmacology and by calculating AMPA/NMDA ratios, is high from P1 to P7 and quickly declines thereafter. This result is consistent with previous findings that both AMPARs and NMDARs initiate calcium entry at AVCN-LSO terminals in early postnatal mice (Ene et al, 2003). Additionally, subunit specific pharmacology and analysis of current kinetics indicates that NMDARs undergo a subunit shift during development, with GluN2B containing receptors being common before P7 and scarce thereafter.

Glutamatergic transmission in the MNTB-LSO pathway

The MNTB-LSO pathway undergoes functional refinement mainly between P3 and P8 (Kim and Kandler, 2003), and glutamate release from developing MNTB-LSO synapses offers an exciting mechanism for the functional refinement of this ultimately inhibitory pathway (Gillespie et al, 2005). Using whole-cell patch-clamp in acute brainstem slices from rats aged P0-P12, we found that NMDAR-mediated transmission was highest at MNTB-LSO synapses between P3 and P8, the period in which these synapses undergo refinement. Additionally, using subunit specific pharmacology, we found that GluN2B-containing receptors were active at MNTB-LSO synapses before P8,

but did not contribute to synaptic current thereafter. The results of this study, taken together with the results of our AVCN-LSO pathway study and the results of Kim and Kandler (2003), indicate that functional refinement of the excitatory and inhibitory pathways mirror one another and likely use similar mechanisms to accomplish this refinement.

Role of VGlut3 in refinement of the MNTB-LSO pathway

Though VGlut3 and VIAAT are expressed at the same MNTB terminals, it is not known whether or not these transporters are expressed in the same synaptic vesicles. This issue is quite important for two main reasons: 1) If VIAAT and VGlut3 are expressed in separate vesicles, there may also be separate vesicle populations that could, in theory, be released by different patterns of activity; 2) If VGlut3 and VIAAT are expressed in the same vesicles, VGlut3 could synergize with VIAAT to increase loading of GABA and glycine into synaptic vesicles at MNTB-LSO synapses, which may be crucial for supporting patterned neurotransmitter release necessary for synaptic refinement.

To address point 1, we used whole-cell patch-clamp in acute brainstem slices from rats aged P0-P7 to determine if GABA/glycine and glutamate exhibit different properties of release at developing MNTB-LSO synapses (Chapter 3). We found that $GABA_AR$/GlyR-mediated responses display greater paired-pulse depression than AMPAR-mediated responses. This result suggests that GABA/glycine and glutamate are released from separate vesicles.

To address point 2, we used whole-cell patch-clamp in acute brainstem slices from mice aged P4-P5 to determine if mice expressing VGlut3 and mice lacking VGlut3 exhibit different properties of neurotransmitter release at developing MNTB-LSO synapses (Chapter 4). We found that paired-pulse ratios, time to recover from paired-pulse depression, and the amplitude of miniature inhibitory events at MNTB-LSO synapses do not differ between mice that express VGlut3 and mice that lack VGlut3. Like the previous result, this result suggests that GABA/glycine and glutamate are released from separate vesicles. Additionally, this result offers further support to the hypothesis that VGlut3 is most important at MNTB-LSO synapses to allow for NMDAR-dependent plasticity during their developmental refinement.

5.2 Implications of results from Chapters 2 to 4

Model for circuit refinement in the LSO

The results described above allow for a rather simple, yet surprising, model for circuit development in the LSO. Because 1) both the excitatory and inhibitory inputs are refined over the same period (~P3-P8; chapter 2, and Kim and Kandler, 2003), 2) NMDAR mediated activity is elevated during the period of refinement (until P8 for the excitatory pathway (chapter 2), P3-P8 for the inhibitory pathway (chapter 3)), 3) VGlut3 is necessary for refinement of the MNTB-LSO pathway (Noh et al, 2010), but VGlut3 does not appear to increase GABA/glycinergic transmission at MNTB-LSO synapses (chapter 4), and 4) spontaneous activity generated in the cochlea begins to increase at the

beginning of the period refinement (P3; Tritsch and Bergles, 2010), it appears that patterned activity generated in the cochlea drives NMDAR-dependent plasticity that underlies functional refinement in both the excitatory and inhibitory input pathways to the LSO. The physiological steps in this model are as follows: 1) Patterned spontaneous activity is generated in the cochlea. This patterned activity propagates through both the excitatory AVCN fibers and the inhibitory MNTB fibers. 2) Neurotransmitter release is initiated at AVCN-LSO synapses and at MNTB-LSO synapses. At AVCN-LSO synapses, glutamate release activates AMPARs and leads to depolarization of the synapse and allows for NMDAR activation by glutamate; at MNTB-LSO synapses, GABA/glycine release at MNTB-LSO synapses activates $GABA_A$Rs and GlyRs and, due to a high chloride reversal potential at this age (Ehrlich et al, 1999), leads to depolarization of the synapse and allows for NMDAR activation by glutamate. The level of NMDAR activation at either synapse may depend on the amount of glutamate that is released, which may be dictated by the patterns of activity that reach the synapses. 3) Calcium entry into the postsynaptic (LSO) cell through NMDARs initiates synaptic plasticity. The direction of plasticity (potentiation versus depression) may be dictated by the subunits that the NMDARs are composed of, and also the overall level of NMDAR activation, which is directly controlled by the amount of glutamate released at the synapse. Though this model has taken shape through the findings of many different studies, several questions remain to be answered to fully understand refinement of the inputs to the LSO.

Does NMDAR-dependent long-term plasticity underlie refinement of inputs to the LSO?

The results from the first two chapters are consistent with the hypothesis that NMDAR activation, specifically GluN2B-containing NMDAR activation, is required for functional refinement in both the excitatory AVCN-LSO pathway and the inhibitory MNTB-LSO pathway. These results are supported by *in situ* hybridization work performed in our laboratory that demonstrated that expression of GluN2B RNA is high in the superior olivary complex in the first postnatal week and declines thereafter; following the first postnatal week, GluN2A RNA expression is most prevalent (Singh et al, unpublished results). However, these results are strictly correlative, and it needs to be determined whether NMDARs actually do contribute to refinement of circuits in the LSO, and, if so, what form(s) of plasticity they mediate. The difficulties with studying NMDAR-dependent plasticity of the excitatory and inhibitory inputs to LSO neurons are essentially the same, but with some added difficulties in the inhibitory pathway. Therefore, I will only discuss what approaches are necessary to study NMDAR-dependent plasticity in the inhibitory MNTB-LSO pathway.

NMDAR-dependent plasticity can arise in different ways at different synapse types, and finding an activity, or stimulation, pattern that elicits plasticity may be the most difficult part of studying plasticity at a particular synapse. In most cases, experimenters use trial and error to find a "plasticity protocol" for a synapse, whether the synapse is excitatory or inhibitory. Usually, it is different stimulation patterns that elicit NMDAR-dependent LTP and LTD at a single synapse; this means that determining two distinct

plasticity protocols, one for LTP and one for LTD, may be required to understand both strengthening and weakening of MNTB-LSO synapses. However, it is possible that a single stimulation pattern can lead to both LTP and LTD at a single synapse; in this case, the direction of plasticity may be determined by the subunits that compose the NMDARs at that synapse (Liu et al, 2004), though this has not been commonly observed. If it is the case that a single stimulation protocol can elicit both LTP and LTD at MNTB-LSO synapses, it will be necessary to determine which subtypes of NMDARs are present when either LTP or LTD occurs; this can be done pharmacologically or by analysing current kinetics.

Though several different forms of NMDAR-dependent inhibitory synaptic plasticity have been observed (for review, see Gaiarsa et al, 2002) and seems to be a likely candidate to mediate functional refinement at MNTB-LSO synapses, other non-NMDAR dependent forms of inhibitory synaptic plasticity exist that must be considered. For example, plasticity may be expressed through changes in the chloride reversal potential: decreasing the chloride reversal potential would make GABA/glycinergic transmission more strongly inhibitory, and vice versa. Spike-timing dependent plasticity at hippocampal inhibitory synapses use this type of plasticity mechanism, as specific patterns of activity lead to changes in the expression of the potassium-chloride co-transporter KCC2 or the sodium-potassium-chloride co-transporter NKCC1, which in turn changes the chloride reversal potential (Woodin et al, 2003; Balena et al, 2008). Though this form of spike-timing dependent plasticity may not be dependent on NMDARs, to fully understand how MNTB-LSO synapses develop it is important to be aware that this

form of plasticity may occur. Additionally, because the chloride reversal potential decreases in MNTB neurons as the neural circuit develops (Ehrlich et al, 1999), it is possible that strengthening or weakening of MNTB-LSO synapses is accompanied by a shift in the chloride reversal potential. It is possible that plasticity of this type could occur at the level of a single MNTB-LSO synapse considering that other changes, such as the shift from GABAergic to glycinergic transmission, is seen at the level of a single MNTB-LSO synapse (Nabekura et al, 2004). Taking in to account this type of plasticity, any study of plasticity at developing MNTB-LSO synapses will ideally be performed using the gramicidin perforated-patch technique rather than whole-cell patch, so that any changes in native chloride concentrations in the neuron can be observed.

In visual cortex and hippocampus, synapses originating from a single neuron can exhibit different forms of plasticity depending on whether the postsynaptic cell is excitatory or inhibitory (Markram et al, 1998; Maccaferri et al, 1998). This finding raises a potential problem for studying plasticity in the LSO, because principal neurons in the LSO are of different phenotypes (Helfert et al, 1989). It is possible that synapse refinement on to excitatory and inhibitory neurons is directed in the same manner, but it is also possible that any plasticity protocol that may be useful in the MNTB-LSO pathway may not produce obvious changes, or may produce inconsistent results, if there is a target-dependent component to synaptic plasticity in this pathway. There are two ways to approach this problem: 1) Include biocytin or a fluorescent dye in the recording electrode so that the neuron can be identified post-hoc and then be counterstained with an excitatory or inhibitory marker. This approach requires a lot of post-hoc experimentation

for every patch recording. 2) Mark a specific cell-type endogenously in the animal you are studying, so that this cell type can be targeted during slice recording. This approach requires developing a mouse that expresses a marker specific for a particular cell-type in the LSO, most likely a marker for a calcium-binding protein specific to an inhibitory cell-type; this is hardly a trivial obstacle to overcome, but would allow for the use of the perforated-patch technique, would reduce the number of patch-experiments in which plasticity protocol failures are observed, and would eliminate problems in cell labelling during the patch recording and also during post-hoc cell identification. However, the concern of target-dependent plasticity is speculative, and it is worth pursuing plasticity at MNTB-LSO synapses without worrying about these problems; however, if plasticity experiments continually fail or produce inconsistent results, these other approaches may need to be considered.

Does patterned activity drive refinement of inputs to the LSO?

Spontaneous retinal waves are crucial for organizing topography in the visual system, creating nearest neighbor relationships between cells in the earliest stages of the visual pathway that are maintained through higher visual processing levels (for review, see Feller, 2009). In the auditory system, tonotopy exists throughout the auditory pathway, but it is unclear how it is directed. Like the retina, the cochlea generates spontaneous activity (Tritsch et al, 2007; Tritsch and Bergles, 2010; Tritsch et al, 2010), and it is possible that spontaneous cochlear activity propagates through the auditory

system to create tonotopy in auditory nuclei, in a manner similar to how retinal waves create topography in the visual system. However, this hypothesis has yet to be examined. The best way to determine what the role of spontaneous cochlear activity is in functional refinement of the MNTB-LSO pathway, and in auditory pathways generally, is to eliminate that spontaneous activity and evaluate the effect this loss has on the system, and ultimately, once the patterns of activity are known, to add back specific portions of that activity to determine which elements may be important for refinement. A previous study has shown that removing the cochlea eliminates anatomical refinement of MNTB-LSO terminals in gerbils (Sanes and Takacs, 1993). However, in this study functional refinement was not examined, and the cochlea was removed at P7, which is near the end of the functional refinement period, and is approaching the age when sound-evoked activity may be more important for any form of refinement. To understand whether loss of activity stops the process of functional refinement, the cochlea could be removed immediately following birth (P0-P1, ideally), and input-output curves similar to those performed by Kim and Kandler (2003), Noh et al. (2010), and by Case et al, (2011, chapter 2 of this thesis) could be performed to evaluate refinement in both the inhibitory and excitatory pathways. An alternative approach to determine whether spontaneous cochlear activity drives functional refinement is to kill cochlear hair cells at a very young age by administering an ototoxic drug. Using this approach would require determining the time it takes for hair cells to die following drug administration, and the amount of variability in the extent of hair cell loss. The best way to approach the question of whether or not spontaneous cochlear activity drives functional refinement in the LSO is to

selectively knock out a protein in the cochlea known to be crucial for the generation of spontaneous cochlear activity during the period of functional refinement, and then examine whether or not functional refinement proceeds normally. Experiments like this have been performed in the retina, and have demonstrated that several different factors drive the development of different aspects of visual processing (for example, Bansal et al, 2000; Mrsic-Flogel et al, 2005; Stacy et al, 2005).

If spontaneous cochlear driven activity does drive tonotopic refinement throughout the auditory system, it will be important to develop a more detailed understanding of what the activity patterns are (but, see Tritsch et al, 2010). Determining these patterns requires *in vivo* recordings throughout the various nuclei in the auditory pathway, and attributing the patterns to spontaneous cochlear activity may also require *in vivo* recordings in genetically manipulated mice that display disrupted cochlear activity. Knowing the patterns of activity that reach LSO neurons during synaptic refinement would make studies aimed at understanding the synaptic mechanisms underlying refinement much simpler, because these patterns of activity can simply be mimicked in a slice preparation, rather than having to search for plasticity protocols at random; the patterns of activity could also be replicated over an extended period of time using a slice culture preparation. Additionally, knowing the patterns of activity that propagate through the auditory system and determining which components of that activity are important for plasticity may aid in the design of therapeutic interventions, such as cochlear implants, for those with hearing disabilities.

Are different transporters directed to specific synaptic vesicles in MNTB terminals?

Release probabilities differ for GABA/glycine and glutamate at MNTB-LSO synapses (chapter 3). Furthermore, release probability of GABA/glycine is the same regardless of VGlut3 expression (chapter 4). These results are consistent with the hypothesis that vesicles expressing VIAAT, and therefore releasing GABA/glycine, and vesicles expressing VGlut3, and therefore releasing glutamate, are separate entities. During development the calcium sensor synaptotagmin 2 (Syt2) is expressed at both AVCN-LSO and MNTB-LSO synapses, whereas synaptotagmin 1 (Syt1) is expressed only at MNTB-LSO synapses (Cooper and Gillespie, 2011); this means that MNTB terminals utilize two different neurotransmitter transporters (VIAAT and VGlut3) and two different calcium sensors (Syt1 and Syt2). Interestingly, the expression pattern of Syt1 closely resembles the expression pattern of VGlut3 (Cooper and Gillespie, 2011); this result suggests that Syt1 localizes specifically with VGlut3 containing vesicles, and corroborates the hypothesis that there are separate populations of VIAAT-expressing and VGlut3-expressing vesicles. Additionally, spillover of glutamate between AVCN-LSO and MNTB-LSO synapses is consistent with glutamate being released ectopically at MNTB-LSO synapses, which could indicate that glutamate-releasing vesicles are in a separate pool from GABA/glycine-releasing vesicles (Alamilla and Gillespie, 2011). However, these results are again only correlative, and further studies are needed to confirm whether or not VIAAT and VGlut3 are directed to separate synaptic vesicles, and whether Syt1 and VGlut3 are directed to the same vesicles. The two best approaches to answer these questions are to either attempt immunoprecipitation from a synaptic vesicle

preparation in order to identify the proteins expressed in vesicles expressing a particular protein, or to use a super-resolution microscopy technique such as two-color STED to attempt to identify the relative locations of these proteins within the synaptic terminal. If useful answers are garnered from these approaches and it turns out that these different proteins are directed to specific vesicles, it would open up interesting basic cell biology questions concerning the mechanisms that guide proteins to specific vesicles, or to specific vesicle pools.

Why is GABA released during the development of an ultimately glycinergic pathway?

The inhibitory MNTB-LSO pathway appears to be purely glycinergic in its mature state, but GABA is prominently released during functional refinement of the pathway (Kotak et al, 1998; Nabekura et al, 2004). In fact, GABA contributes more to transmission at MNTB-LSO synapses than glycine during this refinement period (Kotak et al, 1998). This suggests that GABA is another important factor in the refinement of the MNTB-LSO pathway, but it is unclear how. GABA does not necessarily act on $GABA_A$ receptors - it can also act on metabotropic $GABA_B$ receptors, and can change the kinetics of GlyR-mediated currents (Kotak et al, 1998; Lu et al, 2008). However, these roles of GABA do not explain why $GABA_A$Rs are expressed at developing MNTB-LSO synapses. One hypothesis for why $GABA_A$Rs are expressed at developing MNTB-LSO synapses is that depolarization of the cell membrane through $GABA_A$R-mediated transmission may be trophic during development (Represa and Ben-Ari, 2005); however, GlyR-mediated

transmission is also depolarizing during development, so this is an unsatisfying hypothesis. Another hypothesis is that $GABA_A$Rs are required for receptor clustering at inhibitory synapses during development, and may be required to guide GlyR clustering if gephyrin is unavailable to do so (Levi et al, 2004). A final intriguing hypothesis for the role of $GABA_A$R-mediated transmission during functional refinement of the MNTB-LSO pathway may have something to do with the longer decay time of $GABA_A$R-mediated currents, relative to GlyR-mediated currents; the longer duration of the $GABA_A$R-mediated currents may be important for prolonging the depolarization of the synapse in order to increase NMDAR activation, or for increasing the duration of the synaptic current integration window, which may be important for crosstalk with the excitatory pathway and ultimately circuit alignment.

Determining if GABA is truly important in the functional refinement of the MNTB-LSO pathway is best approached by specifically knocking out GABA release in the LSO and evaluating synapse refinement using slice physiology. In the absence of a conditional knockout like this, a viable alternative is to evaluate MNTB-LSO refinement in a mouse that has had the GABA synthesizing enzyme glutamic acid decarboxylase 65 (GAD65) knocked out. GAD65 is localized to synaptic terminals, whereas another form of glutamic acid decarboxylase, GAD67, is present throughout a neuron. However, GAD65 knockout mice are viable and GAD67 knockout mice are not (Lau and Murthy, 2012). Therefore, in this experiment GABA transmission would likely be decreased rather than eliminated, but this may be enough to observe perturbations in MNTB-LSO synapse refinement. This experiment would only indicate if GABA is truly necessary for MNTB-

LSO functional refinement, but would not determine why it is important; answering the question *why* GABA is important is much more difficult than answering the question *is* GABA important. Determining a way to cause $GABA_A$Rs to behave more like GlyRs while maintaining GABA release may be the best way to answer this question; this would likely require experiments involving chronic pharmacological treatment, or targeted expression of certain $GABA_A$R subunits.

5.3 Summary

The projects described in this thesis have created a strong framework for understanding how functional refinement of the major input pathways into the LSO occurs. However, many experiments remain to be performed in order to fully identify how these pathways develop. To gain a full understanding of circuit development in the LSO several different types of experiments will be required, including slice physiology, *in vivo* physiology, molecular biology, and specialized microscopy. This work may require the collaboration of several groups, but will yield information important not only for understanding the development of the auditory system and sensory systems in general, but also for understanding inhibitory synaptic transmission and plasticity, neurotransmitter release, and synaptic protein trafficking.

References

Alamilla J, Gillespie DC (2011) Glutamatergic inputs and glutamate-releasing immature inhibitory inputs activate a shared postsynaptic receptor population in lateral superior olive. Neuroscience 196:285-296.

Balena T, Woodin MA (2008) Coincident pre- and postsynaptic activity downregulates NKCC1 to hyperpolarize E(Cl) during development. Eur J Neurosci. 27(9):2402-2412.

Bansal A, Singer JH, Hwang BJ, Xu W, Beaudet A, Feller MB (2000)Mice lacking specific nicotinic acetylcholine receptor subunits exhibit dramatically altered spontaneous activity patterns and reveal a limited role for retinal waves in forming ON and OFF circuits in the inner retina. J Neurosci 20(20):7672-7681.

Cooper AP, Gillespie DC (2011) Synaptotagmins I and II in the developing rat auditory brainstem: Synaptotagmin I is transiently expressed in glutamate-releasing immature inhibitory terminals. J Comp Neurol 519(12):2417-2433.

Ehrlich I, Lohrke S, Friauf E (1999) Shift from depolarizing to hyperpolarizing glycine action in rat auditory neurones is due to age-dependent Cl- regulation. J Physiol 520 Pt 1: 121-137.

Ene FA, Kullmann PH, Gillespie DC, Kandler K (2003) Glutamatergic calcium responses in the developing lateral superior olive: receptor types and their specific activation by synaptic activity patterns. J Neurophysiol 90: 2581-2591.

Feller MB (2009) Retinal waves are likely to instruct the formation of eye-specific retinogeniculate projections. Neural Dev. 2009 Jul 6;4:24.

Gillespie DC, Kim G, Kandler K (2005). Inhibitory synapses in the developing auditory system are glutamatergic. Nat Neurosci 8:332-338.

Helfert RH, Bonneau JM, Wenthold RJ, Altschuler RA (1989) GABA and glycine immunoreactivity in the guinea pig superior olivary complex. Brain Res 501(2):269-286.

Kim G, Kandler K (2003). Elimination and strengthening of glycinergic/GABAergic connections during tonotopic map formation. Nat Neurosci 6:282-290.

Kotak VC, Korada S, Schwartz IR, Sanes DH (1998) A developmental shift from GABAergic to glycinergic transmission in the central auditory system. J Neurosci 18:4646-4655.

Lau CG, Murthy VN (2012) Activity-dependent regulation of inhibition via GAD67. J Neurosci 32(25):8521-8531.

Levi S, Logan SM, Tovar KR, Craig AM (2004) Gephyrin is critical for glycine receptor clustering but not for the formation of functional GABAergic synapses in hippocampal lneurons. J Neurosci 24:207–217.

Liu L, Wong TP, Pozza MF, Lingenhoehl K, Wang Y, Sheng M, Auberson YP, Wang YT (2004) Role of NMDA receptor subtypes in governing the direction of hippocampal synaptic plasticity. Science 304:1021-1024.

Lu T, Rubio ME, Trussell LO (2008) Glycinergic transmission shaped by the corelease of GABA in a mammalian auditory synapse. Neuron 57(4):524-535.

Maccaferri G, Toth K, McBain C (1998) Target-specific expression of presynaptic mossy fiber plasticity. Science 279(5355): 1368-1370.

Markram H, Wang Y, Tsodyks M (1998) Differential signaling via the same axon of neocortical pyramidal neurons. Proc Natl Acad Sci U S A 95(9):5323-5328.

Mrsic-Flogel TD, Hofer SB, Creutzfeldt C, Cloëz-Tayarani I, Changeux JP, Bonhoeffer T, Hübener M (2005) Altered map of visual space in the superior colliculus of mice lacking early retinal waves.J Neurosci 25(29):6921-6928.

Nabekura J, Katsurabayashi S, Kakazu Y, Shibata S, Matsubara A, Jinno S, Mizoguchi Y, Sasaki A, Ishibashi H (2004) Developmental switch from GABA to glycine release in single central synaptic terminals. Nat Neurosci 7:17-23.

Noh J, Seal RP, Garver JA, Edwards RH, Kandler K (2010) Glutamate co-release at GABA/glycinergic synapses is crucial for the refinement of an inhibitory map. Nat Neurosci 13: 232-238.

Represa A, Ben-Ari Y (2005) Trophic actions of GABA on neuronal development. Trends Neurosci 28(6):278-283.

Sanes DH, Takacs C (1993) Activity-dependent refinement of inhibitory connections. Eur J Neurosci 5: 570-574.

Stacy RC, Demas J, Burgess RW, Sanes JR, Wong RO (2005) Disruption and recovery of patterned retinal activity in the absence of acetylcholine. J Neurosci 25(41):9347-9357.

Tritsch NX, Yi E, Gale JE, Glowatzki E, Bergles DE (2007) The origin of spontaneous activity in the developing auditory system. Nature 450: 50-55.

Tritsch NX, Bergles DE (2010) Developmental regulation of spontaneous activity in the Mammalian cochlea. J Neurosci 30: 1539-1550.

Tritsch NX, Rodríguez-Contreras A, Crins TT, Wang HC, Borst JG, Bergles DE (2010) Calcium action potentials in hair cells pattern auditory neuron activity before hearing onset. Nat Neurosci 13(9):1050-2.

Woodin MA, Ganguly K, Poo MM (2003) Coincident pre- and postsynaptic activity modifies GABAergic synapses by postsynaptic changes in Cl- transporter activity. Neuron 39(5): 807-820.